Design and Control of a Knee Exoskeleton for Assistance and Power Augmentation

UNIVERSITÀ DEGLI STUDI
DI GENOVA

Lorenzo Saccares

University of Genova, Italy

Istituto Italiano di Tecnologia (IIT)

Submitted in partial fulfilment of the requirements for the degree of

Doctor of Philosophy (Ph.D.)

February 2018

Thesis Supervisors:

Dr. Ioannis Sarakoglou

Research Engineer

Department of Advanced Robotics

Istituto Italiano di Tecnologia (IIT)

Dr. Nikos Tsagarakis

Senior Researcher

Department of Advanced Robotics

Istituto Italiano di Tecnologia (IIT)

ABSTRACT

Thanks to the technological advancements, assistive lower limb exoskeletons are moving from laboratory settings to daily life scenarios. This dissertation makes a contribution toward the development of assistive/power augmentation knee exoskeletons with an improved wearability, ergonomics and intuitive use. In particular, the design and the control of a novel knee exoskeleton system, the iT-Knee Bipedal System, is presented. It is composed by: a novel mechanism to transmit the assistance generated by the exoskeleton to the knee joint in a more ergonomic manner; a novel method that requires limited information to estimate online the torques experienced by the ankles, knees and hips of a person wearing the exoskeleton; a novel sensor system for shoes able to track the feet orientation and monitor their full contact wrench with the ground.

In particular, the iT-Knee exoskeleton, the main component of the aforementioned system, is introduced. It is a novel six degree of freedom knee exoskeleton module with under-actuated kinematics, able to assist the flexion/extension motion of the knee while all the other joint's movements are accommodated. Thanks to its mechanism, the system: solves the problem of the alignment between the joint of the user and the exoskeleton; it automatically adjusts to different users' size; reduces the undesired forces and torques exchanged between the attachment points of its structure and the user's skin.

From a control point of view, a novel approach to address difficulties arising in real life scenarios (i.e. noncyclic locomotion activity, unexpected terrain or unpredicted interactions with the surroundings) is presented. It is based on a method that estimates online the torques experienced by a person at his ankles, knees and hips with the major advantage that does not rely on any information of the user's upper body (i.e. pose, weight and center of mass location) or on any interaction of the user's upper body with the environment (i.e. payload handling or pushing and pulling task). This is achieved

by monitoring the full contact wrench of the subject with the ground and applying an inverse dynamic approach to the lower body segments.

To track the full contact wrench between the subject's feet and the ground, a novel add on system for shoes has been developed. The iT-Shoe is adjustable to different user's size and accommodates the plantar flexion of the foot. It tracks the interactions and the orientation of the foot thanks to two 6axis Force/Torque sensors, developed in-house, with dedicated embedded MEMS IMUs placed at the toe and heel area.

Different tasks and ground conditions were tested to validate and highlight the potentiality of the proposed knee exoskeleton system. The experimental results obtained and the feedback collected confirm the validity of the research conducted toward the design of more ergonomic and intuitive to use exoskeletons.

ACKNOWLEDGEMENT

First, I would like to thank my advisors, Dr. Ioannis Sarakoglou and Dr. Nikos G. Tsagarakis. Without them, the work presented in this thesis would not exist. They gave me full freedom to conduct my research and they were always present to discuss about it. My gratitude goes also to Anais Brygo, Joao Bimbo and Vasiliki-Maria Katsageorgiou. They supported me in many ways: on the set up of the experiments and on their execution, in writing as well as in programming. I am grateful also to Prof. Darwin Caldwell, director of the department of Advanced Robotics at IIT. He always supported my Ph.D. research and his department has an excellent work environment. I would also like to acknowledge also Dr. Roberto Cingolani, scientific director of the IIT-Istituto Italiano di Tecnologia. Thanks to his work, Italy can boast of one of the best research institutes in the world.

My gratitude goes also to all the technicians of the department of Advanced Robotics at IIT. In particular, I would like to thanks Giuseppe Sofia and Gianluca Pane, for their advices on mechanical aspects, as well as Phil E. Hudson and Marco Migliorini for their support on software and electronic components.

I am grateful to my colleagues and friends at IIT: Nawid Jamali, Anays Brigo, Bilal Rehman, Soraia Fernandes, Dina Niculaes, Javad Shamsi, Jorghe Fernandez, Joao Bimbo, Olmo Moreno, Stefano Toxiri, Jesus Ortiz, Alperen Acemoglu, Zhuoqi Cheng, Matteo Rossi, Marco Laghi, Andrea Ciullo, Tommaso Poliero, Francesca Negrello, Veronica Penza, Lucia Schiatti, Sara Moccia, Dimitris Kanoulas, Wansoo Kim, Arash Ajoudani, Josephus Driessen and Wesley Roozing. It was a pleasure to stay with them inside an outside IIT.

Special thanks go to Prof. Giovanni B. Broggiato. Without his support my PhD would not have begun.

I would like also to thank my old and new friends. In particular Stefano Balsamo, Dario Cassano, Antonio Caizzi and Matteo Busatto for making feel Genoa as home to me.

I am grateful to my parents and my family for their support and for encouraging me in my endeavors.

Finally, my last words of gratitude are saved for Olga Tsorokh, my love, for her faith, support and cheerfulness.

CONTENTS

LIST OF FIGURES

LIST OF TABLES

NOMENCLATURE

AKHFE plane	Ankle, Knee and Hip Flexion-Extension plane
DoF	Degree of Freedom
FEA	Finite Element Analysis
GRF	Ground Reaction Forces
GRT	Ground Reaction Torques
ICR	Instantaneous Centre of Rotation
IMU	Inertia measurement unit
pHRi	physical Human-Robot interaction
RoM	Range of Motion
S2AP	Series of two Articulated Parallelograms
SLLE	Static Lower Limbs Equilibrium

1 INTRODUCTION

1.1 Motivation

Exoskeletons are wearable devices that acts in parallel to the muscles of the human body to assist the segments motion. Even if in 1890 Yagn had already seen their potentiality [1], due to the human body complexity and technological limitations, research and development activities are still undergoing in this field. Nowadays exoskeletons have different fields of application and they are grouped in three main categories according to their scope [2]. These categories are: rehabilitation, assistive augmentation exoskeletons and power augmentation exoskeletons.

Rehabilitation exoskeletons aim at recovering the neuro-musculoskeletal function of stroke or post-surgical patients. They are typically not portable and are used in clinical environments. The introduction of this kind of robots can allow patients to receive a more effective and stable rehabilitation process, as well as therapists to reduce their workload and at the same time increase their productivity, providing quantitative measurements of patients' progress. Within this context, a remarkable example is Lokomat, refer to Fig. 1.a, a treadmill-based exoskeleton for gait training commercialized by Hocoma company [3]. LOPES is a treadmill-based lower limp exoskeleton, which utilizes Bowden cables to transmit the mechanical power from a motor placed out of the exoskeleton structure [4]. The NEUROBOTICS Elbow Exoskeleton (NEUROExos), on the other hand, is an elbow exoskeleton device for post-stroke physical rehabilitation that incorporates four passive Degrees of Freedom (DoF) to improve the users' interaction with the device [5]. Finally, the AssistOn-Knee exoskeleton is a self-aligning active exoskeleton for robot-assisted knee rehabilitation. Using a Schmidt coupling, this device can accommodate the Instantaneous Center of Rotation (ICR) translation on the sagittal plane [6].

Assistive exoskeletons on the other hand, are aimed to support, partially or fully, the motion of elderly people or of individuals with impaired functions, while performing daily tasks. The EMG-controlled HAL 5 full-body exoskeleton is an example of such a device developed by Tsukuba and Cyberdyne Inc. [7],[8]. Additionally, the AlterG Bionic Leg robot, commercialized by Tibion Corporation, implements the polycentric motion of the knee [9], [10]. Argo Medical Technologies has developed ReWalk [11], a lower body assistive exoskeleton with a single DoF, target for paraplegics. Ekso Bionics at Berkeley has developed Ekso, refer to Fig. 1.b, a medical gait training exoskeleton, previously called eLEGS, which helps individuals with various levels of paralysis and hemiparesis [12],[13]. In [14], a 6-DoF exoskeleton for the knee joint has been presented. This device assists the flexion/extension motion of the knee, while all the other DoF of the knee are accommodated. However, this kinematic redundancy is attained through a bulky and heavy implementation, which might become a drawback for such a system. More recently, in [15], a 3 DoF knee exoskeleton based on a polycentric four-bar linkage was developed, while a similar concept was used in [16], where the polycentric four-bar linkage was driven by a linear actuator placed on the user's thigh.

Finally, power augmentation exoskeletons target to the power capacity of the healthy operator by enhancing his ability to execute higher load demanding tasks as well as extending his endurance during these operations. This type of devices can be useful for disaster relief workers, firefighters, but also for factory workers. BLEEX (Berkeley Lower Extremity Exoskeleton) developed by the University of California [17], [18] and XOS 2 [19], by Raytheon SARCOS, belong to this category and are able to increase the human strength and endurance capabilities. More recently, the University of California teamed up with Lockheed Martin to spread in the market the HULC exoskeleton [20], a device that can provide strength and endurance augmentation characteristics, as Fig. 1.c depicts.

Despite the fact that exoskeletons have different applications, common technological requirements have to be satisfied. Indeed, as robots operating in close physical contact with humans, exoskeletons have to always guarantee comfort and

safe interactions. As a consequence, multiple requirements, such as wearability, ergonomics, actuation systems, interaction control and energetics, have to be fulfilled.

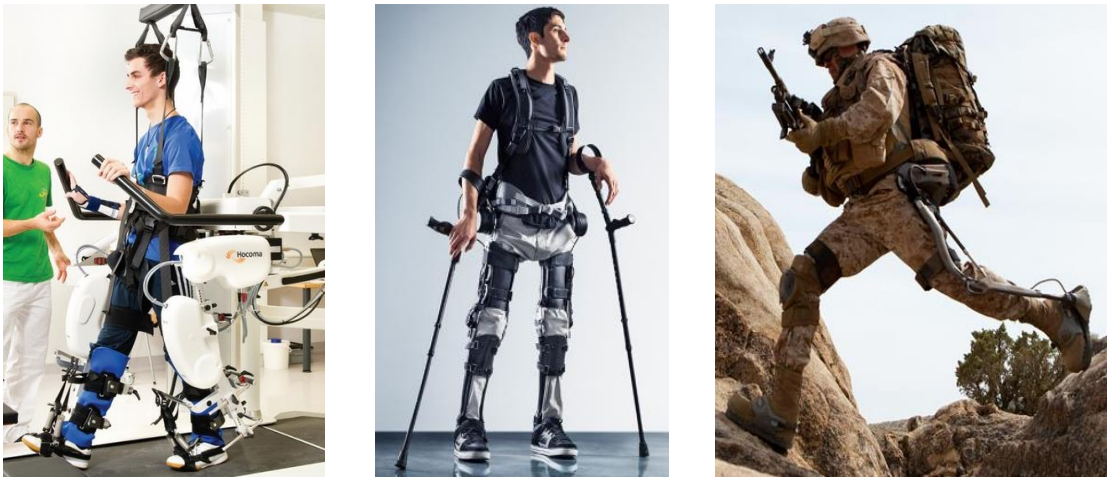

(a) (b) (c)

Fig. 1– (a) the rehabilitative exoskeleton Lokomat. (b) the assistive exoskeleton Ekso Bionics–eLEGS. (c) the power augmentation exoskeleton HULC.

1.2 Objective and Approach

To become widespread in the society, exoskeletons, as wearable devises, should be ergonomic, user-friendly and effective. The objective of this thesis is to contribute toward the design and the control of assistive/power augmentation lower limbs exoskeletons that are characterized by an improved wearability, ergonomics and intuitive use. Specifically, the research attention was focused on the design of exoskeletons that exhibit fast donning, removal and setup procedures as well as adaptability to different users' sizes. Moreover, exoskeletons should not impose motion constraints to the assisted joint and they should not generate undesired interactions (forces/torques) while they provide assistance to the user. To design exoskeleton systems intuitive to use and effective, the second objective of this thesis was the development of an accurate method to detect the users' intension in terms of motion in all loading conditions and of a precise approach to estimate on-line the users' effort during such tasks. Finally, the attention was focused on the design of

sensory systems rich of information but at the same time compact, portable and ergonomic. Indeed, especially in outdoor scenarios, the control architecture of the exoskeletons should rely on portable sensing systems in order to not reduce the user's workspace [21].

To improve the wearability and the ergonomics, attention was firstly given to the study of the human knee anatomy and kinesiology and then on the design of a knee exoskeleton that accounts for the human joint complexity. Such an approach permitted to design systems fully kinematic coupled with the human knee, adjustable to different users' size and ergonomic in the way the assistance is transmitted from the exoskeleton to the user's body segments. To improve the capability of lower limb exoskeletons in estimating the user's state with reduced information in real time, the research attention was focused on the design of a novel method capable of evaluating online the torques generated by the user at the ankles, knees and hips, without the need for any information of the user's upper body and of possible interactions occurring between the user's upper body and the environment. Finally, to test the implemented control strategy on the exoskeleton system and to improve its portability, the work presented in this thesis is focused on the design of a novel sensorized add-on system for shoes able to monitor the feet orientation and their full contact wrench with the ground. As a result, the development of a wearable, ergonomic, and portable exoskeleton system has been achieved.

1.3 Main Contributions

This dissertation contributes on the investigation of novel design and control approaches for assistive/power augmented lower limb exoskeletons. Result of this research activity is the development of the iT-Knee Bipedal System that gathers together the following contributions.

The contributions regarding the design are listed below:

• A modular six degree of freedom knee exoskeleton (iT-Knee exoskeleton) with under-actuated kinematics able to assist the flexion/extension motion of the knee while all the other joint's movements are accommodated. In particular, two iT-Knee exoskeletons were developed and used to perform assistive tasks within the iT-Knee bipedal system.

• A first sensory system for shoes (iT-Shoe) to monitor the interaction of the feet with the ground. It was used for preliminary evaluations of the SLLE method, refer to control contribution list.

• A second version of the iT-Shoe. In particular, an add on system for shoes adjustable to different users' size, able to accommodate the plantar flexion and to monitor the interaction and the orientation of the toes and heels, was designed. It was used in different tasks (i.e. lifting and pushing tasks) and terrains (i.e. flat grounds, inclined surfaces, steps, irregular terrains) to validate the SLLE method, refer to control contribution list.

The contributions regarding the control are listed below:

• A method (the SLLE method) that estimates online the torques generated by the user's ankles, knees and hips with the major advantage that it does not require any information about the user's upper body (i.e. pose, weight and center of mass location) and about any interaction of the user's upper body with the environment (i.e. payload handling or pushing and pulling task). This is achieved by monitoring the full contact

wrench of the subject with the ground and applying an inverse dynamic approach to the lower body segments.

• A state machine to modulate the assistance of the iT-Knee bipedal system while a locomotion task is performed. Torque references for the iT-Knee actuators are generated based on the values estimated online by the SLLE method. The controller is based on the detection of gait events.

1.4 Outline

The rest of this thesis is organized as follows. Chapter 2 provides the state-of-the-art of exoskeletons with a focus on their design characteristics. In addition, the so far implemented control strategies for lower limb exoskeletons are reported.

Chapter 3 presents the hardware components of the iT-Knee Bipedal System. In particular, a detailed description of the iT-Knee exoskeleton (i.e. its kinematics, design and actuation system) and of the iT-Shoes is presented.

Chapter 4 describes the control architecture of the iT-Knee Bipedal System. Firstly, a detailed description of the SLLE method is given, followed by the state machine implemented to modulate the assistance of the iT-Knee Bipedal System.

Chapter 5 describes and discusses the experiments conducted to test and validate the property of the iT-Knee exoskeleton, the accuracy of the iT-Shoes, the precision of the SLLE method and finally the capability of the iT-Knee Bipedal System to generate assistance.

Chapter 6 addresses the conclusions and highlights the main contributions of the work presented in this dissertation. Finally, future research directions are outlined.

1.5 Publications

- **L. Saccares**, I. Sarakoglou, and N. G. Tsagarakis, "iT-Knee: An exoskeleton with ideal torque transmission interface for ergonomic power augmentation," in *2016 IEEE/RSJ International Conference on Intelligent Robots and Systems (IROS)*, 2016, pp. 780-786.
- **L. Saccares**, A. Brygo, I. Sarakoglou, and N. G. Tsagarakis, "A Novel Human Effort Estimation Method for Knee Assistive Exoskeletons," in *ICORR 2017-15th IEEE International Conference on Rehabilitation Robotics*, 2017.
- **L. Saccares**, I. Sarakoglou, and N. G. Tsagarakis, " A Novel Joint Torque Estimation Method and Sensory System for Assistive Lower Limb Exoskeletons" under review at *2018 IEEE/RSJ International Conference on Intelligent Robots and System* (IROS), 2018.

1.6 Patent

The design of the iT-Knee exoskeleton has be patented, refer to:

- Patent Application IT 102016000099694 (UA2016A007086) (PT160339): *"Esoscheletro per arti inferiori"*.

2 Background and Related Work

2.1 Mechatronic Design of Lower Limb Exoskeletons

The development of effective lower limb exoskeletons is still an open challenge in robotic research [2, 22-24]. Their design is a highly demanding task: requirements that are characteristic of industrial products need to coexist with necessities arising from to their wearable nature. Features as wearability, ergonomics, adaptability [25], portability and aesthetics must go hand in hand with more traditional aspects as the correct sizing of the actuation unit, reliability of the structure, maintainability of the assembly, modularity of the system, energy autonomy, cost and safety. Moreover, such requirements become stricter if from laboratory setting, lower limb exoskeletons have to be effective in real scenarios. Always the main challenge is to define the best trade-off between all the characteristics of a product. Indeed, often during the design process of a system, in order to improve one of its aspects, another feature is penalized.

Aligned with the contribution of this thesis, in the following sections a review of knee exoskeleton systems that have been proposed so far with respect to their ergonomics is given.

2.1.1 Ergonomics

As wearable devices, lower limb exoskeletons need to be ergonomic [26]. Different design aspects define the overall ergonomics of such systems. An exoskeleton will be more ergonomic if: its movements are harmonized with the motion of the assisted user's joint [27]; its structure has low mass and inertia; during assistive phases, its physical interaction with the user is comfortable.

If such requirements are not achieved, the usage of these systems can became early uncomfortable or even painful and dangerous, limiting their use to short periods of operation [28].

2.1.1.1 Kinematics

Exoskeletons need to exhibit proper kinematics to fully follow the motions of the assisted joint. To this end, such devices should be designed with the same DoF of the assisted joint. If this is not taken into consideration, the user will be constrained in his motion and the device will be perceived with reduced ergonomics. In lower limb exoskeletons this also represents a safety issue since a reduced mobility of the user's lower limbs negatively influence his self-balancing capability [27]. Due to the human body complexity, a full kinematic coupling is not a trivial objective to achieve for many of the human joints. Their functionality is always the result of multiple passive and active DoF (rotations and translations) between the articulated links. For instance, as proposed by [29] and also suggested by the International Society of Biomechanics [30], the human knee should be modelled as a 6-DoF system, see Fig. 2. Even if, the knee is a joint with a single principal DoF (flexion/extension), it is not a simple revolute joint, but it should be modelled as a condyloid hinge joint. Indeed, due to the limbs' shape, the joint surface shape and the functionality of the ligaments, it also allows for the internal/external and the abduction/adduction rotation of the tibia with respect to the thigh. Moreover, during the flexion/extension movements, the tibia roll and slide against the femur generating the translation of the Instantaneous Centre of

Rotation (ICR). Such a translation mainly occurs on the sagittal plane, refer to XY plane in Fig. 2.

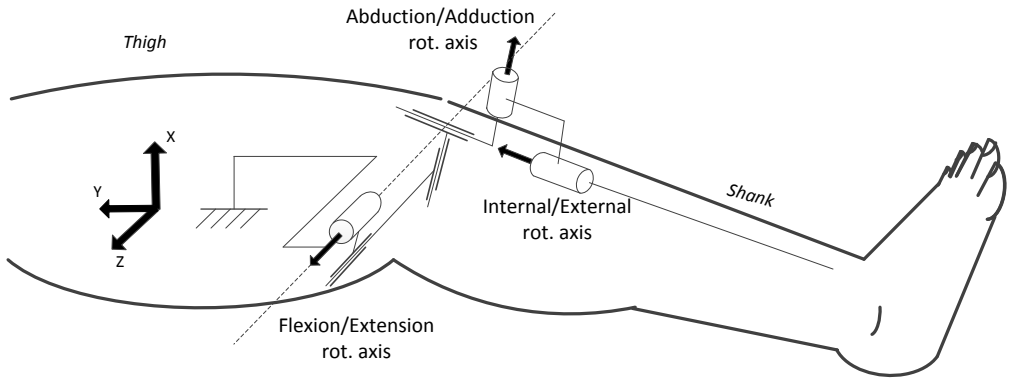

Fig. 2 – The human knee and its kinematics model, adapted from [29].

Nevertheless, lower limb exoskeletons often adopt oversimplified kinematic models of the human joints. This occurs due to limited considerations of the human anatomy and kinesiology or due to design choices that focus more on the reduction of the structure mass, inertia and complexity.

As far as knee exoskeleton devices are concerned, several systems have been proposed over time with an increasing effort to move from exoskeletons that model the knee as a simple revolute joint, to platforms that take into account also its polycentric motion (i.e. 3 DoFs knee exoskeletons) and to devices that take into account the full knee complexity (i.e. 6 DoFs knee exoskeletons).

Among the lower limb exoskeletons described in Section 1.1, systems that model the human knee as a single DoF joint are: the rehabilitate exoskeletons Lokomat [3] and LOPES [4]; the assistive exoskeletons HAL 5 [7], ReWalk [11], Ekso [12],[13], the 10 DoFs full-body exoskeleton presented in [31, 32], the 1 DoF knee exoskeleton proposed in [33],[34] refer to Fig. 3.a.; as well as the power augmentation exoskeletons BLEEX [17],[18], XOS 2 [19] and HULC [20].

Among the exoskeletons that model the knee as a 3 DoF joint, taking into account also the translation in the sagittal plane of the axis of the flexion/extension rotation, further distinction can be done. Indeed, the translation of the axis of the flexion/extension rotation can be accommodated imposing a fixed path based on

statistical studies on the morphology of the human knee, or designing devices able to passively follow the translation of the axis. Examples of the first category are: the AlterG Bionic Leg robot [9], [10], refer to Fig. 3.b; the 3 DoF knee exoskeleton based on a polycentric four-bar linkage actuated by a rotary actuation unit presented in [15]; and the 3 DoF knee exoskeleton based on a polycentric four-bar driven by a linear actuator placed on the user's thigh [16]. Finally, to the best of the author's knowledge, the AssistOn-Knee exoskeleton represents the only 3 DoFs knee exoskeleton that is able to accommodate (i.e. passively follow) the translation of ICR of the user's knee on the sagittal plane [6]. This is achieved thanks to the adoption of a Schmidt coupling.

The only knee exoskeleton with 6 DoFs developed so far was presented in [14] , refer to Fig. 3.c. This device assists the flexion/extension motion, while the internal/external and the abduction/adduction rotations are accommodated. However, due to its mechanical complexity, the device is heavy and bulky.

(a) (b) (c)

Fig. 3– (a) a knee exoskeleton with 1 DoF is depicted. (b) the AlterG Bionic Leg robot that models the knee as a 3 DoFs joint is shown. (c) a 6 DoFs knee exoskeleton is depicted.

2.1.1.2 Joint misalignment

Another important aspect in the ergonomics of exoskeletons is the problem known in literature as “the human-robot axes misalignment” [5, 28, 35]. Indeed, normally, exoskeletons assist the joints’ rotation with a mismatch between the location of their axis of rotation with respect to the axis of rotation of the assisted joint. This is due to multiple reasons: the complexity of the human kinematics that cannot be modeled as simple collections of kinematic pairs; the difficulty in knowing precisely the configuration of the human joints if special image equipment is not utilized; and the natural variability in exoskeleton placement with respect to the human limbs. Misalignments of joint axes cause undesirable internal reaction forces on the corresponding human joints and at the mounting locations. Such parasitic forces produce discomfort, pain or even injury. Important axis misalignments can also force compensatory movements of the assisted joint, drastically decreasing the ergonomics of the devices. To solve this problem, exoskeletons with the so called self-aligning mechanism have been proposed. In the design of these structures, the revolute joint that provides assistance (i.e. the actuated DoF or active DoF) has its rotation decoupled by its translations. In the case of knee exoskeletons with 3 DoF self-aligning mechanisms, the flexion/extension motion will be assisted while the translation of the axis defining the flexion/extension rotation of the knee will be accommodated/follow by the 2 passive DoF.

To the best of the author’s knowledge, currently three are the exoskeletons that show self-aligning property: the LIMPACT exoskeleton [36] with an under actuated 3 DoFs self-aligning mechanism for the elbow joint; the AssistOn-Knee [6] with an under actuated 3 DoFs self-aligning mechanism for the knee joint; and the NEUROExos [5], an elbow exoskeleton with an under actuated 4 DoFs self-aligning mechanism. In the case of the LIMPACT exoskeleton, the two passive DoFs are realized with the adoption of two parallelogram mechanisms, while in the AssistOn-Knee through a Schmidt coupling. Finally, in the NEUROExos the 3 passive DoFs are

added to the structure through a sophisticated closed chain composed by 13 passive joints: 4 prismatic, 4 spherical, 2 circular sliders, 2 universal and 1 rotational joint.

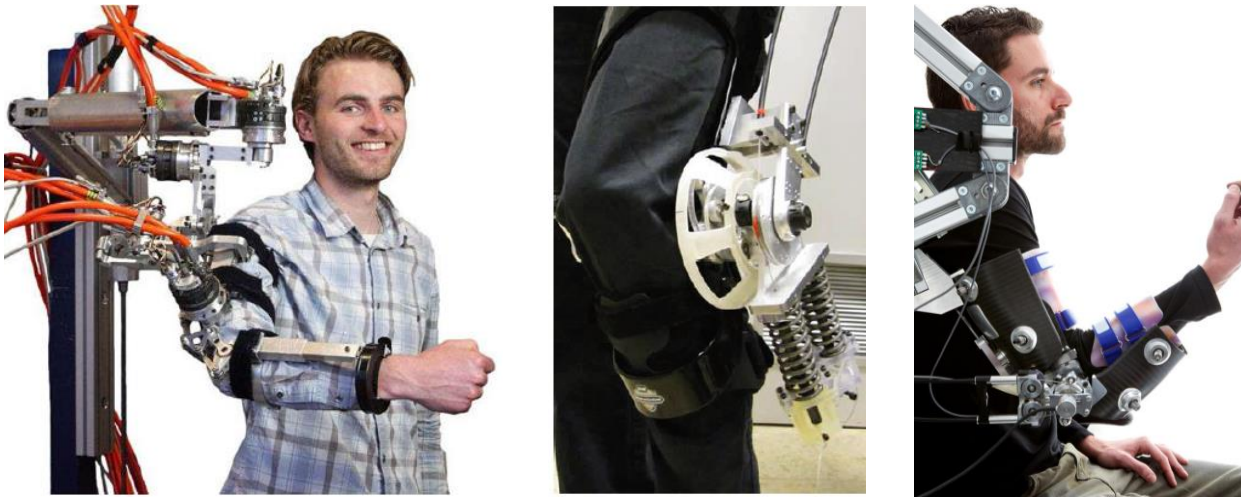

(a) (b) (c)

Fig. 4– (a) the LIMPACT exoskeleton. (b) the the AssistOn-Knee. (c) NEUROExos.

Finally, exoskeletons with self-aligning property are also self-adjustable to different users thanks to their passive DoFs implemented. They automatically adjust themselves to different users' anatomy, such as limb girth, bone shape, joint orientation and length of limbs. This feature reduces the mounting and setup time required by such systems, improving their wearability.

2.1.1.3 Structure

Mass and inertia are also fundamental aspects that contribute to determine the overall ergonomics of exoskeletons. Indeed, heavy and bulky devices may be difficult to wear and to keep them in place. They might also not be acceptable from an aesthetic point of view. In addition to this, they may cause a decrement of the overall agility of the user, not letting the user access narrow spaces and finally they might become counterproductive with respect to a reduction of the total effort produced by the user to complete a generic task.

Active soft orthotics represent an alternative to rigid exoskeletons [37]. These devices, composed by soft materials, can provide a significant improvement to the wearability and ergonomics of exoskeleton devices. They can be significantly lighter and compact than rigid exoskeletons. Due to their flexible frame, soft exoskeletons are fully kinematic coupled with the user, overcoming the joints misalignment problem. On the other hand, they cannot provide high level of assistance since high pressure on the user's skin would become uncomfortable. Moreover, since soft exoskeletons use unidirectional linear actuators (e.g. pneumatic actuators), the number of actuation units that are necessary to assist the same number of DoF assisted by a rigid exoskeleton powered by rotary motors, is doubled. This aspect and the flexible nature of their structure make the control of soft exoskeletons complex, especially when a torque trajectory has to be followed. Finally, because of their flexible nature, these wearable suits cannot be used to design load-carrying augmentation exoskeletons.

A representative device of this category is a bio-inspired active soft orthotic device for ankle foot pathologies presented in [37] (refer to Fig. 5.a). In this system, three artificial muscles aim to mimic the muscle-tendon-ligament structure in order to assist the dorsiflexion as well as inversion and eversion of the user's ankle. In [38], a soft lower-extremity robotic exosuit actuated by pneumatic actuators is presented, refer to Fig. 5.b. This device assists the flexion/extension motion of the leg joints. Finally, a soft cable-driven exosuit that can generate assistance at the hip and ankle joints in the sagittal plane is presented in [39], as depicted in Fig. 5.c.

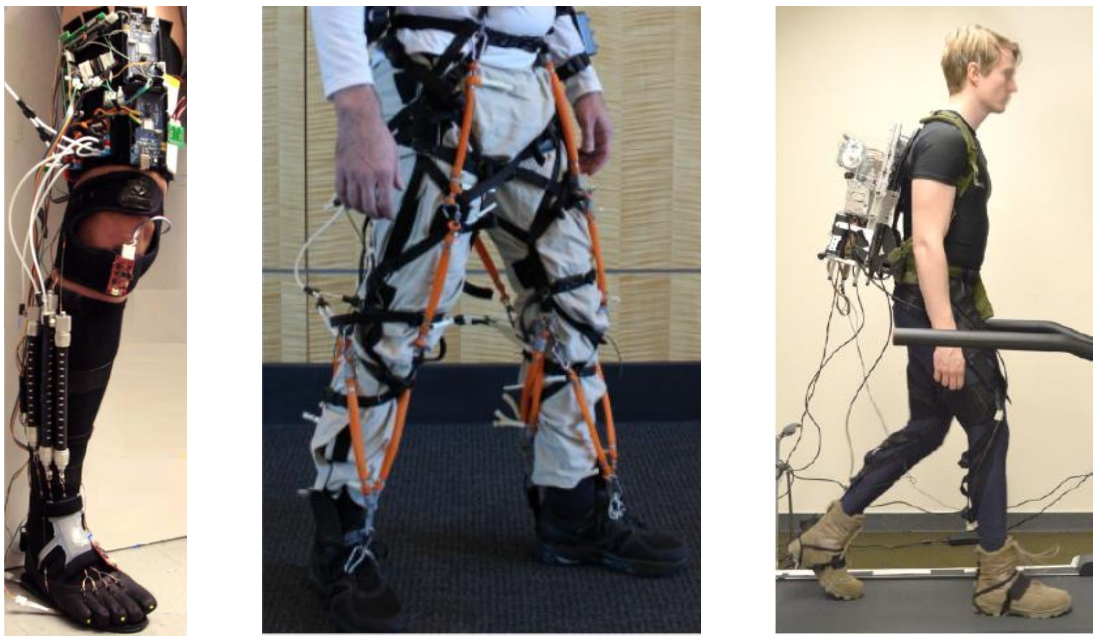

(a) (b) (c)

Fig. 5– (a) a bio-inspired active soft orthotic device for ankle foot pathologies. (b) a soft lower-extremity robotic exosuit to provide assistance at the leg joints. (c) a soft cable-driven exosuit that generates assistance at the hip and ankle joints.

2.1.1.4 Interaction

Physical Human-Robot interaction (pHRi) has a big impact on the exoskeletons' ergonomics. Assistance is transmitted by exoskeletons to the users' body through interaction forces between the exoskeletons' attachments and the users' skin. To improve the devices' ergonomics, exoskeletons should reduce the stress generated on the users' skin while the required assistance is delivered [5]. Indeed, pressure and friction forces deform tissues with the possibility to induce early uncomfortable or even painful and dangerous pHRi. This aspect is even more crucial if long tasks need to be performed wearing exoskeletons.

To reduce, on the user's skin, friction forces generated by the exoskeletons' actions, from devices that act on the assisted body segments generating a single force, refer to Fig. 6.a and Fig. 6.b, research is moving toward systems that transmit pure torque along with their mechanism, refer to Fig. 6.c. Systems as LIMPACT, indeed, interact

with the user, generating pairwise forces acting only perpendicularly with respect to the users' bones axis [35]. To generate such pairwise forces, this type of exoskeletons requests two attachment points for each assisted body segment. Nevertheless, due to space limitation, this additional cuff may represent a disadvantage for the proper attachment of this type of mechanism on small body segments.

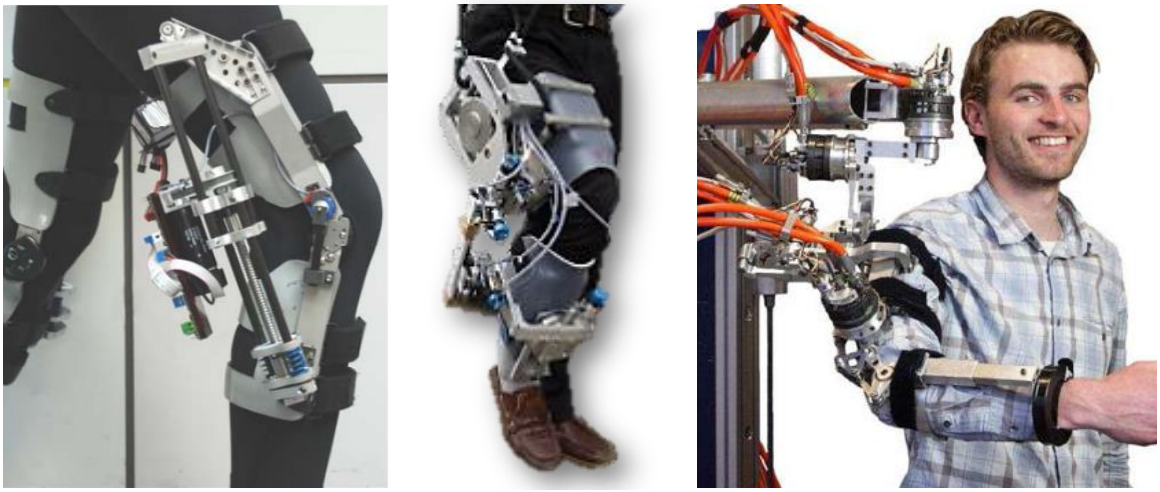

(a) (b) (c)

Fig. 6– In (a) and (b) knee exoskeletons that engage the user's shank with a single attachment area. In (c) LIMPACT, an elbow exoskeleton that interacts with the user's forearm with two cuff.

2.2 Control Strategies of Lower Limb Exoskeletons

Exoskeletons are wearable systems that must provide mechanical assistant to the users' synchronously with their intentions. In particular, appropriate sensing systems should be able to monitor the users' state while control systems should interpret their intentions and properly modulate the assistance of exoskeletons based on such information. These aspects are even more crucial if lower limb exoskeletons move from laboratory settings to daily life scenarios. From a control point of view, indeed, unknown environments require strategies that cope with irregular and noncyclic locomotion (e.g. walking in a crowd or standing and shuffling), unexpected ground conditions (e.g. walking on rough terrain), as well as interactions of the user with the surroundings (e.g. lifting, pulling and pushing task) [21]. Therefore, information like the user's state (i.e. position, orientation, velocity and acceleration of each body segments), user-exoskeleton interaction, user-environment interaction and the ability to predict and detect the user's intentions are fundamental. At the same time, especially in outdoor scenarios, the objective of rich sensory information must coexist with that of compactness, high degree of portability, reliability and ergonomy; for the exoskeleton itself and for the associated sensing systems [21].

In the context of assistive strategies for elderly or healthy subjects various assistive strategies have been adopted so far. As suggested by [40], exoskeleton controllers can be classified based on the strategy used to estimate the user's joint effort: between controllers adopting muscle model approaches or body model methods. In the first group, as described in [41] and [42], the user's effort is measured by monitoring the muscle activity through EMG sensors once a human muscle model has been developed. In [43] an EMG based method, taking into account also the variability of human joints impedance, is presented. Nevertheless, outside laboratory settings, extract meaningful and precise data form the EMG signals could not be always easy to

acquire due to placement and calibration of the EMG electrodes, noise, muscle fatigue and also by natural muscular variability [44].

Among the human-exoskeleton model-based controllers, as suggested by [21], a further distinction can be adopted: controllers dependent by gait phase or controllers independent by gait events. A well know example of strategies not phase dependent is the one proposed to control BLEEX [45], a lower limb exoskeleton developed by the University of California. Thanks to the measurement of the ground reaction forces (GRF) and the measurement from the exoskeleton itself (i.e. motor position velocity and torque), BLEEX helps the user to carry his backpack, while at the same time keeping constantly zero the Human-Robot interaction (HRi) forces [46]. Such a method, called Sensitivity amplification control (SAC), has the particularity to not use direct force measurement coming from the HRi. Indeed, the HRi forces are considered as disturbance from a control point of view. The torques, that BLEEX has to generate to carry the user's backpack are estimated based on an inverse dynamic method applied to a model that accurate reconstructs the exoskeleton where its state information is used as input.

The lower limb exoskeleton proposed by Honda [47] and the RoboKnee exoskeleton [48], instead, aim to support both the weight of the user itself and of any carried payload. While the first device assists the user's walking, RoboKnee helps the user to climb stairs and perform deep knee bends while also carrying a load in a backpack. Both systems are implemented with a control architecture that uses only the measurement of the ground reaction force (GRF).

In [22] and [49] the effort at the leg joints for sit to stand tasks is estimated monitoring the body's posture through an optical tracking system. Then, using a lumped mass model of the human body, the muscles' activity is estimated. Such an approach could be suitable for clinic scenario, where, in dedicated indoor ambient, patients that have to retraining own muscles needs a sensing system less invasive as possible to wear. On the other hand, in outdoor scenario, such a strategy is hard to adopt due to the low portability of the required instrumentation (camera system), the calibration procedure and the possible shift or detachment of the markers form the

user. Moreover, in the case of load handling, with the proposed method it is necessary to know in advance the mass and the location of the center of mass (CoM) of the load during the task in order to incorporate this information in the human model for the joint torque estimation.

In [50] and [51], instead, control strategies based on a disturbance observer, which estimate respectively the torques produced by elbow and knee joint, are presented. These approaches rely on an initial accurate identification and compensation of the disturbance torques (stiction, viscous friction, and gravitational loads) at the joint level. In this manner any additional torques' input can be detected and compensated via feedforward loops without the need for torque sensor.

On the other hand, in the predefined action based on gait patter, the assistive strategies implemented in the lower limb exoskeletons act synchronously with expected gait events; as an example, in [52] the pneumatic actuators change the inner pressure depending on swing or stance phase of the assisted limb. The gait events are detected with insole sensors. In [39], a soft cable-driven Exosuit is presented, where Bowden cables are driven by geared motors to pull the suit in proximity of the ankle joint and assist its propulsion. The control regulates the position trajectory of the cable as function of the gait percentage. Finally, in [53] the MIT Exoskeleton for load-carrying augmentation is presented, where in order to assist more synchronously the gait motion, control strategies based on a state machine implementation have been realized. Using position information and/or ground-exoskeleton force sensing, each different phase of the gait can be detected and, according to human walking data, the most appropriate assistance profile can be delivered.

3 THE iT-KNEE BIPEDAL SYSTEM: HARDWARE SETUP

3.1 Introduction

This chapter describes the hardware setup of the iT-Knee Bipedal System, refer to Fig. 7. The exoskeleton system assists the flexion/extension of the human knees. Its purpose is to support elderly people in daily tasks (i.e. walking, sit to stand task, climbing a stair) and to improve the strength and/or the endurance of healthy subjects (i.e. workers or militaries) with an improved ergonomics. As Fig. 7 shows, from an hardware point of view the iT-Knee Bipedal System is composed by:

- two iT-Knee exoskeletons that generate the mechanical assistance to the knees.
- two iT-Shoes that monitor the feet's orientation and the full contact wrench between the user and the ground.

In future, thanks to its modular design, the iT-Knee exoskeleton could form the primitive block of a full body exoskeleton system.

The rest of this chapter is structured as follows: section 3.2 describes features, kinematic model, mechanical components and mechanical requirements of the iT-Knee exoskeleton. Section 3.3 discusses the proposed sensorized add-on system for shoes. In particular, the mechanical and sensing requirements of the iT-Shoes and the two prototypes so far developed are addressed. Finally, section 3.4 describes the architecture of the iT-Knee Bipedal System.

Experiments conducted to validate the iT-Knee exoskeleton and the iT-Shoes and to test them in the context of the iT-Knee Bipedal System are reported in chapter 5.

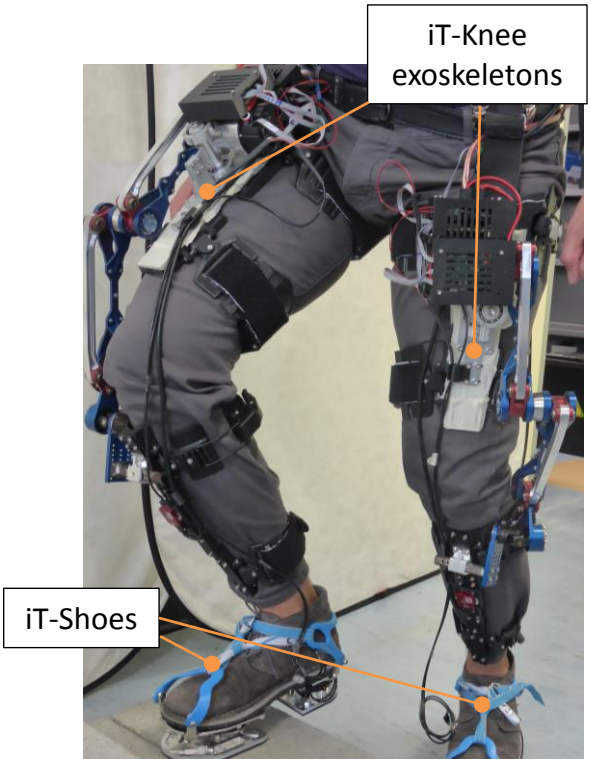

Fig. 7– The iT-Knee Bipedal System and its main components: the iT-Knee exoskeletons and the iT-Shoes.

3.2 iT-Knee exoskeleton

As introduced in Chapter 2, the design of effective exoskeletons represents a highly challenging task. Ideally these systems should be easy to wear, ergonomic while providing assistance, safe, portable, attractive from an aesthetic point of view and they should not limit the user's mobility. According to these requirements, the design of the iT-Knee exoskeleton was based on the following concepts:

- the exoskeleton should accommodate all the motions of the knee joint.
- the exoskeleton should have the same range of motion as the human knee.

- the system should be lightweight and compact in order to be portable and easy to wear.
- the iT-Knee exoskeleton should be suitable for different user sizes.
- the exoskeleton should be compact on the lateral side of the user's leg therefore it should be developed also on the front side of user's leg.
- the iT-Knee exoskeleton should be modular to result the primitive block of a full body exoskeleton system.
- the iT-Knee exoskeleton should satisfy the power and structural requirements for completing standing-up, sitting-down, walking, and stair climbing tasks.

The design of a knee exoskeleton, that satisfies the aforementioned requirements, was one of the main objective of this thesis. To this end, the effort was focused on the design of a novel mechanism able to provide the required assistance to the knee with an improved ergonomics, resulting, at the same time, fully kinematic coupled with the joint, adjustable to different user's size, compact and light as possible.

The design requirements of the iT-Knee exoskeleton span across performance and ergonomic specifications that were satisfied with the appropriate selection of the system kinematics and range of motion as well as by its structural components and its actuation unit. Specifically, the structural and kinematic requirements of the iT-Knee mechanism were based on the knee biomechanical data obtained from the literature. In particular, the structural design of the iT-Knee mechanism was defined by a balancing of the maximum torque output and an overall effort to reduce the form factor of the system and increase its wearability and its power to weight ratio. The actuation unit of the iT-Knee exoskeleton was selected to fulfil the requirements of a standard walking task in terms of peak velocity and peak torque. This choice was also made as a trade-off between the actuation unit's performance, dimensions and weight. The maximization of the range of motion of the structure as well as the optimization of the structure form factor were the result of an iterative design process. FEA analyses were employed for all structural components, while additive printing technology allowed

the evaluation of several different versions of the mechanism until the functional requirements were achieved.

3.2.1 Features

The core of the iT-Knee Bipedal System is the iT-Knee exoskeleton. The iT-Knee exoskeleton, refer to Fig. 8, is a modular knee exoskeleton that ergonomically assist the knee flexion/extension motion.

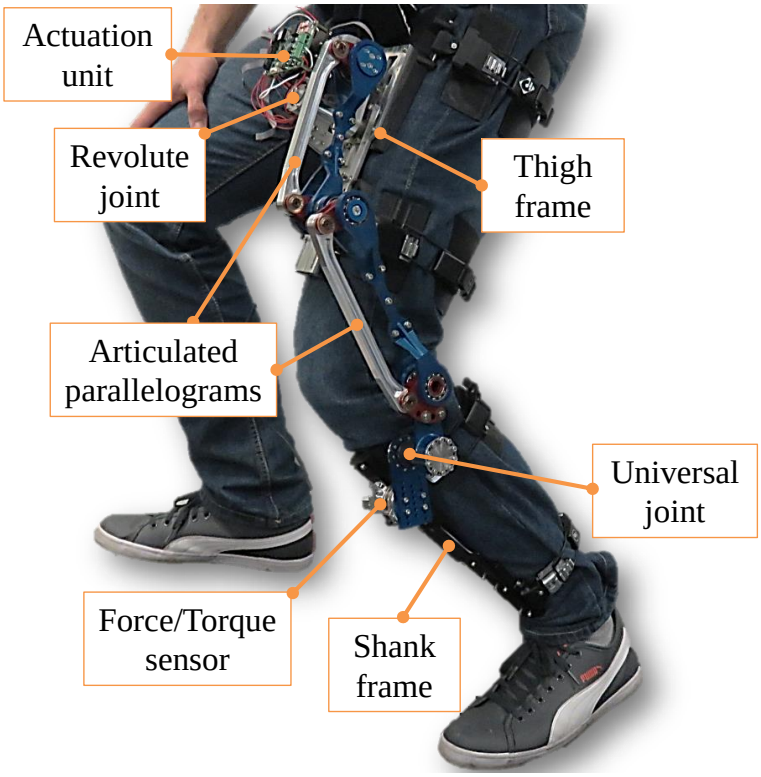

Fig. 8– The developed iT-Knee device mounted on a human leg.

It consists of an under-actuated 6 DoFs self-aligning exoskeleton mechanism. It has 1 active DoF to assist the flexion/extension movement of the knee and 5 passive DoFs to passively accommodates: the translations in the sagittal plane and in its orthogonal direction of the instantaneous center of rotation (ICR) of the flexion/extension movement for the knee joint; the knee abduction/adduction rotation; and the internal/external rotation motions of the knee. It has a range of motion (RoM) of 120°

on the flexion/extension motion of the knee. Thanks to its 6 DoFs, the iT-Knee exoskeleton does not impose any motion constrain to the user. This is an important feature especially in lower limb exoskeletons where a reduction of the mobility imply a minor capability of the user of balancing himself and then a reduced safety of the device.

Thanks to the self-aligning property of the mechanism, the iT-Knee exoskeleton overcomes problems generating by misalignments between the flexion/extension axis of rotation of the knee joint and of the exoskeleton. As consequence no undesirable reaction forces on the assisted human joints and at the mounting locations are generated.

Moreover, the self-aligning property allows iT-Knee to automatically adapt itself to different users' anatomy. No manual and time consuming adjustments are necessary to fit the iT-Knee exoskeleton with respect to users' anatomical different such as limb girth, bone shape and joint orientation.

In addition the iT-Knee transmits pure torque along with its mechanism. As advantage, no sliding motions between the user's leg skin and the attachments of the exoskeleton are generated when iT-Knee exoskeleton is providing assistance since pairwise forces always acting perpendicular to the bones axis are generated. This aspect is crucial if long tasks want to be performed with exoskeletons. Indeed, undesired interaction can induce early uncomfortable or even painful and dangerous situation.

Finally, iT-Knee targets an overall compact design with low mass/inertia and a small form factor. The mass of each iT-Knee exoskeleton is 3.75 kg, which can be supported without causing significant burden. Special attention has been put on the thigh area, favoring a frontal over the more classical lateral implementation/mounting of the actuation and transmission mechanisms, as seen in the majority of the existing devices. This feature could also make the iT-Knee suitable for wheelchair users since the mainly frontal implementation of the system would be less likely to cause mechanical obstructions.

3.2.2 Mechanism

The mechanism of the iT-Knee and its kinematic representation are shown in Fig. 9. The mechanism of the iT-knee, refer to Fig. 9.a, is composed by: the thigh attachment; a revolute joint grounded on the thigh attachment of the exoskeleton with its rotation axis orthogonal to the plane of the attachment; an actuator frame rigidly linked with the revolute joint that passively rotates around it; an actuator, fixed on its frame; a series of two articulated parallelograms mechanism (S2AP), that transmits the torque generated by the actuator, to the shank attachment through an universal joint interposition.

The S2AP mechanism is a cascade of two articulated parallelograms, where the B pulley, Fig. 9.a, is coaxial and rigidly coupled with the C one, while the A pulley is directly linked with the actuation unit. The A and D pulleys represent respectively the input and output of the S2AP mechanism. As [35] introduced, the main feature of these type of mechanisms is to decouple the relative rotation between the input joint and the output joint with respect to their translations. Moreover, since in iT-Knee the A pulley is connected to the actuation unit, the D pulley can independently translate with respect to the A pulley while is providing torque. As consequence, the iT-Knee exoskeleton results self-aligning with respect to the axis of the knee flexion/extension motion. Indeed iT-Knee exoskeleton can assist the knee flexion/extension motion, while passively following the translation of the axis defining this movement. As result, undesired forces, due to misalignment between the knee rotation axis and the exoskeleton, are prevented. Moreover, since the iT-Knee mechanism transmits pure torque to the user's thigh and the shank, as [35] underlines, on the involved body segments the pure torque is felt only as pairwise forces acting perpendicular to the axis of the bones. As result, any sliding forces between the iT-knee attachments and the user' skin are generated.

Finally, since these two cascaded 4-bar mechanisms are parallelograms the rotation of the actuator is transmitted from the motor output (pulley A) to the output (pulley D) with a ratio of 1:1 in the entire RoM. If less than 180° of flexion extension is required,

as it is the case for the flexion/extension RoM of the human knee, the S2AP mechanism is able to transmit the torque in a more rigid and compact way compared to the transmission chain propose in [14].

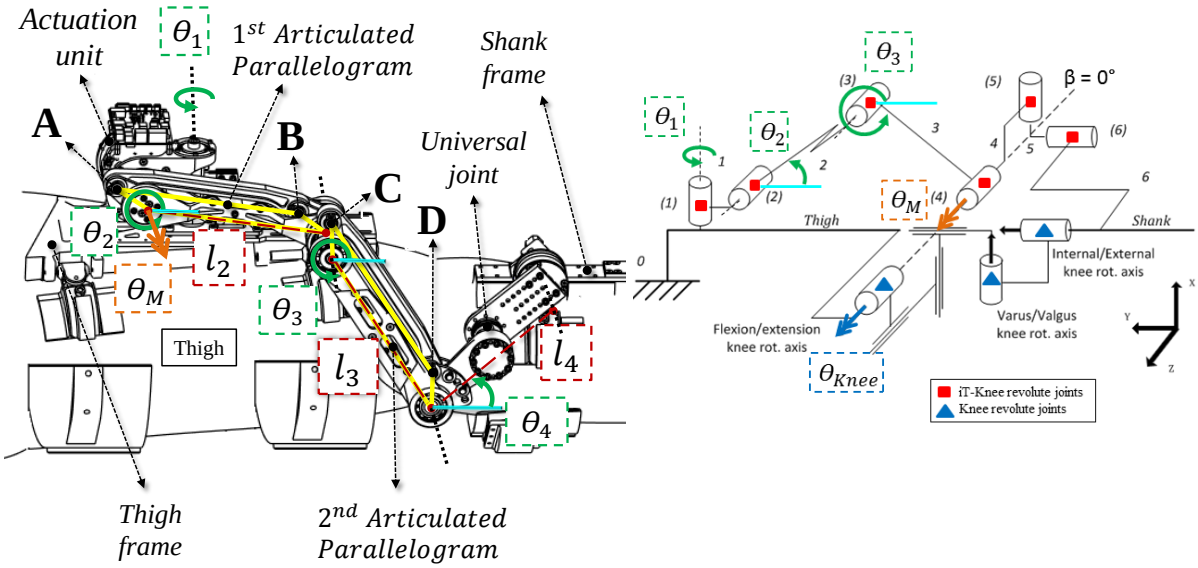

(a) (b)

Fig. 9– In (a) the iT-Knee exoskeleton showing the main mechanical components of the device; in (b), its kinematic representation (red revolute joints) mounted on the human knee kinematic model (blue revolute joints) with an ideal match between the human and exoskeleton flexion/extension rotation axis.

3.2.3 Kinematic model

As shown in Fig. 9.b, the iT-Knee is composed of 7 links and 6 revolute joints forming a 6-DoF mechanism. Using the Grübler formula, the number of parameters necessary and sufficient to univocally define the mechanism configuration(F), is evaluated as follow:

$$F = \lambda(l-1) - \sum_{i=1}^{j}(\lambda - f_i) \quad (1)$$

Where λ is the mobility number, equal to 6, l is the link number with frame included, and f_i defines numerically the DoF of the elementary joints. iT-Knee exoskeleton has only 1 DoF active, the one responsible for the flexion/extension

motion of the knee, i.e. joint (4). The other 5 DoFs are passive and they accommodate all the other motions of the knee. Since Fig. 9.b is a kinematic representation of iT-Knee mechanism, the S2AP mechanism is not directly presented in this figure. Nevertheless, joint (2), (3) and (4) represent the DoFs introduced by the S2AP mechanism. Finally, the S2AP mechanism allows transmitting torque to joint (4) by placing the actuator on joint (2) on the thigh. This reduces the perceived inertia as the effect of the actuator mass is lower during motions of the leg.

The translations of the knee are accommodated by joints (1),(2), and (3), and they are described by the following equations:

$$\begin{cases} X_4 = -l_{1_z} \sin\theta_1 + (l_{1_x} + l_2 \cos\theta_2 + l_3 \cos\theta_3) cos\theta_1 \\ Y_4 = l_2 \sin\theta_2 + l_3 \sin\theta_3 \\ Z_4 = -l_{1_z} \cos\theta_1 - (l_{1_x} + l_2 \cos\theta_2 + l_3 \cos\theta_3) sin\theta_1 \end{cases} \quad (2)$$

Where X4, Y4 and Z4 are the translations of the joint (4) with respect to the leg frame XYZ; θ_1, $\theta_2$and θ_3 represent respectively the rotation of the joint (1), (2) and (3) with respect to their principal axis; l_1,l_2 and l_3 are the distance respectively between joints (1)-(2), (2)-(3) and (3)-(4). In particular l_{1_x} and l_{1_z} are the components of l_1 with respect to the leg frame when θ_1 is zero. The abduction/adduction and the internal/external knee rotations are accommodated by the revolute joint (1) and by a universal joint represented by joint (5) and (6), see Fig. 9. The effect of this set of joints can be also seen in Fig. 11 where the iT-knee is shown to be able to follow a mechanical human leg replica, that will better introduced in Section 5.2.

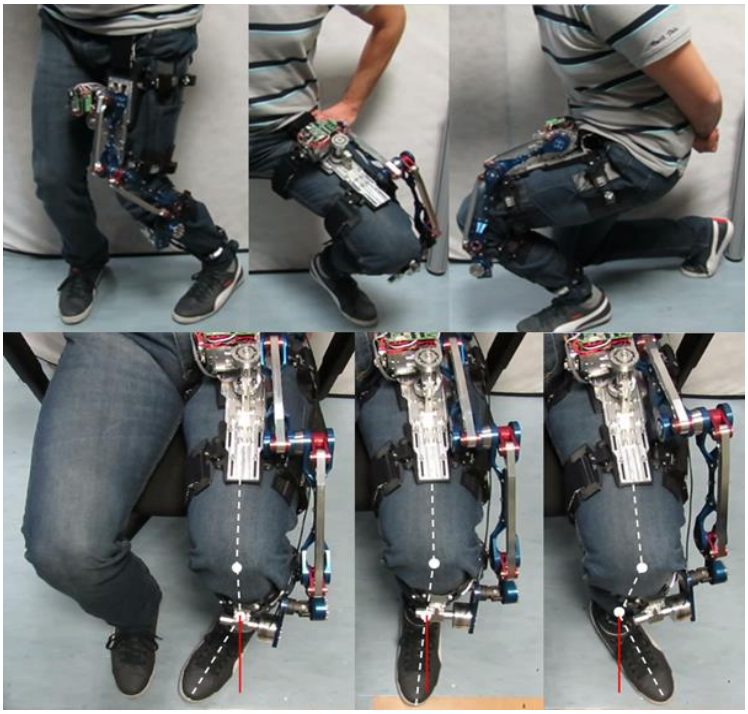

Fig. 10 – The mobility of the iT-Knee exoskeleton provides wide range of motion while accommodating all knee motions and potential misalignments of the device against the human knee.

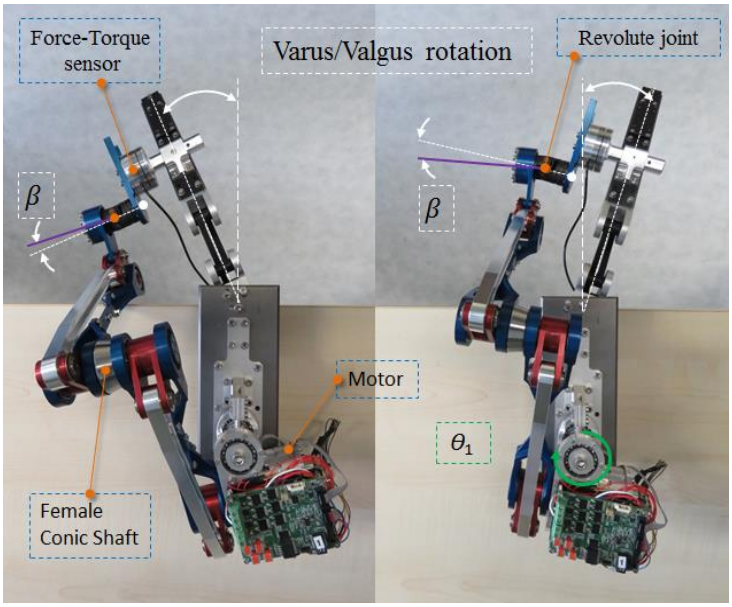

Fig. 11 – The revolute and universal joints arrangement permitting the varus/valgus, the internal/external knee rotations and the perpendicular translation with respect to the sagittal plane of ICR.

Finally, due to the universal joint, the output rotation (i.e. θ_{Knee}) and velocity as well as the transmission ratio are affected by the inclination between the rotation axis of θ_{M} angle and θ_{Knee} one (i.e. β angle), see Fig. 9.b and Fig. 11:

$$\tan\theta_{\text{Knee}} = \cos\beta \tan\theta_{\text{M}}$$

$$\dot{\theta}_{Knee} = \frac{\cos\beta(1+\tan^2\theta_M)}{(1+\tan^2\theta_{Knee})}\dot{\theta}_{\text{M}} \quad (3)$$

$$t_{\text{r}} = \dot{\theta}_{Knee}/\dot{\theta}_{\text{M}}$$

Nevertheless, the universal joint influence on the iT-Knee system can be reasonable omitted. Indeed, a universal joint, performing a rotation of 130° with a fix value of 15° for the β angle, generates a temporary maximum angular displacement between the input and output rotation of less than one degree, with a transmission ratio medium value of 0,988 and a maximum difference from the unit value of 3,4%.

3.2.4 Range of Motion

As shown in Fig. 9.a, the S2AP transmission mechanism is a cascade of two articulated parallelograms connected at a common point (joint (3)) through the fastening of pulleys B and C. Each articulated parallelogram has been designed to have a range of motion (RoM) of 130°. Nevertheless, the RoM of the S2AP will be equivalent to the RoM of each single articulated parallelogram only if in its initial configuration: the two articulated parallelogram that define the S2AP are aligned (i.e. $\gamma = 0°$, refer to Fig. 12.a) and the B and C pulleys have the same orientation (i.e. $\varphi = 0°$, refer to Fig. 12.a); or if the two articulated parallelogram that define the S2AP are not aligned, defining an angle γ different from zero, and the B and C pulleys have a relative angular offset (φ) equal to γ, refer to Fig. 12.a. If one of these two conditions are not verified the S2AP will have a RoM smaller than the RoM of the single articulated parallelograms. In particular, if in the initial configuration, the two articulated parallelograms that define the S2AP are aligned but the B and C pulleys

have an angular offset of φ, the RoM of the S2AP will be equivalent to the RoM of the single articulated parallelograms minus the φ value; or, if in the initial configuration, the two articulated parallelogram that define the S2AP are not aligned, defining an angle (γ), and the B and C pulleys have a relative angular offset (φ) different from γ, the RoM of the S2AP will be equivalent to the RoM of the single articulated parallelograms minus the difference between φ and γ angles.

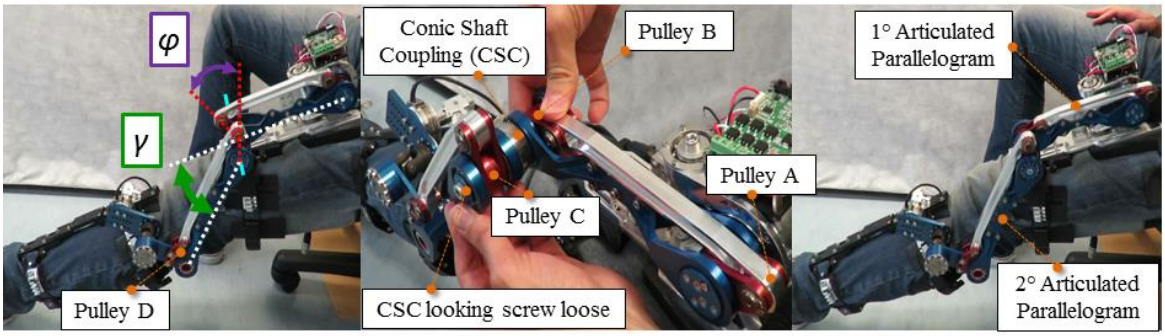

(a) (b) (c)

Fig. 12 – In (a) the iT-Knee mechanism unadjusted is shown, with the S2AP mechanism with limited total RoM. In (b) the adjustment phase is highlight, with the CSC looking screw unlocked and B pulley adjusted for RoM_1 and RoM_2 alignment. In (c) the iT-Knee mechanism adjusted and locked is shown.

In the iT-Knee case, due to the human physical variability and the objective difficulty to place the exoskeleton's attachments always in the same location among trials, the initial distance between the thigh and shank mounting frames will be always different. As consequence, the initial configuration of the S2AP will be always different as well, especially with different values of γ , refer to Fig. 12.a. Then, in order to maximize the RoM of the iT-Knee exoskeleton, before to use it, the relative angular offset (φ) between the B and C pulleys should be always similar to γ, refer to Fig. 13. In the iT-Knee exoskeleton this is achieved thanks to the Adjustment for Range of Motion that consists of a Conical Shaft Coupling (CSC), which allows to set the fixed angle φ between pulley B and C, as the cross section in Fig. 13 depicts. This is done by releasing the locking mechanism and rotating the pulley B to set the angle φ, refer to Fig. 12.b. This routine is implemented when the user's knee is fully

extended so that the RoM of the S2AP is aligned with the RoM of the knee flexion/extension, see Fig. 12.c.

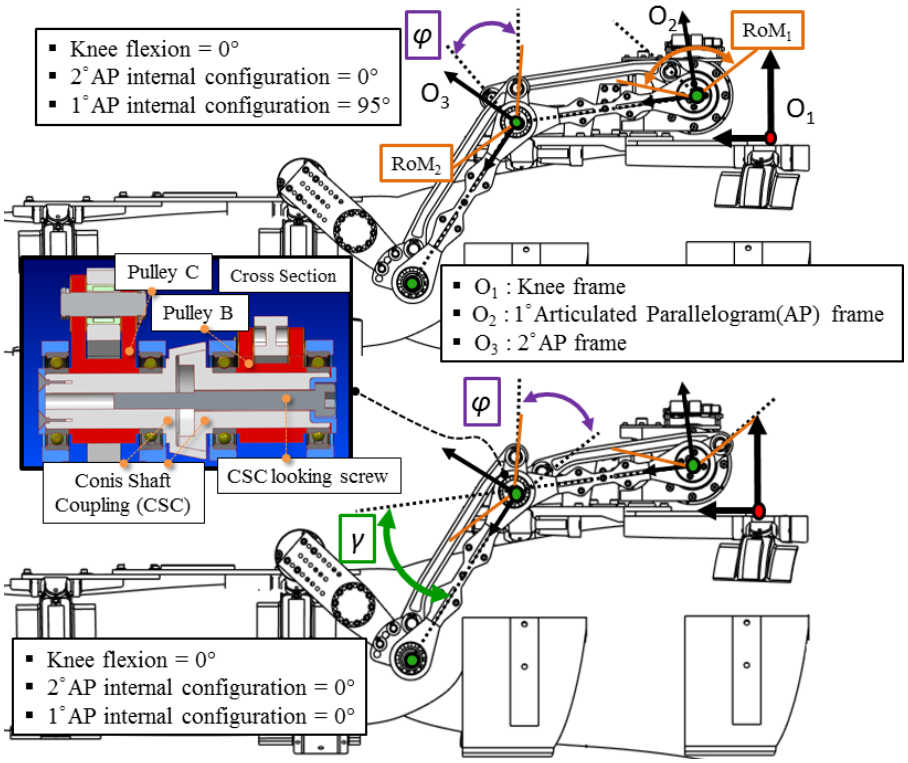

Fig. 13 – The iT-Knee 3D model mounted on a manikin. On the top and on the bottom are respectively shown the mechanism before and after the adjustment. The cross section highlight how this is mechanically achieved.

3.2.5 Torque-Force transmission

The mechanism of the iT-Knee is designed to support the load required on the knee joint of an average adult to stand up from a sitting position on a chair while the person is completely passive. According to [22] approximately a maximum peak torque of 100 Nm have to be provided to perform such task. Nevertheless, iT-Knee can transmit up to140 Nm, taking in account higher peak torques.

In an articulated parallelogram, the torques present on the input and the output joints are always equal, independently of the system configuration. Nevertheless, this is not true for the internal forces developed on the links of the mechanism, which are

dependent on the system configuration. Taking into account the maximum internal stress of the S2AP components, it is possible to define the maximum allowable torque that can be transmitted from the mechanism as a function of the knee flexion/extension angle, refer to Fig. 14. Finally, the mechanism of the iT-Knee, excluding the gearbox of the actuation unit, provides a constant transmission ratio of 1:1 along all its RoM.

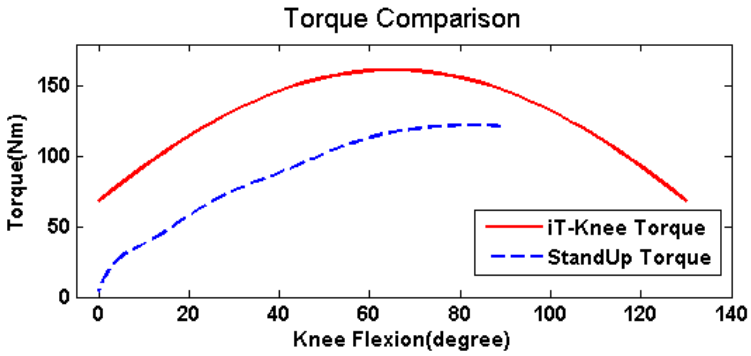

Fig. 14 – Red trend: Maximum transmissible torque from the iT-Knee mechanism during the flexion movement according to its maximum mechanical stress. Blue trend: Torque profile required at the knee joint of an average adult during a standing up motion from a sitting posture.

3.2.6 Actuation unit and sensory system

The iT-Knee is equipped with a series elastic actuation(SEA) unit, developed in [54] and [55]. This custom SEA is equipped with embedded electronics, position, torque and temperature sensors.

The actuator unit consists of a frameless brushless DC motor, a Harmonic Drive (HD CSD series) gearbox with reduction ratio of 80:1 and a flexible element (a torsion bar) that connects the output of the gearbox to the output flange of the actuator. This actuator can provide a continuous torque of 30Nm and an intermittent torque of 60Nm, while the output velocity can reach ~ 585 deg/s (10.2 rad/s) at the continuous maximum torque level. This actuation system permits the iT-Knee can follow the human gait at its natural speed of 1,37 m/s [56], with knee angular velocity peaks of

around 390 °/s [57], and it can also provide support for assistive tasks up to 60 Nm within its RoM.

The actuation module incorporates two high resolution (19 bit) position sensors for measurement of the flexion/extension movements of the knee and for torque measurement by monitoring the differential deflection of the series elastic element under load. The torsional stiffness of the actuator is 1000 Nm/rad, while its torque resolution provided by the 19bit differential deflection measurement is 12mNm. Embedded control is implemented on a 50MHz microcontroller which is communicating to a host master through a dedicated Ethernet 1kHz link for high level mode commands and for direct feed trajectories.

In addition to the embedded torque sensor the exoskeleton is equipped with an ATI 45mini force-torque sensor mounted at the output (shank mounting see Fig. 8 and Fig. 11). The purpose of this additional force/torque sensor is to monitor the forces and torques that are transmitted by the iT-Knee between the thigh and the shank, including the system's internal forces and torques.

3.3 iT-Shoes

This section focuses on the iT-Shoes. They represent the key components of the sensing system of the iT-Knee Bipedal System. They were realized to test the control strategy implemented on the iT-Knee Bipedal System, refer to Chapter 4. iT-Shoes were designed based on the following requirements:

- iT-Shoes should monitor the full contact wrench between the user's feet and the ground.
- the sensing system should track the orientation of the user's feet.
- iT-Shoes should allow natural walking therefore the plantar flexion of the feet have to be accommodated.
- iT-Shoes should be lightweight and compact.
- the sensing system should be adjustable to different foot size.

The design of a sensing system for shoes, that satisfies the aforementioned requirements, was one of the main objectives of this thesis. To achieve this, two different sensorized add-on systems for shoes were designed. In particular, the second prototype has a compact and light design, it is adjustable to different foot sizes and it monitors the feet's orientations as well as their interactions with the ground.

The two version of the iT-Shoes were designed to sustain a vertical load of 120 kg. This value was defined based on the weight of an average adult with the addition of a safety margin to account for possible payloads carried by the user.

3.3.1 Prototype 1

As Fig. 15 depicts, the first prototype version of the iT-Shoes [58] is composed of two aluminum plates with a footprint shape, which are connected to each other with a force/torque sensor. Their purpose is to monitor the interaction forces and torques applied between the ground and the user's feet. In particular, they provide information on how users distribute their weight on their feet and which amount of torque is provided by the ankle joint. The force/torque sensors are in-house developed semiconductor strain gauge sensors, model IIT-FT50. They have a force measurement range of Fx,y,z ±2000N and a torque measurement range of Txyz±40Nm. The measurement resolution is approximately 500mN and 20mNm for forces and torques respectively.

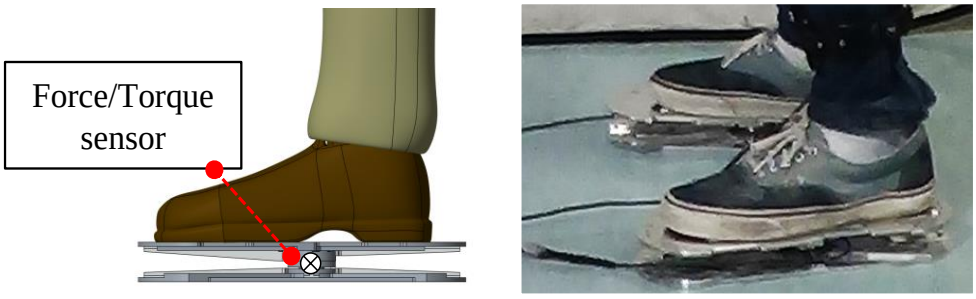

Fig. 15– The first iT-Shoe prototype. It is equipped with a 6 DoF Force/Torque sensor to monitor the interactions of the foot with the ground.

As Chapter 5 presents, several experiments were conducted with the first iT-Shoe prototype. Thanks to its simple design, the first version of the iT-Shoes allowed to obtain quick initial evaluations of the overall control system capability implemented in the iT-Knee Bipedal System, refer to Chapter 4. Subsequently, in order to perform more complex tasks the iT-Shoes were upgraded. The main reasons that determined an upgrade of this sensing system were the following:

- over no flat terrains, the first version of the iT-Shoes cannot properly reconstructs the interaction of the feet with the ground since the orientation of the feet is not monitored.
- the system does not allow for a natural walking since the feet plantar flexion is not accommodated.

Moreover, due to the above limitations and the overall design, if a plantar flexion motion is performed on the first iT-Shoe prototype, as Fig. 16 depicts, it is no possible to reconstruct the effort that the ankle is producing. Indeed, in the first version of the iT-Shoes the variation of the distance (*d*) between the ankle joint and the *z* axis of the force/torque sensor cannot be tracked. As consequence, the torque ankle (τ_{ankle}) cannot be computed properly since it is dependent by *d* as follow:

$$\tau_{ankle} = \tau_{GRT} + F_{\mathrm{gr}} d \qquad (4)$$

where τ_{GRT} stands for the torque measured by the foot sensor in the sagittal plane, and F_{gr} represents the ground reaction force measured by the foot sensor in the *z* direction, refer to Fig. 16.

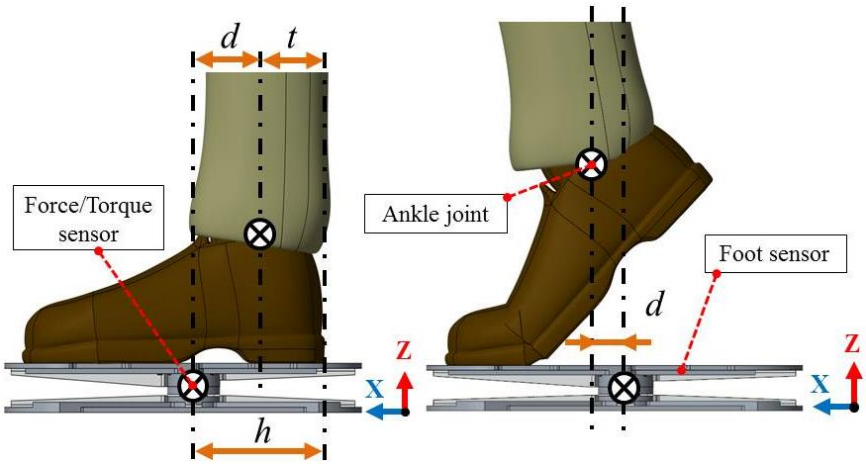

(a) (b)

Fig. 16 – In (a) and (b) is shown the variation to the distance (*d*) between the ankle joint and the z axis of the force/torque sensor as a result of the change to the configuration of the user's foot while on the first iT-Shoe prototype.

3.3.2 Prototype 2

The second version of the iT-Shoes has been designed as a sensorized add on system for shoes. Each iT-Shoe integrates two 6axis Force/Torque (F/T) sensors with dedicated embedded MEMS IMUs in their electronics, shown in Fig. 17. The F/T sensors measure the interaction with the ground, while the embedded IMUs measure the plantar flexion of the feet. This version of the iT-Shoes is composed of two main parts: a first subassembly (A) shaped to be mounted at the user's toes and a second (B) shaped for mounting at the user's heel. A flexible steel component (C) connects A with B and is designed to allow regulation of the distance between A and B for different foot sizes. Its flexibility accommodates plantar flexion and allows for natural walking, climbing stairs etc. The fastening structure (D) holds the iT-Shoes onto the user's shoe. Components A.1, B.1 and A.3, B.3 are respectively the top and the bottom plates of the in-house developed F/T sensors (model IIT-FT50) shown as parts A.2 and B.2. Plastic covers protect the sensors from dust and particles. The F/T sensors use semiconductor strain gauges for low noise and high sensor stiffness. They have a measurement range of Fx,y,z ±2000N and Tx,y,z ±40Nm and a resolution of 500mN for forces and 20mNm for torques. The measurement rate is up to 1kHz

through a UDP connection. Embedded IMUs provide readings of the toe and heel inclination (parts A and B) at a resolution of 14bits with an update rate of 100Hz embedded in the force torque measurement UDP data. Fig. 21.b depicts the adopted F/T sensor reference frames. Each iT-Shoe weighs 1.6 kg and is mainly made of aluminium 7075-T6; components A.2 and B.2 are made of steel; textured rubber is attached on A.3 and B.3 to improve traction. A similar shoe sensing system has been presented in [59]. However, the novelty of the system presented here lies with its add-on characteristics, which make it a universal wearable device suitable for different settings, its adjustability for different user's foot sizes, its reliable construction, its high degree of mechanical and electronics and software integration.

In section 4.2.2, equation (5) describes how the effort generated by the subject's ankle is evaluated based on the information gathered by the second prototype of the iT-Shoes. Finally, experiments conducted to validate the second prototype of iT-Shoes and to test them in the context of the iT-Knee Bipedal System are reported in chapter 5.

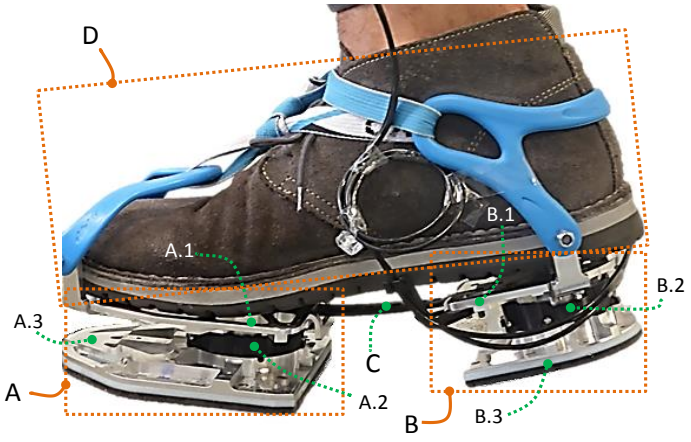

Fig. 17– The developed iT-Shoes equipped with two 6 DoF F/T sensors and two IMUs to monitor the toe and heel orientation and the contact wrench. It is adjustable to different user's size and accommodates the foot plantar flexion motion.

3.4 System Architecture

This section discusses the system architecture and the communication used to control the iT-Knee Bipedal System, refer to Fig. 18. Currently, the proposed system is connected to an external power supply at 36V through a power tether; in future, it could be powered by Li-Po batteries. The iT-Knee actuators work at 36V while the force/torque sensor, embedded in the iT-Shoes, at 3.2V. The voltage transformer as well as all the switches necessary to run the system are located in the user's backpack.

The iT-Knee actuators are controlled by custom driver electronics. Their low level control comprises position, velocity and torque loops that run at 1KHz. As result, actuators can be operated with torque or impedance control. The actuators are brushless DC electric motors driven with 40kHz PWM. The motor controller board communicates with the PC through Ethernet. As described in chapter 4, the high level controller of the iT-Knee Bipedal System, coded in C++, is implemented in the PC. Then, the PC sends the torques references to the iT-Knee exoskeletons, through a custom software called RoboLLI. Two types of connections are implemented in such framework: the UDP protocol to send/receive broadcast data, and the TCP connection to stream commands. Possible broadcast data are: position and velocity trajectories and their measurements, setting of the PID controllers as well as their errors and outputs. On the PC the framework updates at 500 Hz. iT-Shoes communicate with the PC through Ethernet cable. iT-Shoes adopt the same communication infrastructure used by the iT-Knee actuators. Their custom electronics communicate with the force/torque sensors at 1kHz through a UDP connection. The MEMS IMUs embedded in the electronics of the force/torque sensor has an update rate of 100Hz. Finally, the sensing system of the iT-Knee Bipedal System comprise two more commercial Inertia Measurement Unit (IMU) sensors (model VN-100T Rugged from VectorNav) used to monitor the orientation of the user's shanks. They communicate with the PC through USB connections using the VectorNav library. The USB connection insures also power supply to the IMUs.

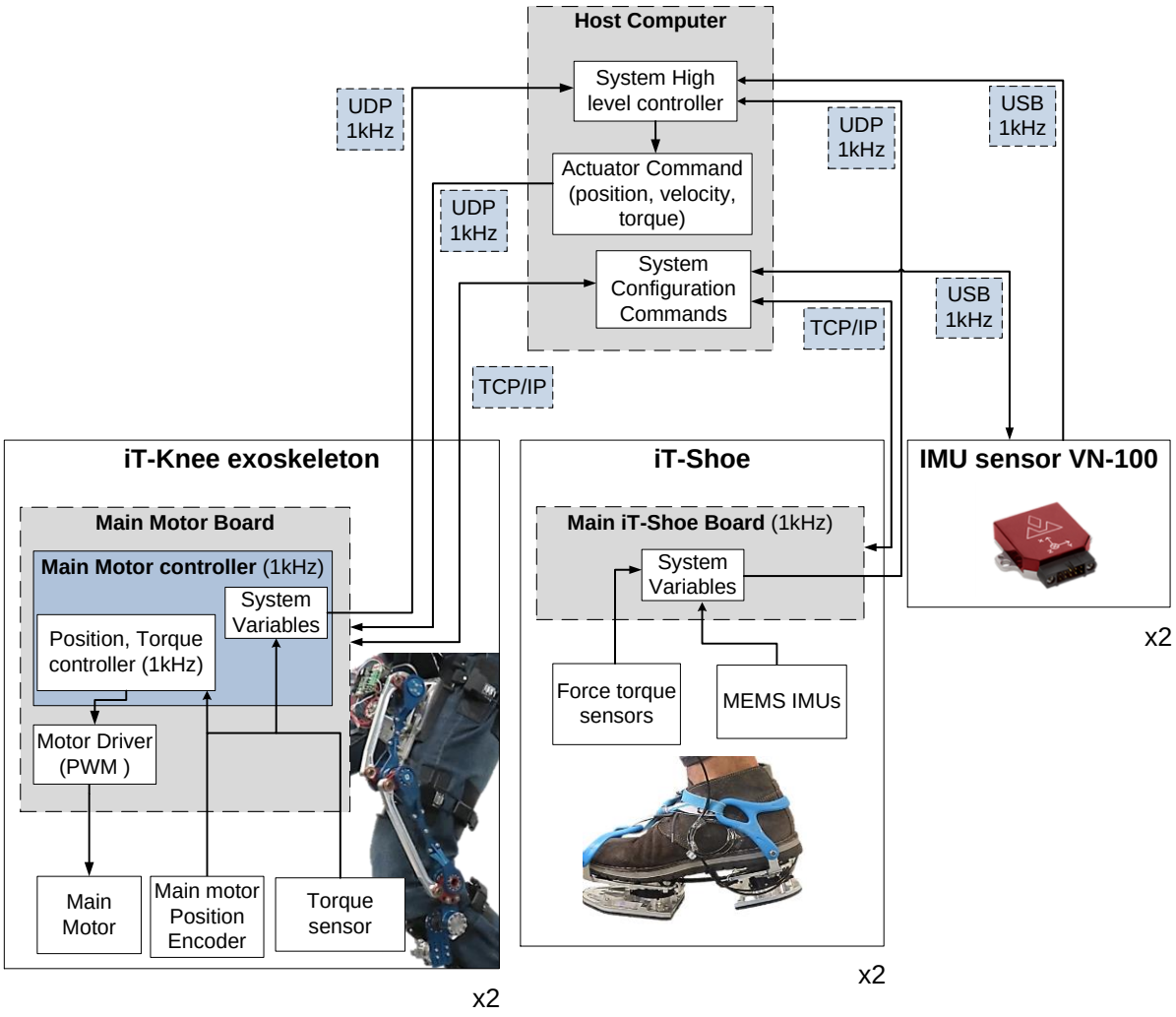

Fig. 18– The architecture of the iT-Knee Bipedal System.

4 THE iT-KNEE BIPEDAL SYSTEM: CONTROL

4.1 Introduction

The iT-Knee Bipedal System aims to assist elderly people and to augment the strength and the endurance of healthy subjects to accomplish daily life activities. As consequence, the control of iT-Knee Bipedal System must exhibit robust behaviors across different user's actions and with respect to unpredictable user-environment interactions. At the same time, the desirable control should evaluate the user's intentions and acts synchronously with the user's actions, requiring a sensing system less invasive as possible to obtain an overall system as portable as possible.

In the rest of this chapter the control strategy implemented on the iT-Knee Bipedal System is presented. In the author's opinion, it represents a valuable contribution toward the capability to drive lower limb exoskeletons in scenarios where unexpected ground conditions or unpredicted interactions with the surroundings (i.e. payload handling or pushing and pulling task) can occur. In particular, in section 0 a novel approach (the SLLE method) to estimate online the torque generated by the user's ankles, knees and hips is presented. Finally, section 4.3 discusses the implemented state machine that generates online the reference signals for the iT-Knee actuators based on the torques at the knees estimated by the SLLE method.

4.2 Joint torque estimation

This section presents a novel method, the SLLE method, for estimating online the torques at the ankle, knee and hip of a user with the goal of generating reference signals for torque controlled lower limb exoskeletons. In particular, this approach attempts to address difficulties arising in real scenarios when noncyclic locomotion activity, unexpected terrain or unpredicted interactions with the surroundings occur. As main advantage, the proposed method does not require any information on the user's upper body (i.e. pose, weight and center of mass location) or on any interaction of the user's upper body with the environment (i.e. payload handling or pushing and pulling task). By monitoring the interaction of the user's feet, possible thanks to the development of the iT-Shoes, refer to Section 3.3.2, the method applies an inverse dynamic approach on the user's lower limbs to estimate in real time the torque at each leg joint. As second advantage the sensing system, required by the SLLE method, results fully wearable, ergonomic and portable, since no sensors are necessary on the user's upper body.

The rest of the section firstly describes the inverse dynamic method that inspired the development of the proposed method to estimate the torque at the leg joints, then the SLLE method is described in detail. Experiments performed to validate the proposed approach under different tasks (i.e. payload handling and pushing task) and terrains (i.e. flat ground, inclined surface, irregular terrains and stairs) are presented in chapter 5.

4.2.1 The Inverse Dynamic method: an overview

In the field of robotics, the inverse dynamic method is generally applied to robotic arms. Such an approach estimates the torque that the motors of a manipulator have to deliver in order to perform a generic task, refer to Fig. 19. The peculiarity of the method is that it does not require sensors that monitor the torque output of the robot's

actuators. Indeed, the inverse dynamic method estimates the torques at each joint of the robot (q_i) based on: an accurate model of the manipulator; the knowledge of the state of each link of the robot (i.e. pose, velocity and acceleration); the measurement of all the forces and torques exchanged by the manipulator with the environment.

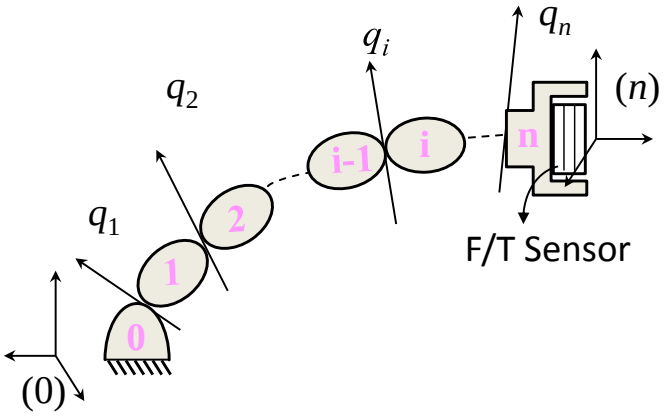

Fig. 19– A planar robotic arm composed by *n*+1 links and *n* revolute joints.

Once this information is available, starting from the last link of the manipulator (i.e. the end effector or link *n*) to the first one, recursively, a dynamic equilibrium is imposed. In particular, the torque that each actuation unit of the robot is generating is equivalent to the internal torque estimated by the inverse dynamic method.

As the next section discusses, the inverse dynamic method can be also applied on the human lower limbs to compute the effort that a person is generating at his ankles, knees and hips. Indeed, the human leg can be considered as a robotic manipulator composed by three links, where: the ground to which the manipulator is fixed symbolizes the user's upper body; each link of the system, from the first to the last, respectively represents the user's thigh, shank and foot; and the F/T sensor, attached to the last element of the system, can be substituted by the iT-Shoes, presented in section 3.3, to monitor the interaction of the user with the ground. The main advantage in using the inverse dynamic method on the human leg is that no information of the user's upper body is required to estimate the torques generated at the leg joints.

4.2.2 The Static Lower Limbs Equilibrium (SLLE) method

The Static Lower Limbs Equilibrium (SLLE) method applies an approximate inverse dynamic analysis on the user's lower limbs to estimate online the torque at each user's leg joint in quasi-static condition. In particular, the acceleration and velocity terms contributing to the estimation of the joint torques are assumed negligible. The inputs required by the SLLE method are: the monitoring of the interactions between the user's feet and the ground; the tracking of the orientation of the lower limbs; the implementation of a model of the human lower limbs. As Section 3.3.2 describes, the iT-Shoes monitor the orientation of the user's feet and their interaction with the ground, while four commercial IMUs (model VN-100T Rugged from VectorNav) track the orientation of the shanks and of the thighs with respect to the ground. The method uses a planar lumped mass model of the human lower limbs, where the parameters (i.e. masses, lengths and CoM locations) of the lumped model of the thighs and shanks are computed from the user's weight and height using the statistical model presented in [60] and adjusted in [61]. Finally, the feet parameters are derived from [62].

Fig. 20– A manikin is shown where the green plane represents its sagittal plane and the grey and red planes depict respectively the AKHFE plane for the right and left leg.

In the SLLE method, each user's leg model is implemented in an independent plane that vary from the sagittal one, as Fig. 20 depicts. The considered planes are called AKHFE planes defined as the planes containing the Flexion-Extension rotations for the Ankle, Knee and Hip joint. Their orientation with respect to the sagittal plane in the transverse one follow the feet disposition. As consequence the SLLE method works also in case of no symmetrical user's lower body posture with respect to the sagittal plane. The SLLE method treats as full independent entities the user's legs, where the torques estimated on one leg do not influence the one computed on the other and vice versa.

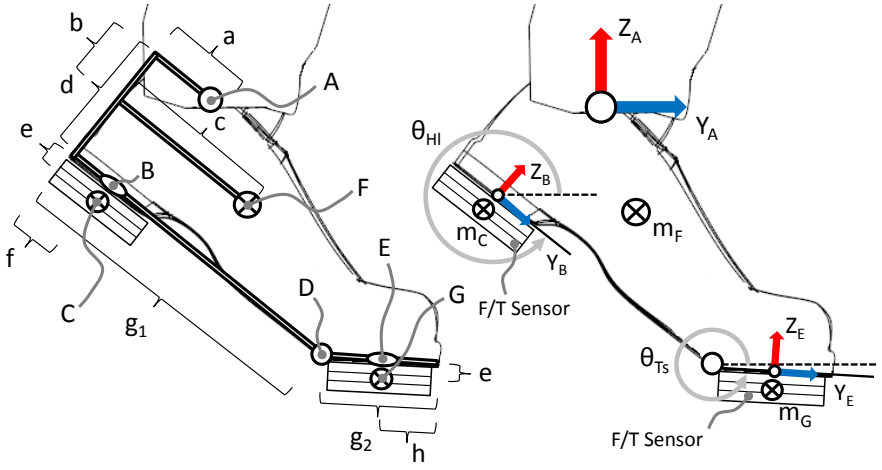

(a) (b)

Fig. 21– The adopted lumped mass model of the user's foot. (a) depicts the lengths chosen to describe with respect to the ankle joint (A) the position of: the CoM of the foot (F); the F/T sensors located at the heel (C); the F/T sensors located at the toe (G) ;and the point where the GRFs are measured (B, E). In (b) the angles monitored by the embedded IMU sensors to track the orientation of the heel (θ_{Hl}) and of the toes (θ_{Ts}) in the AKHFE plane are shown.

In Fig. 21 the adopted lumped model of the user's feet is shown. In Fig. 21.a the lengths chosen to defined the feet model are depicted, while in Fig. 21.b the angles describing the feet orientation in the AKHFE plane and the considered frames are shown. The system of equations (5) imposes a static equilibrium at each foot in its AKHFE plane. The equations (5) are solved with respect to the origin of the ankle frame (A). As consequence, the GRF monitored in the F/T sensor frame are projected in the ankle one.

$$\begin{cases} \tau_A + \tau_B + \tau_E + \tau_{m_{C,F,G}} + \tau_{B_y} + \tau_{B_z} + \tau_{E_y} + \tau_{E_z} = 0 \\ A_y + B_y + E_y = 0 \\ A_z + B_z + E_z + m_C g + m_F g + m_G g = 0 \end{cases} \quad (5)$$

Where τ_A represents the torque generated by the user's ankle to compensate for: the Ground Reaction Torque (GRT) (τ_B, τ_E) measured by the F/T sensors; the sum of the torques generated by the action of gravity ($\tau_{m_{C,F,G}}$) on C (τ_{m_C}), G (τ_{m_G}) and on F (τ_{m_F}); the torques (τ_{B_y}, τ_{B_z}, τ_{E_y}, τ_{E_z}) produced by the GRF (E_y, E_z, B_y, B_z). In particular:

$$\tau_{m_F} = m_F g\overline{AF}\cos(\theta_{\mathrm{Hl}}), \qquad \tau_{m_C} = m_C g\overline{AC}\cos(\theta_{\mathrm{Hl}}),$$

$$\tau_{m_G} = m_G g(\overline{AD}\cos(\theta_{\mathrm{Hl}}) + \overline{DG}\cos(\theta_{Ts})), \qquad \tau_{B_y} = B_y\,\overline{AB}\sin(\theta_{Hl}),$$

$$\tau_{E_y} = E_y(\overline{AD}\sin(\theta_{Hl}) + \overline{DE}\sin(\theta_{Ts})), \qquad \tau_{B_z} = B_z\,\overline{AB}\cos(\theta_{\mathrm{Hl}}),$$

$$\tau_{E_z} = E_y(\overline{AD}\cos(\theta_{Hl}) + \overline{DE}\cos(\theta_{Ts})).$$

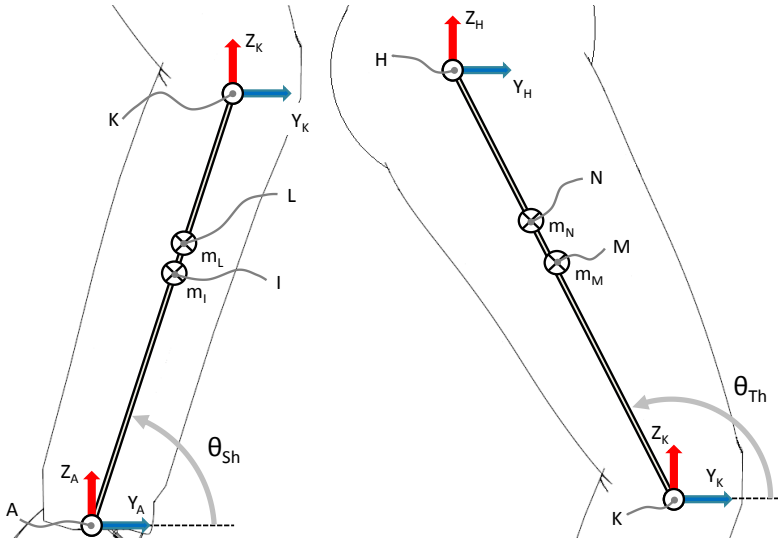

(a) (b)

Fig. 22– The adopted lumped model of the user's shanks (a) and thighs (b). A, K and H represent the location of the Ankle, Knee and Hip joint in the AKHFE plane. I, L, M and N the CoM location respectively of the shank (m_I), shank attachment (m_L), thigh (m_M) and thigh attachment (m_N). θ_{Sh} and θ_{Th} are the shank and the thigh angles in the AKHFE plane.

The adopted lumped model for the user's shanks and the angle chosen to define their orientation in the AKHFE planes are shown in Fig. 22.a. The system of equations (6) imposes a static equilibrium at each shanks in the AKHFE plane. The equations (6) are solved with respect to the reference frame in K.

$$\begin{cases} \tau_K + \tau_A + \tau_{m_I} + \tau_{m_L} + \tau_{A_y} + \tau_{A_z} = 0 \\ A_y + K_y = 0 \\ A_z + K_z + m_I g + m_L g = 0 \end{cases} \qquad (6)$$

Where τ_K represents the torque generated by the user's knee to compensate for: the torque generated by the action of gravity on m_I (τ_{m_I}) and m_L (τ_{m_L}); the pure reactive torque generated by the ankle (τ_A); and the torques (τ_{A_y}, τ_{A_z}) produced by ankle

reaction forces (A_y, A_z). The values of τ_A, A_y and A_z are estimated through (5). In particular:

$$\tau_{m_I} = m_I g\overline{KI}\cos(\theta_{Sh}+\pi), \qquad \tau_{m_L} = m_L g\overline{KL}\cos(\theta_{Sh}+\pi),$$

$$\tau_{A_y} = A_y\,\overline{KA}\sin(\theta_{Sh}+\pi) \quad \text{and} \qquad \tau_{A_Z} = A_Z\,\overline{KA}\cos(\theta_{Sh}+\pi).$$

The adopted lumped mass model for the user's thighs and the angle chosen to define their orientation in the AKHFE planes are shown in Fig. 22.b. The system of equations used to impose the static equilibrium at each thigh in the AKHFE plane is equivalent to the one adopted for the knees where: *K*, *A*, *I*, *L*, m_I, m_L and θ_{Sh} are respectively replaced by *H*, *K*, *M*, *N*, m_M, m_N and θ_{Th}. τ_A, K_y and K_z are estimated in (6).

Since no information of the user's upper body is required, thanks to the data collected by the iT-Shoes, as (5) and (6) highlight, the SLLE method is intended as a contribution toward a control strategy able to drive lower limb exoskeletons in scenarios where unexpected ground conditions or unpredicted interactions with the surroundings (i.e. payload handling or pushing and pulling task) may occur. Finally, the action of gravity on the lower body segments is the only interaction accounted for by the implemented lower limbs model, as (5) and (6) highlight. The effect of other types of interactions between the user's lower limbs (e.g. collisions-contacts of objects with the legs) are not considered by the SLLE method. As a consequence, estimation of the torque of leg joints above the lower body segment where such un-modelled situations occurred would be not accurate.

4.3 Control strategy

To design effective exoskeletons the detection of the user's intention and the modulation of the exoskeletons' assistance based on the user's actions are crucial. This is true especially in every-day scenarios where all the interactions of the user with the environment cannot be predicted. As consequence, from a control point of view, the design of control strategies able to adapt to different user's states is fundamental.

To address this issue, as reported in [63], state machines represent powerful tool to implement different controllers. Nowadays, state machines are often used in lower limb exoskeletons to specify diverse strategies to adopt along the different phases of the human gait (i.e. the stance and the swing phase). Nevertheless, many systems provide walking assistance based on time, normalizing each subject's step timing. As [63] highlights, to achieve more robust behavior in every-day scenarios, where changes on the step length, walking speed or terrain profiles can occur, state machines based on time parameter should be replaced by state machines that combine user's state (i.e. joint orientation and velocities) and interaction force measurements (i.e. ground reaction forces).

The rest of this section describes the state machine implemented in the iT-Knee Bipedal System. It is based on information about the user's state and on the interaction forces exchanged by the user with the ground. Section 5.4.2 reports the experiment conducted to test the implemented control strategy.

4.3.1 A State Machine based on the gait phases

Based on the torques estimated online at the user's knees by the SLLE method, refer to Section 4.2.2, for each iT-Knee actuator, a state machine has been developed to modulate the assistance of the iT-Knee Bipedal System during a walking task. In particular, based on the different phases of the gait, the state machines define the

reference signals for the actuators of the iT-Knee exoskeletons. The torque references are followed by actuators based on a PID torque regulator. Fig. 23 shows the overall control architecture and the torque trajectory generator of the iT-Knee actuators. According with the system architecture of the iT-Knee Bipedal System, presented in section 3.4, the SLLE method and the implemented state machine define the high level controller implemented in the host computer, refer to Fig. 18.

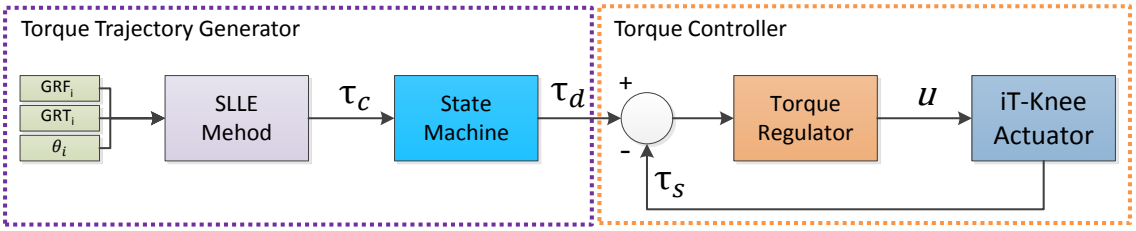

Fig. 23– The iT-Knee trajectory generator and torque controller.

As Fig. 24 depicts, the state machines modulate the assistance of the iT-Knee actuators synchronously with the gait events detected from system variables such as the Ground Reaction Forces (GRF), measured by iT-Shoes, and the orientation (θ_{Sh}) and the angular velocity ($\dot{\theta}_{\mathrm{Sh}}$) of the shanks monitored respectively by the IMUs placed on the attachments of the exoskeleton and by the actuation units. In particular, the stance phase of the gait is detected by the presence of GRF bigger than $threshold_1$, defined to overcome the signal noise, refer to Fig. 24. During the stance phase and at the initial part of the swing phase (State 1) the state machine sends to the motors a percentage of the joint torques estimated by the SLLE method. Assistive action during the initial part of the swing compensates for the knee torque due to the shank-foot and exoskeleton hardware mass, reducing the hamstring muscle effort. After the inversion of the shank's rotation at the rear extreme of the swing toward the extension direction, State3 is entered and the reference signals are set to zero torque tracking to let user move the shank forward with the assistance of gravity. To smoothen the transition between the zero torque tracking State3 and the assistive torque State1, two intermediate states exist (i.e. State0 and State2) which ramp the reference from the current torque to the desired value.

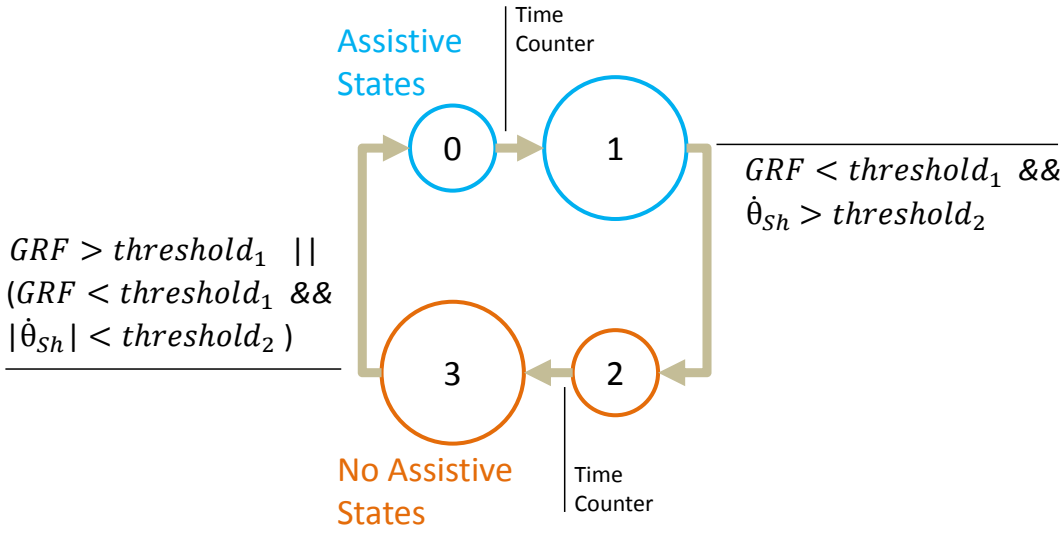

Fig. 24– The iT-Knee Actuator state machine.

As [63] describes, state machines are powerful tool toward the human's intention detection. Their goal is to identify the different conditions in which the system of interest can pass through. Controls, that implement state machines, have the possibility to adopt multiple strategies along a complex task characterized by different sub tasks. As example, walking can be assisted by a lower limb exoskeleton that implements an impedance-based controller when the stance is detected and an admittance controller for the swing phase. To improve the controllers' robustness, crucial is the capability of state machines to correctly detect and distinguish tasks. To this end, as [63] suggest, approaches, such as the SLLE method, that combine posture and interaction force measurements rather than approaches based on time specific parameters allow the design of control strategies which are more robust in daily life scenarios where changes on the step length, walking speed or terrain profiles can occur.

In Section 5.4.2 an assisted walking task performed by the iT-Knee Bipedal System is presented. Among the experiments results, the capability of the proposed state machine to detect the different phases of the gait will be discussed.

5 EXPERIMENTAL RESULTS

5.1 Introduction

This chapter collects all the experiments aimed to test and validate the iT-Knee exoskeleton, the IT-Shoes, the SLLE method and the iT-Knee Bipedal System. The chapter is organized as follow: firstly the mechanism of the iT-Knee exoskeleton and the performance of its torque controller are analyzed; then, the iT-Shoes and the SLLE method are validated under different tasks and ground conditions; finally, the capability of the iT-Knee Bipedal System to provided assistance in a lifting task and in a motion tasks are tested.

5.2 iT-Knee exoskeleton

5.2.1 Trajectory tracking with different load conditions

The objective of this experiment was to verify whether the iT-Knee exoskeleton is able to transmit only pure torque along with its mechanism to the user's shank. To evaluate this, iT-Knee was mounted on a mechanical replica of a human leg/knee, inspired from [64], refer to Fig. 25. This setup assisted to perform a controlled test by eliminating uncertainties that would be otherwise inserted by the attachment on the soft skin of the human leg. The knee of the Human Leg Replica is modelled as a 5 DoF joint, where the internal/external rotation is omitted for mechanical simplicity. The omission of this axis does not affect the test validity, since the iT-Knee should be expected to accommodate the internal/external knee rotation in the same way that it does for the varus/valgus rotation.

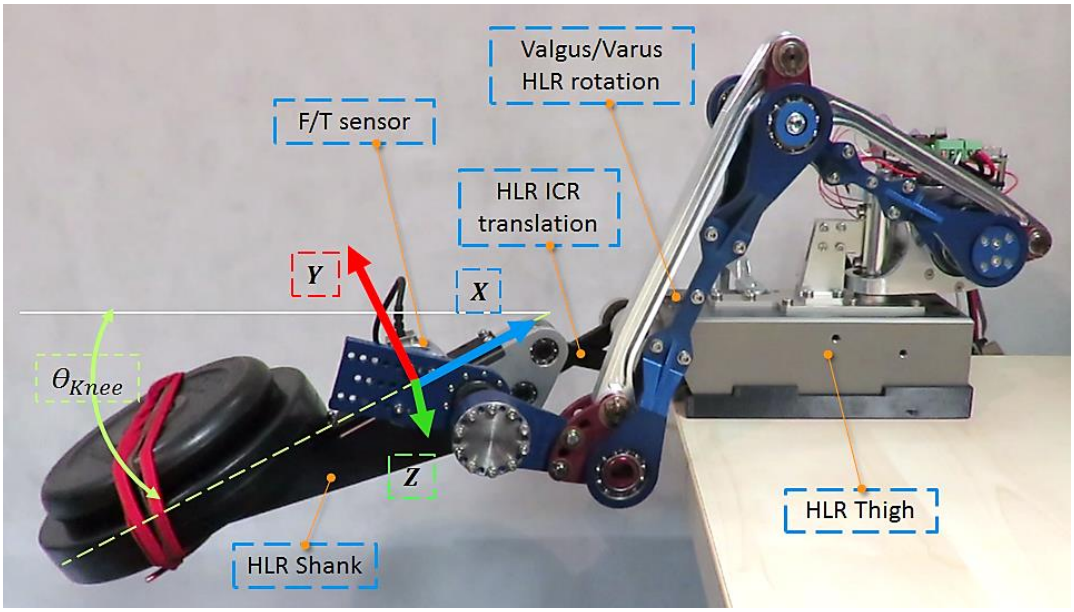

Fig. 25– iT-Knee mounted on the HLR, while it is performing the task in loaded condition. F/T sensor frame is shown.

Measurements of the force/torque sensor, located at the end of the mechanism, see Fig. 25, were recorded, while slow flexion/extension motions within a range of 0°-120° were performed at a constant angular velocity of 6° $/sec$. The, varus/valgus angle was kept at 0°. The device was tested under unloaded and loaded conditions. In Fig. 25, the iT-Knee is shown while performing the task with a payload of 3kg, located on the Human Leg Replica shank.

The upper plot of Fig. 26 depicts the motion performed by the iT-Knee exoskeleton during the experiment and its tracking performance in the loaded condition. The remaining graphs of Fig. 26 depict the interaction loads recorded by the force/torque sensor, placed between the iT-Knee mechanism and the shank of the HLR, for the load and unload conditions, according to the frame shown in Fig. 25. Trends in the middle and bottom plot of Fig. 26 show as only the value of the torque applied by the motor (T_z) changes between the loaded and unloaded condition when the same motion is performed. Even if, the variation of the torque applied by the motor could be easily predicted, the same cannot be said for the other torque and force components. Indeed, their trends are invariant with respect to different load conditions. Those experimental results demonstrate that iT-Knee exoskeleton is able to transmit only a pure torque to

the user's shank to assist the knee flexion/extension motion without the generation of any other force/torque interactions. In particular, according to the frame of the F/T sensor, reported in Fig. 25, the sum of F_x and F_y components, shown in Fig. 26, represents the forces generated due to the mass/inertia that are supported by the shank. This not only gives the possibility to evaluate better the mass distribution of iT-Knee over the user's shank and thigh, but especially to prove that the propose platform does not generate any sliding motion between the skin and its attachments while assistance is provided. Indeed, as aforementioned, the middle plot of Fig. 26 shows no tangent forces (i.e. F_x and F_z), between the skin and the shank frame of the iT-Knee, are generated by its action but mostly due to the mass/inertia of the iT-Knee transmission. As its fully kinematic coupling with the knee, this feature represent another important aspect in order to claim that iT-Knee offer high ergonomics.

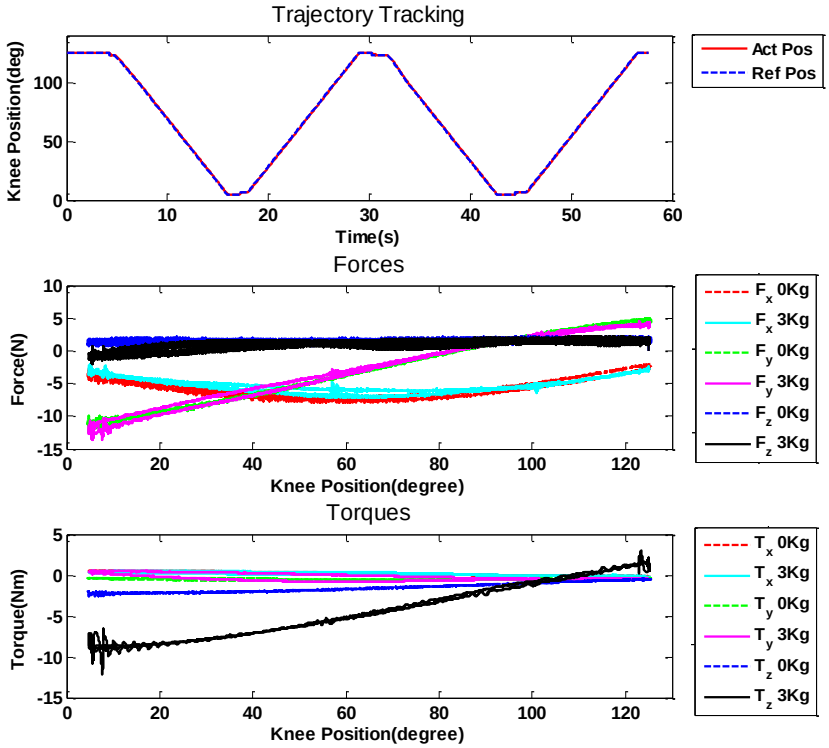

Fig. 26– The upper plot depicts the flexion/extension motion performed by the iT-Knee and the trajectory tracking performance of the system in the loaded condition. Interaction forces and torques measured by the 6 DoFs F/T sensor, installed between the iT-Knee and the shank of the mechanical leg, under unloaded (0Kg) and loaded (3kg) conditions are respectively reported in the middle and bottom plot.

5.2.2 Trajectory tracking with different varus/valgus angles

The goal of this experiment was to evaluate whether different varus/valgus configurations, would affect the torque transmission while performing flexion and extension motions under load, as well as the level of other parasitic interaction forces and torques during these motions.

As in the previous experiment, the iT-Knee exoskeleton was mounted on a human leg replica (HLR), refer to Fig. 25. Slow flexion/extension motions were performed within a range of 120° at different values of the varus/valgus angle (i.e. 0°, -15°, +15°) with a constant angular velocity (i.e. $6° / sec$) moving a payload of 3 kg . The varus/valgus setting of the knee replica was manually changed. An example of varus/valgus variation with the knee replica is shown in Fig. 11.

Trends in Fig. 27 demonstrate that different values of the varus/valgus angle do not affect significantly the force/torque transmission of the iT-Knee mechanism. These results can be safely extended to the behavior of the iT-knee under different internal/external knee angle values, since, the latter DoF are mechanically accommodated in the same way by the exoskeleton. These results reinforce the hypothesis that the iT-Knee exoskeleton manages to reach a high level of ergonomics and compatibility with the native knee not only from a kinematic point of view but also from a force/torque transmission aspect.

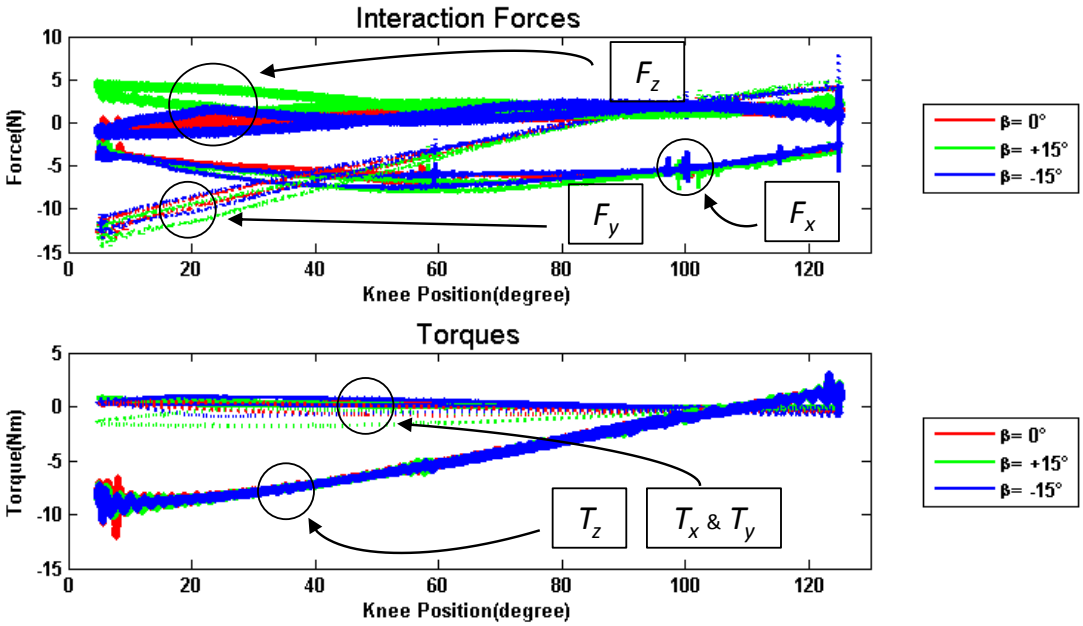

Fig. 27– Interaction forces measured by the 6-DoF F/T sensor installed between the iT-Knee and the shank of the mechanical leg under loaded (3kg) conditions for different varus/valgus angle.

5.2.3 Torque control Performance

The aim of this experiment was to transparently accommodate the knee flexion/extension movements of a healthy subject while the subject is walking on a treadmill at the speed of 3km/h. An impedance control law with an inner torque controller was implemented, as shown in Fig. 28. By setting the spring and damping gains of the external impedance loop to zero, a zero torque reference is generated for the inner torque loop requesting from the iT-Knee to provide an unconstrained knee motion during the entire gait cycle following the zero torque reference.

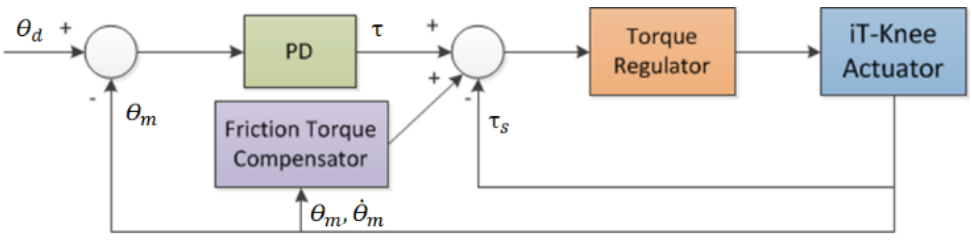

Fig. 28– Torque control scheme of the iT-Knee device.

The iT-Knee position and velocity during the walking experiment are shown in Fig. 29. The reduced velocity amplitude seen when the torque control is disabled is due to a certain level of resistance experienced by the human due to the friction and damping forces generated by the actuation and transmission system.

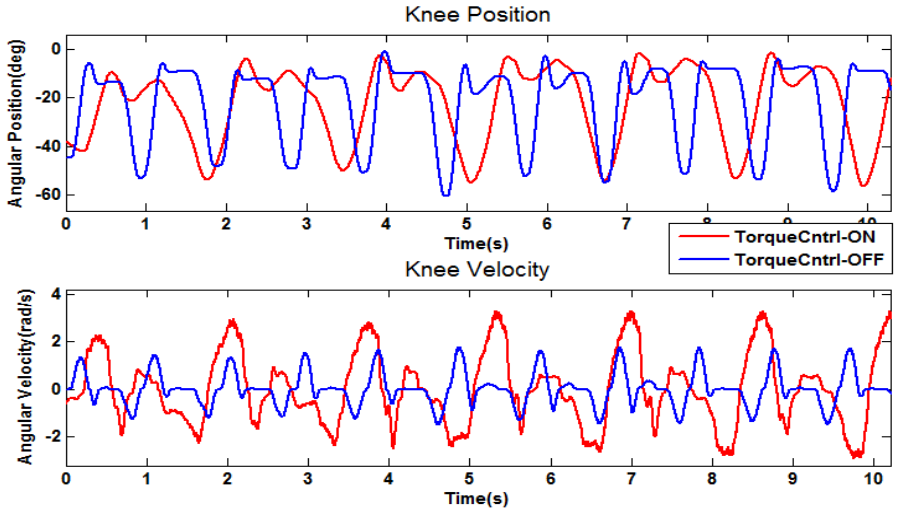

Fig. 29– Position and angular velocity of the actuated joint during multiple gait cycles. Results with torque control on and off are shown.

The enhanced transparency of the exoskeleton and the functionality of the torque controller is clearly demonstrated by looking on the interaction torque along the flexion/extension axis in Fig. 30 when the torque controller is active. It is evident that with the torque control enabled the interaction torque experienced by the human user is significantly reduced by almost an order of magnitude compared to the level measured when the torque control is disabled, and remains bounded within +/-2Nm during the entire duration of the walking experiment.

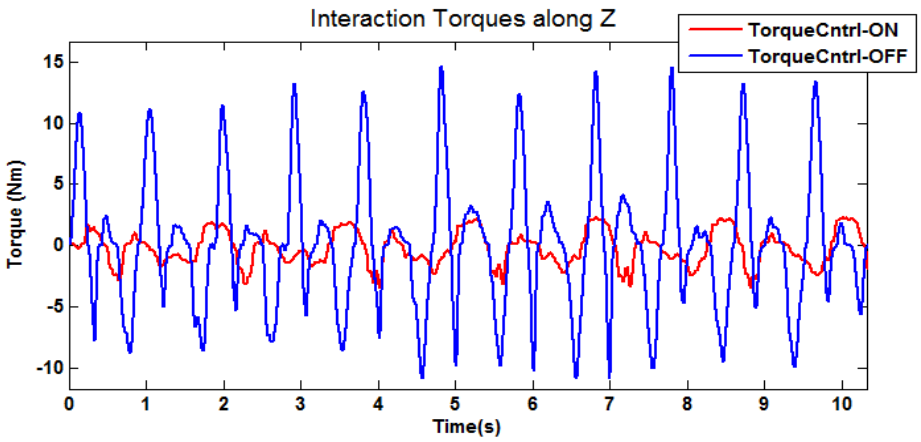

Fig. 30– Interaction torque between iT-Knee and user's leg during multiple gait cycles. Results with torque control on and off are shown.

Finally, Fig. 31 shows the other components of the interaction forces and torques generated at the knee during the walking; verifying that the exoskeleton's self-aligning mechanism provides adequate decoupling between the assisted flexion/extension motion and the other ideally passive axes of the human leg during dynamic natural motions reaffirming the observations of the experiment in Section 5.2.1.

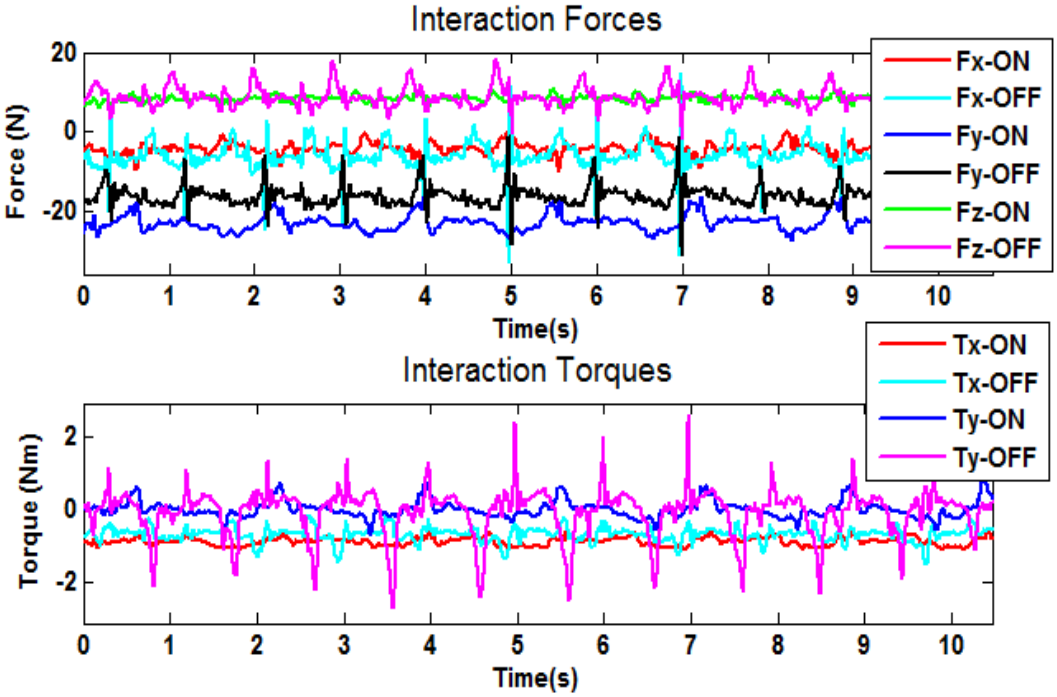

Fig. 31– The other interaction force/torque components between iT-Knee and user's leg. Results with torque control on and off are shown. Peak differences are made by harder

ground impact while the user exerts higher effort to move the joint due to the larger resistance forces when the torque controller is off.

As part of the same experiment we evaluate the power cost of the transparency mode when the torque control is enabled. In particular, the electrical power consumed by the actuation unit with the torque control active was measured to understand its power cost. As it can be seen in Fig. 32 the absolute peak power, during the zero torque tracking during the 3Km/h walking, reached levels of 34Watts while the corresponding RMS power indicated by the green line was at the level of 17 Watts. In the same plot the instantaneous values of current and voltage demands are presented showing in overall that the power cost is not significant given the free motion transparency improvement achieved in the system.

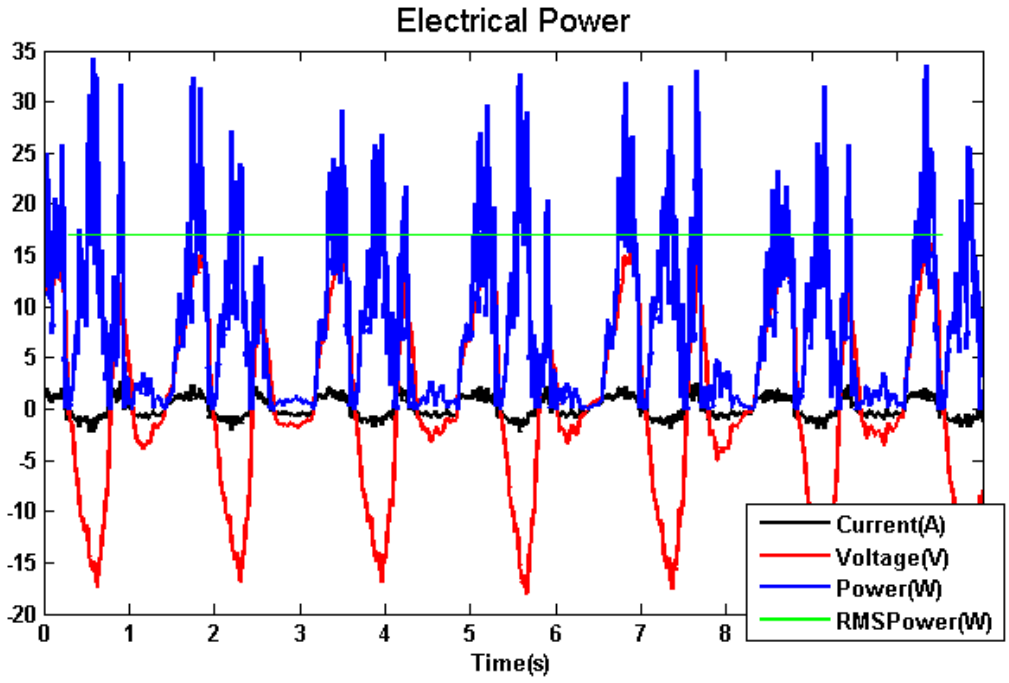

Fig. 32– The iT-Knee's RMS Power consumption during a human gait in Torque control mode active (reference value set to zero).

5.3 iT-Shoes and the SLLE method

This section presents the experiments conducted to validate the iT-Shoes and the SLLE method. In particular, the proposed sensing system and algorithm are tested in squat motions, asymmetric body postures with respect to the sagittal plane, payloads holding, payloads lifting, pushing task on different ground conditions (i.e. flat ground, upward slope, irregular terrains and stairs).

5.3.1 Squat motions

The aim of this experiment was to compare the knees' torque estimated by the Static Lower Limb Equilibrium (SLLE) method, with the approach presented in [22] and [49]. In these works the knees' torque in the sagittal plane is computed as the sum of the action of gravity on the body segments above the knees with respect to the knee location, refer to Fig. 33.b. This approach relies on a rigid human planar model. Such technique will be referred to as the Body Posture method (BP) in the rest of the experiment. Equation (7) describes computation of the knee torque with this method.

$$\tau_{knee} = g\left(m_2\, l_2^{com} c_2 + m_{iT_{up}}\, l_2^{iT_{up}} c_2 + m_3 d_1 + m_4 d_2 + m_5 d_3 + m_6 d_4 + m_7 d_5 + m_8 d_6\right) \quad (7)$$

With: $d_1 = l_2 c_2 + l_3^{com} c_3$, $d_2 = l_2 c_2 + l_3 c_3 + l_4^{com} c_4$,

$d_3 = l_2 c_2 + l_3 c_3 + l_5^{com} c_5$,

$d_4 = l_2 c_2 + l_3 c_3 + l_5 c_5 + l_6^{com} c_6$,

$d_5 = l_2 c_2 + l_3 c_3 + l_5 c_5 + l_6 c_6 + l_7^{com} c_7$,

$d_6 = l_2 c_2 + l_3 c_3 + l_5 c_5 + l_6 c_6 + l_7 c_7 + l_8^{com} c_8$

where τ_{knee} is the torque of the knee joint; g is the acceleration of gravity; c_i=cos ϑ_i and m_i, ϑ_i and l_i are the i-th limb's mass, orientation and length; l_i^{com} refers to the distance from the CoM of the limb *i* to the joint connecting it with the limb *i-1*; $m_{iT_{up}}$ and $l_2^{iT_{up}}$ are the mass of the exoskeleton supported by the thigh and the distance of the device's CoM to the knee joint, see Fig. 33.

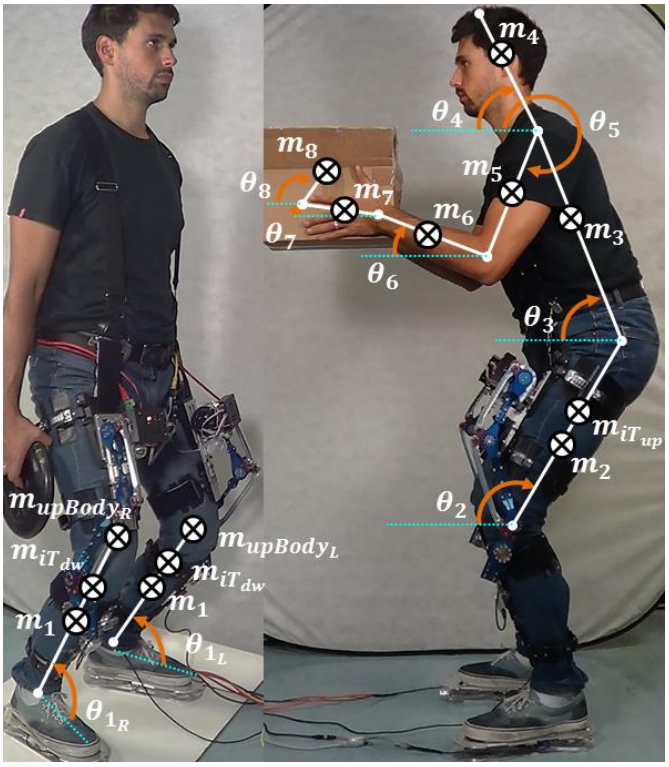

(a) (b)

Fig. 33– Human model representations for computing the torque that the human knee applies to compensate for the action of the gravity on the body as well as on eventual payload carried by the user with the Static Lower Limb Equilibrium method (a) and with the Body Posture method (b) .

As Fig. 33 depicts, the SLLE method and the BP method represent opposite approaches to estimate the knee's torque; indeed, while the SLLE method considers the body segments under the knees and the interaction of the user's feet with the ground, the BP relies on the body segments above the knees and on the interaction of the user's upper body with the environment.

As Fig. 33 shows, the experiment was performed with the first prototype version of the iT-Shoes and the ankles' torque was computed based on (4). Terms in (6) as τ_A, τ_K, θ_{Sh}, τ_{m_I}, τ_{m_L} and τ_{A_z} are respectively labelled in Fig. 33.a as τ_{ankle}, τ_{knee}, θ_1, τ_{m_1}, $\tau_{m_{iTdw}}$ and $\tau_{m_{upBody}}$.

To compare the torque estimated at the knees by the two methods, a user was instructed to perform two squats while maintaining the torso vertical. This motion as well as the posture of the torso were chosen because they are very torque demanding for the knee joint. To know the subject's upper body posture, the experimental setup was enriched with an IMUs attached to the torso and the user was instructed to keep the neck straight and to align the arms alongside the torso, such that $\vartheta_4 = \vartheta_3$, $\vartheta_5 = \vartheta_3 + 180°$, $\vartheta_6 = \vartheta_5$, $\vartheta_7 = \vartheta_5$ and $\vartheta_8 = \vartheta_5$. The readings of the foot plate sensors, the shank's and torso's IMUs and the exoskeleton's motor position encoders were recorded and used to compute the trajectories of $\{\vartheta_1, \tau_{ankle}, Fz\}$ and $\{\vartheta_2, \vartheta_3\}$, which are respectively used to compute the knee torque in the SLLE and BP methods. As in the SLLE method, the limbs' mass, length and CoM location parameters, necessary for the BP method, are computed from the user's weight and height using the statistical model presented in [60] and adjusted in [61].

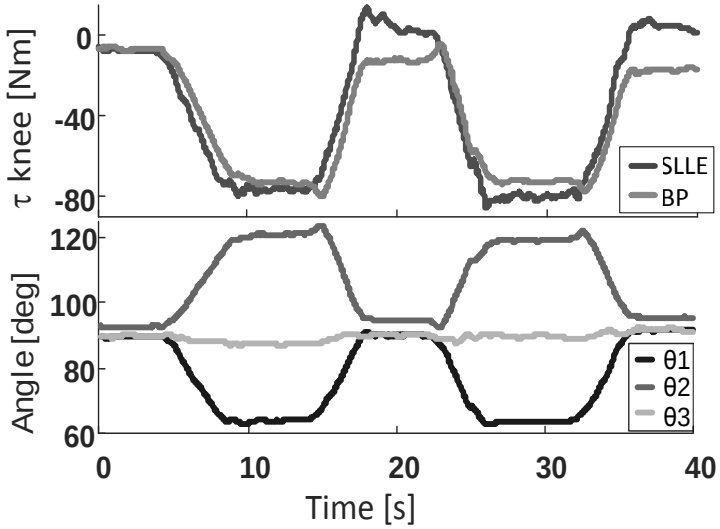

Fig. 34– The upper plot compares the torque estimated by the proposed method (SLLE) with respect to the (BP) method while squat motions were performed. In the bottom plot the orientation of the shank (ϑ_1), thigh (ϑ_2) and trunk (ϑ_3) of the subject with respect to the sagittal plane are depicted.

The experimental results are presented on Fig. 34. The upper plot of Fig. 34 shows some discrepancies between knee torque computed from both methods. They might stem from deviations from the assumptions associated with the implementation of the BP method. Indeed, in the present implementation of the BP model the torso has been modelled as a rigid body whose orientation is set according to the IMU sensor reading. However, in reality the torso is a flexible body, and a single IMU which measures the slope only at a single attachment point is unable to capture the articulation of the whole upper body and therefore its true CoM. Additionally, the forearms, upper arms, hands and head may not be perfectly aligned with the torso during the entire motion as assumed to be by this implementation of the BP model. Due to the above, while the changes of the body mass distribution are ignored by the implemented BP method they are taken into account by the proposed SLLE method since the foot sensor torque measurement contains the effects of actual CoM location of all parts of the body.

Although, it would be interesting to perform a comparative analysis implementing a more complex human body model toward a more accurate implementation of the BP method, even with this simple approach it can be observed that the torque synthesized from both methods does follow the same trend and is of a similar magnitude. These results thus provide a preliminary validation of the proposed approach in symmetrical body configurations.

5.3.2 Asymmetric postures

The aim of this experiment is to analyze how the proposed method handles asymmetric body postures with respect to the sagittal plane. To this end, the user was instructed to translate his CoM in the frontal plane as shown on Fig. 35.

The motion consisted of four phases shown in Fig. 35 and indicated on Fig. 36, such that the user, starting from a standing position with slightly bended knees (a), shifted most of his weight on his right leg (b) and then on his left leg (c) before lifting his right foot off the ground (d). During these phases the upper body was kept at

relatively constant inclination with respect to the frontal plane so as to not affect the knee torques by bending forward or backward. The experiment was performed with the first prototype version of the iT-Shoes and the ankles' torque was computed based on (4).

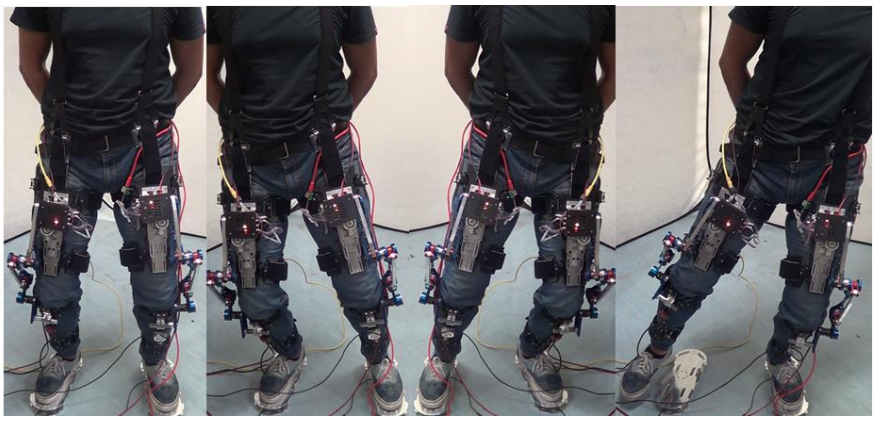

(a) (b) (c) (d)

Fig. 35– Different body postures corresponding, from left to right, to the phases "a", "b", "c" and "d" defined in Fig. 36.

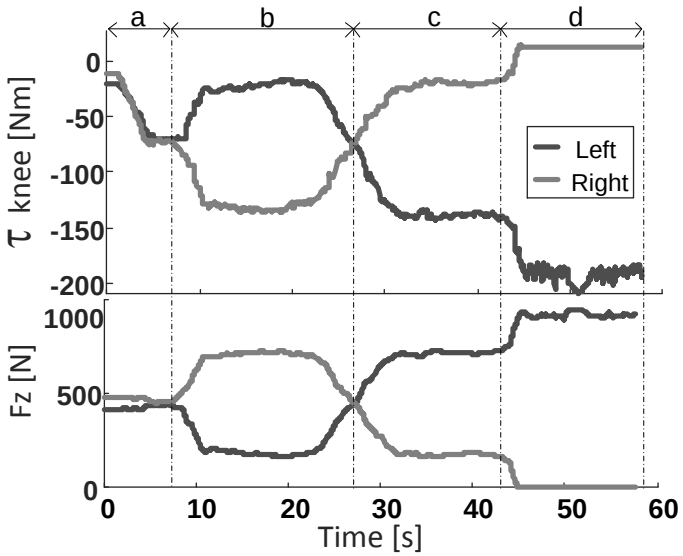

Fig. 36– The upper plot shows the torque generated at the knees joints (Left and Right), estimated by the proposed method (SLLE), while the subject was translating on the frontal plane the distribution of his body's weight (F_z) from a foot to the other and vice versa (lower plot), see Fig. 35.

As shown on Fig. 36, the shift of the body mass from one leg to the other is reflected by the vertical forces measurement of the feet sensors and are properly translated into the estimated torque of the knee. In particular, the estimated knee torque increases in the leg on which the body mass is shifted on, while the estimated torque of the other knee decreases proportionally. Finally, in the phase (d), where the right foot is lifted from the ground, it can be noticed that the estimated torque of the right knee is nonzero and in fact positive. This is the torque that the knee has to apply against gravity (i.e. the weight of the shank, the foot and of the lower part of the exoskeleton) to hold this flexed position.

5.3.3 Holding payloads

This experiment focuses on assessing the capability of the SLLE method to account for the extra loading of the knee joints occurring when the user picks up an object with considerable mass. To evaluate this, a user was instructed to hold, in a constant whole-body posture shown on Fig. 37: no payload, phase (a); 5 kg weights in each hand, phase (b); 10 kg in each hand in phase (c). The arms were vertical along the body, while the subject's was standing on a flat surface. In this body configuration, the torque needed at the knee joint increases with the mass of the payload. This compensation torque was adequately estimated by the implemented SLLE method, as shown on Fig. 38. The experiment was performed with the first prototype version of the iT-Shoes and the ankles' torque was computed based on (4). Finally, in the bottom plot of Fig. 38, a difference between the measured ground reaction force (GRF) of the user's feet can be noticed. This can be explained by a natural asymmetric posture of the subject.

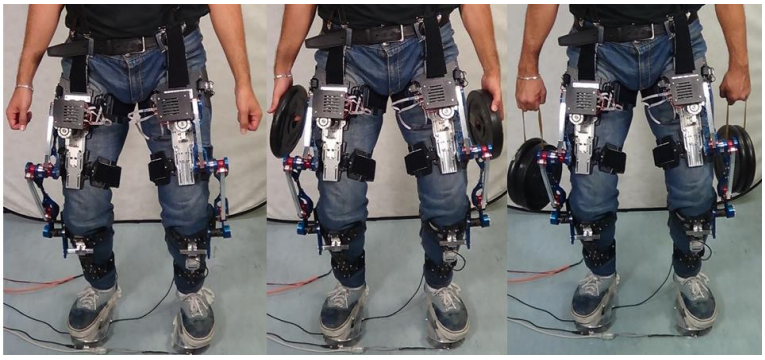

(a) (b) (c)

Fig. 37– The subject is shown when in the same posture was holding different payloads. From the left to the right, respectively, no payload (a), 5kg (b) and 10kg (c) on each hand.

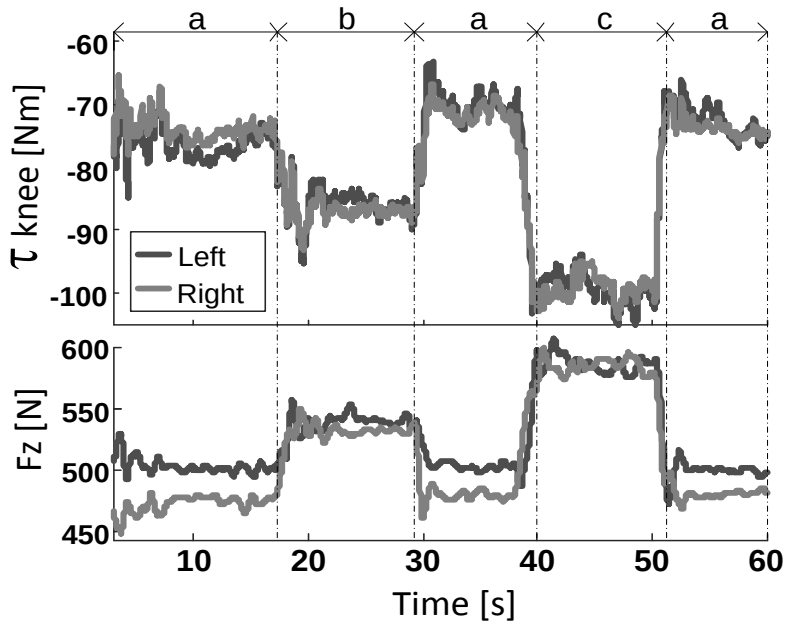

Fig. 38– The upper plot shows the torque generated at the knees joints (Left and Right), estimated by the proposed method (SSE), while the subject in the same posture was holding different payloads, refer to Fig. 37. In the lower plot the vertical forces (Fz) monitored by the foot sensors are depicted.

5.3.4 Lifting task on a flat surface

The aim of this experiment was to evaluate the effectiveness of the SLLE method and of the second prototype of the iT-Shoes in estimating the effort generated by the user's lower limbs at the ankles, knees and hips to lift payloads, standing on a flat surface, without any information about the user's upper body and about the lifted loads.

Task:

The user was instructed to hold, standing on a flat surface, a specific posture for a few seconds, refer to Fig. 39 with no payload, phase (a), with 3,1 kg weights in each hand, phase (b) and with 4,85 kg in each hand, phase (c). During the task the subject was instructed to keep a symmetrical posture with respect to the sagittal plane. To focus on the results of interest, the transition (t) between each phase of the experiment will be not discussed.

Setup:

The experimental setup was enriched with an IMUs attached to the torso and an Optitrack tracking system. The IMUs was placed on the user's trunk to track its orientation (θ_{Tr}), while the Optitrack tracking system was used to monitor the user's ankle, knee, and hip location as well as the payload's CoM position. To track the payload's CoM location a marker was placed at the center of the user's hand with the addition of an appropriate offset. The Optitrack system monitored only the user's left side since a symmetrical posture with respect to the sagittal plane was assumed to be adopted by the subject during the experiment.

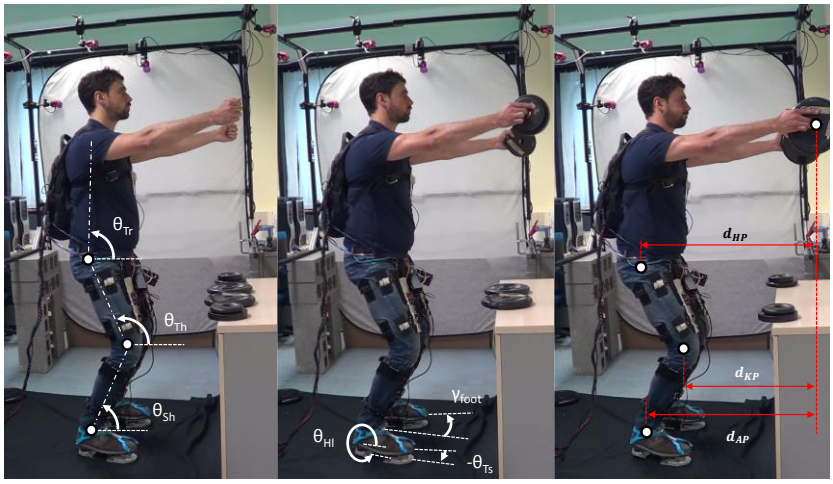

(a) (b) (c)

Fig. 39– The lifting task is shown while the subject was holding a position with no payload (a), with 3,1 kg weights in each hand (b) and with 4,9 kg in each hand (c) on a flat terrain. In (c) the distances monitored by the Optitrack are depicted.

Methodology:

To validate the iT-Shoes the values of the GRF measured by the proposed sensing system were analyzed. According with the task described, during the experiment, the horizontal GRF, projected in the ankle frame, as Fig. 21 depicts, should not be affected by the payload increment. Moreover since there are no external horizontal forces or fast dynamic motions creating horizontal forces (i.e. static friction), the measured horizontal GRF should ideally remain constant and close to zero. The vertical GRF, instead, projected in the ankle frame, should vary according with the payload increments. To evaluate the SLLE method the torques computed for the ankle, hip and knee joints between the experimental phases (b-a) and (c-a) were investigated. These torques were compared with the torques generated by the lifted weights multiplied by the distances, computed by the Optitrack, between each leg joint and the payloads, refer to Fig. 39.c. In the rest of the this section these torques computed by the Optitrack will be referred to as the expected torque variations. Crucial, in this experiment, is the user's ability to maintain a constant body posture between the unloaded and loaded conditions to avoid that the torques variation between the experimental phases (b-a) and (c-a) were generated not only by the payload presence, but also affected by the torque generated by variations of the body

posture. Finally, looking at the torque differences between the unloaded and loaded conditions allowed to investigate the ability of the SLLE method to estimate the joint torques without being affected by possible inaccuracies in the parameters adopted for the lower limbs model.

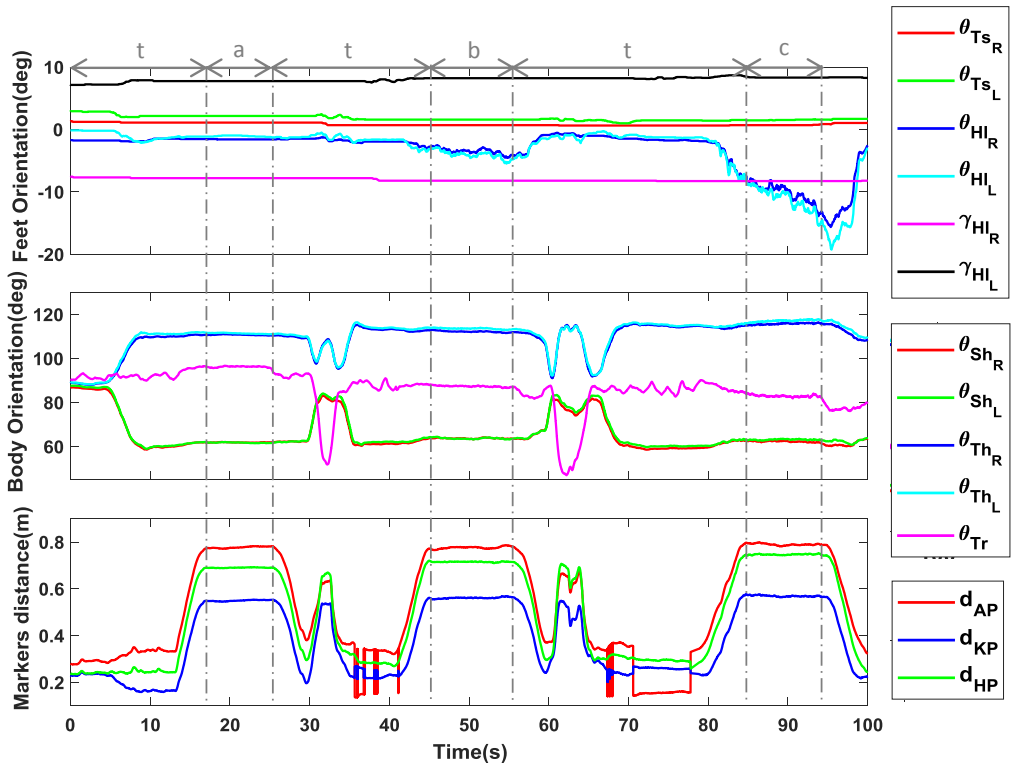

Fig. 40– The upper plot shows the orientation in the AKHFE plane, while the lifting task on a flat terrain was performed, of the right and left toe ($\theta_{Ts_R}, \theta_{Ts_L}$) and of the right and left heel ($\theta_{Hl_R}, \theta_{Hl_L}$) as well as the placement of the right and left foot with respect to the sagittal plane (γ_R, γ_L); the middle plot presents the pose in the AKHFE plane of the left and right user's shank ($\theta_{\mathrm{Sh}_L}, \theta_{\mathrm{Sh}_R}$), of the left and right user's thigh ($\theta_{\mathrm{Th}_L}, \theta_{Th_R}$) and of the user's trunk (θ_{Tr}) in the sagittal plane; the bottom plot reports the distance in the sagittal plane between each lower joint and payloads. The ankle-payload distance, the knee-payload distance and the hip-payload distance are respectively indicated as d_{AP}, d_{KP} and d_{HP}.

Results:

Although care was taken by the subject, Fig. 40 and Table 1 highlight the subject's difficulty to keep the same posture during the task. The upper and middle plot of Fig. 40 depict the orientation of the user's lower limbs during the experiment, while the bottom plot show the distance of the leg joints with respect to the payload position.

Although the subject kept a symmetrical posture with respect to the sagittal plane, the body posture did not remain constant among the different phases of the task. In particular, in the upper plot is evident that heels lift up ($\theta_{Hl_R}, \theta_{Hl_L}$) in phases (b) and (c); in the middle plot the orientation of the subject's thighs ($\theta_{\mathrm{Th}_L}, \theta_{Th_R}$) and trunk ($\theta_{Tr}$) change, while in the bottom plot the distance between the hip and payloads (dAP) sensibly vary.

Table 1, on its left part, for each phase (j), reports the mean (m) between the orientation of the left and the right side (${}^{j}\theta_{k}^{m}$) of each type of body segment (k), while, on its right part, the distance (${}^{j}d_{iP}$), in the sagittal plane, between each leg joint (i) and the payload (P) held by the subject are depicted. As Fig. 40 shows, Table 1 highlights the subject's posture variation during the experiment. The variation of the orientation of the heels (${}^{j}\theta_{Hl}^{m}$) can be noticed, as well as the different posture of the thighs (${}^{j}\theta_{Th}^{m}$) and the increment of the distance between the hip and the payloads (${}^{j}d_{HP}$). On the other hand, the orientation of the toes (${}^{j}\theta_{Ts}^{m}$) of the shanks (${}^{j}\theta_{Sh}^{m}$) and of the feet (γ_R, γ_L), following the external-internal rotation of the legs with respect to the sagittal plane, can be considered constant along the task. In particular, the orientation of the toes highlights how the flat surface was correctly detected by the iT-Shoes.

TABLE 1 BODY POSTURE VARIATION ON A FLAT TERRAIN

Body Segment *(k)*	**Mean orientation in the AKHFE plane in phases (a), (b) and (c) (deg)**			**Leg joint *(i)***	**Distance with respect to the payload in the transverse plane (cm)**		
	$^{a}\boldsymbol{\theta}_{\boldsymbol{k}}^{\boldsymbol{m}}$	$^{b}\boldsymbol{\theta}_{\boldsymbol{k}}^{\boldsymbol{m}}$	$^{c}\boldsymbol{\theta}_{\boldsymbol{k}}^{\boldsymbol{m}}$		$^{a}\boldsymbol{d}_{\boldsymbol{iP}}$	$^{b}\boldsymbol{d}_{\boldsymbol{iP}}$	$^{c}\boldsymbol{d}_{\boldsymbol{iP}}$
Toes *(Ts)*	+1,6	+1,1	+1,1	Ankle *(A)*	77,8	77,6	79,0
Heel *(Hl)*	-1,3	-3,8	-10,7	Knee *(K)*	55,0	56,2	57,0
Shank *(Sh)*	+61,9	+63,8	+62,7	Hip *(H)*	69,1	71,5	74,7
Thigh *(Th)*	+111,1	+112,9	+116,4				
Trunk *(Tr)*	+96,2	+87,4	+83,0				

As Fig. 40 and Table 1 highlight, the assumption of a constant posture of the subject during the experiment was not verified. As it will be further discussed, from the difference between the torques estimated in the unloaded and loaded conditions by the SLLE the torque contribution generated by the variations of body posture have to be compensated in order to obtain the torque generated solely by the weights.

Fig. 41 shows the subject's feet interaction with the ground measured by the four force/torque sensors of the iT-Shoes. In the upper plot the sum of the vertical GRF is also depicted as well as its mean values during each phase of the task. The trend of the vertical GRF sum highlights clearly the payload increment during the experiment, while its mean values the accuracy of the iT-Shoes. The error in the estimation of the lifted weight in phase (b) and (c) is around the 2%. The middle plot of Fig. 41, instead, depicts the horizontal GRF in the AKHFE planes. As mention in the methodology paragraph, the values of the horizontal GRF, projected in the ankle frames, should not be affected by the payload increment. Moreover since there are no external horizontal forces or fast dynamic motions creating horizontal forces (i.e. static friction), the measured horizontal GRF should ideally remain constant and close to zero. However in the middle plot of Fig. 41 can be seen that the horizontal GRF, measured by the left and the right iT-Shoe, show a significant increment in phase (c). This discrepancy from the expected zero value might be the result of a non-optimal calibration of the force/torque sensors of the iT-Shoes, which seems to not resolve with high precision the applied wrench at the foot sensor. In our experience, this could be rectified by an adaptation of the calibration mechanical setup and will be considered as part of future work.

On the other hand, in the bottom plot of Fig. 41, the GRT measured by the iT-Shoes are reported. Their trends are similar and consistent with respect to the different phases of the experiment. Indeed, their increment in phase (b) and (c) are determined by the shifting of the subject's body weight on the extremity of the front subassembly of the iT-Shoes and by the payloads lifting. Finally, in Fig. 41 an asymmetry between the interactions measured at the left and right foot can be explained by a slight asymmetry in the subject's stance and feet placement, refer to Fig. 40.

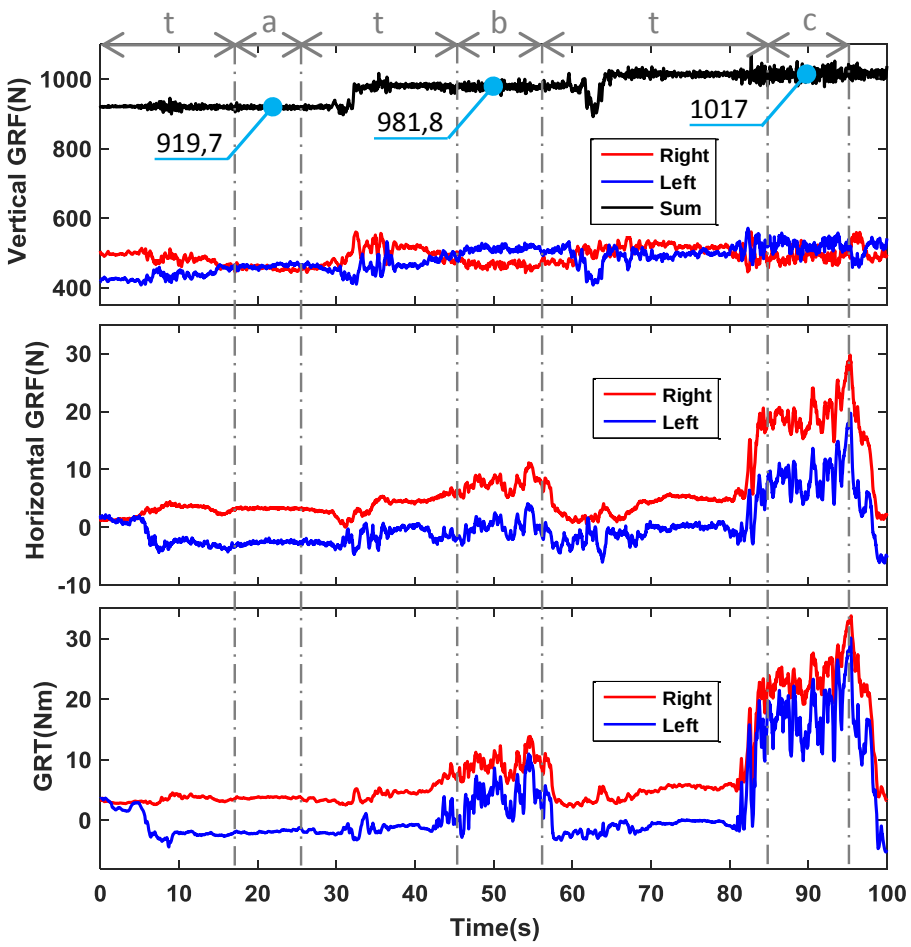

Fig. 41– Measurements of the GRF and of the GRT monitored by left and right iT-Shoe during the lifting task on a flat terrain are shown. The values are expressed with respect to the ankle frame, refer to Fig. 21, in the AKHFE planes. In the upper plot the trend of the sum of the GRF is also reported.

The torques estimated by the SLLE method are shown in Fig. 42. The torques show the expected trends according to the lifted weights. For an increment of the payloads, the effort of the extensor muscles of the ankle and of the hip joints increase, while for the knees the activity of the extensor muscles decrease. Indeed, in phases (b) and (c) the CoM position of all the elements above each leg joint moved progressively toward the payload CoM position, generating the aforementioned effort variation in the leg muscles to balance the action of the gravity.

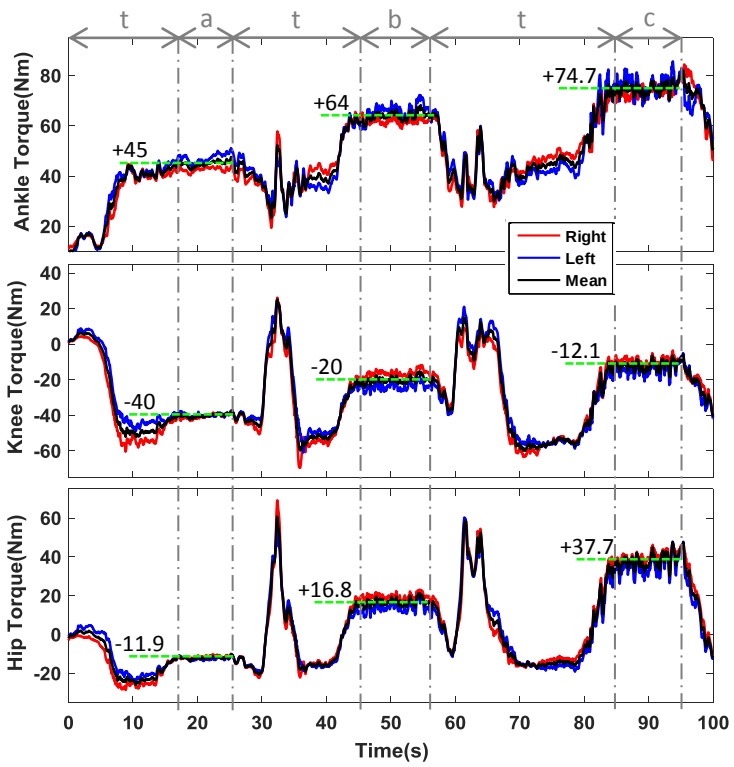

Fig. 42– Torques estimated by the SLLE method for both legs in the AKHFE planes during a lifting task on a flat terrain are reported. The values are expressed in the joint coordinate frame, refer to Fig. 21 and Fig. 22. Black lines represent the mean between the right and the left legs, red and blue lines respectively. In each phase the mean value of the black trend is depicted.

To compare the differences between the torque estimated by the SLLE method in the unloaded and loaded conditions with respect to the expected torques estimated by the Optitrack, the torque contributions generated by the variations of body posture had to be compensated. To this end, the influence of the variation of posture was estimated using the implemented lower limbs model and an approximate model for the upper body taking the IMUs outputs. These bias values for the torques at the ankle, knee, and hip were subtracted to the values estimated by the SLLE method, defining the effective torque variation computed by the proposed approach. In Table 2 the effective torque variations estimated by SLLE are reported. ${}^{ba}\Delta\tau_i^{me}$ represents the variation between phases (a) and (b), while ${}^{ca}\Delta\tau_i^{me}$ the variation between phases (a) and (c) for each joint (i).

TABLE 2 SLLE METHOD: OUTPUT COMPARISON ON A FLAT TERRAIN

	SLLE Effective Torque Variation between phases (b-a) and (c-a) (Nm)		**Expected Torque Variation in phases (b-a) and (c-a) (Nm)**		**Percentage Error (between torques)**	
Joint *i*	$^{ba}\Delta\tau_i^{m^e}$	$^{ca}\Delta\tau_i^{m^e}$	$^{ba}\Delta\tau_i^*$	$^{ca}\Delta\tau_i^*$	$^{ba}e_i$%	$^{ca}e_i$%
Ankle	+22,8	+33,0	+22,6	+37,2	0,8	11,4
Knee	+18,6	+28,8	+16,4	+26,8	13,5	7,4
Hip	+22,8	+39,7	+20,9	+35,2	9,7	12,8

The expected torque variations ($^{ja}\Delta\tau_i^*$), calculated using the known weight of the payload (m_jg) and its distance from the joints ($^{j}d_{iP}$) tracked by Optitrack on the transverse plane, are reported in Table 2 and computed in (8). $cos(\gamma^m)$ accounts for the non-parallel disposition of the subject's feet with respect to the sagittal plane projecting in the AKHFE planes the desired torque. The mean of the values in module (γ^m) along the task was almost constant a 8°.

$$^{ja}\Delta\tau_i^* = m_j\text{g}\ ^{j}d_{iP}cos(\gamma^m) \qquad (8)$$

Discussion:

The obtained results validate of the iT-Shoes and of the SLLE method. iT-Shoes showed sufficiently accurate measurement of the GRF. The SLLE method between phases (b-a) and (c-a) get respectively a mean percentage error ($^{ja}e_i$%) of 8% and 10,5 %. Assuming negligible the optical tracking errors in the measurement of $^{j}d_{iP}$, then in phase (b) the 3,1 kg payload held by the subject in each hand is estimated with a mean error of 0,25 kg, while in phase (c) the 4,85 kg payload with 0,51 kg of error. Possible sources of errors in the presented data are: inaccuracies on the upper body model adopted; inaccuracy on the measurement of the feet-ground interactions monitored by the iT-Shoes; errors in the lower limb orientation measurement (i.e. imperfect alignment of the limbs and the IMUs); inaccuracy in the tracking of the joint positions by imprecise placement of the markers, affecting the calculation of the expected joint torques; errors induced by the approach of tracking only one side of the user's body and assuming a symmetrical body posture with respect to sagittal plane.

5.3.5 Lifting task on an inclined surface

The aim of this experiment was to evaluate the effectiveness of the SLLE method and of the second prototype of the iT-Shoes in estimating the effort generated by the user's lower limbs at the ankles, knees and hips to lift payloads, standing on inclined surface, without any information about the user's upper body and about the lifted loads.

Task:

The user was instructed to hold, standing on a 10° upward slope, a specific posture for a few seconds, refer to Fig. 43 with no payload, phase (a), with 3,1 kg weights in each hand, phase (b) and with 4,85 kg in each hand, phase (c). During the task the subject was instructed to keep a symmetrical posture with respect to the sagittal plane. To focus on the results of interest, the transition (t) between each phase of the experiment will be not discussed.

Setup:

As in the previous experiment, the setup was enriched with an IMUs attached to the torso and an Optitrack tracking system. The IMUs was placed on the user's trunk to track its orientation (θ_{Tr}), while the Optitrack tracking system was used to monitor the user's ankle, knee, and hip location as well as the payload's CoM position. To track the payload's CoM location a marker was placed at the center of the user's hand with the addition of an appropriate offset. The Optitrack system monitored only the user's left side since a symmetrical posture with respect to the sagittal plane was assumed to be adopted by the subject during the experiment.

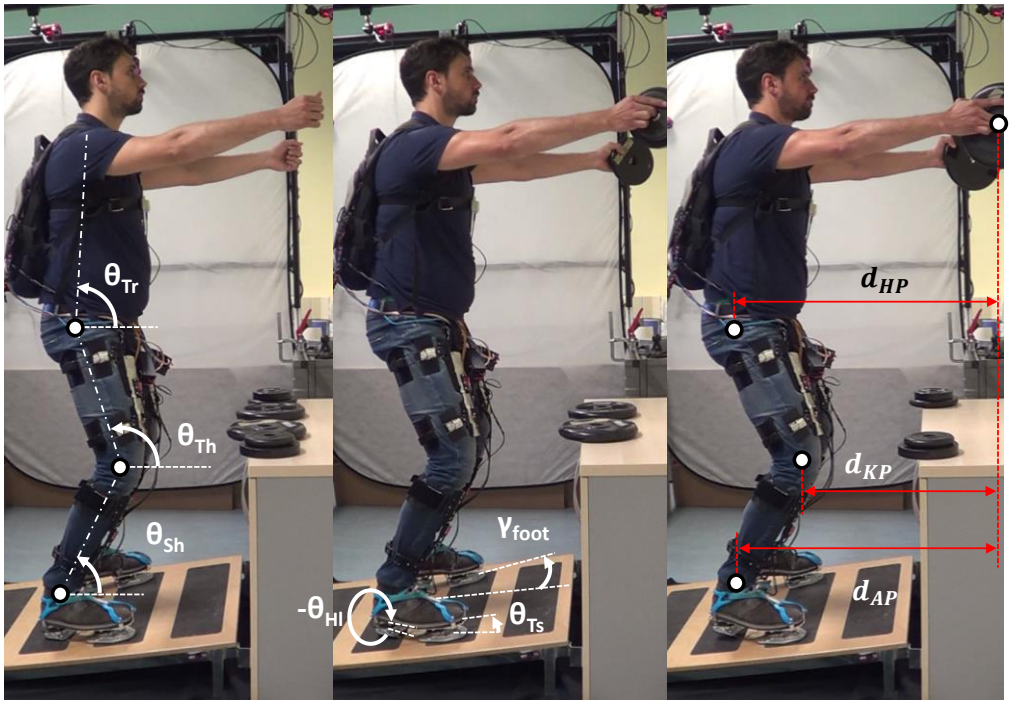

(a) (b) (c)

Fig. 43– The lifting task is shown while the subject was holding a position with no payload (a), with 3,1 kg weights in each hand (b) and with 4,9 kg in each hand (c) on a 10° upward slope. In (c) the distances monitored by the Optitrack are depicted.

Methodology:

As in the previous experiment, to validate the iT-Shoes the values of the GRF measured by the proposed sensing system were analyzed. According with the task described, during the experiment, the horizontal GRF, projected in the ankle frame, as Fig. 21 depicts, should not be affected by the payload increment. Moreover since there are no external horizontal forces or fast dynamic motions creating horizontal forces (i.e. static friction), the measured horizontal GRF should ideally remain constant and close to zero. The vertical GRF, instead, projected in the ankle frame, should vary according with the payload increments. To evaluate the SLLE method the torques computed for the ankle, hip and knee joints between the experimental phases (b-a) and (c-a) were investigated. These torques were compared with the torques generated by the lifted weights multiplied by the distances, computed by the Optitrack, between each leg joint and the payloads, refer to Fig. 43.c. In the rest of the this section these

torques computed by the Optitrack will be referred to as the expected torque variations. Crucial, in this experiment, is the user's ability to maintain a constant body posture between the unloaded and loaded conditions to avoid that the torques variation between the experimental phases (b-a) and (c-a) were generated not only by the payload presence, but also affected by the torque generated by variations of the body posture. Finally, looking at the torque differences between the unloaded and loaded conditions allowed to investigate the ability of the SLLE method to estimate the joint torques without being affected by possible inaccuracies in the parameters adopted for the lower limbs model.

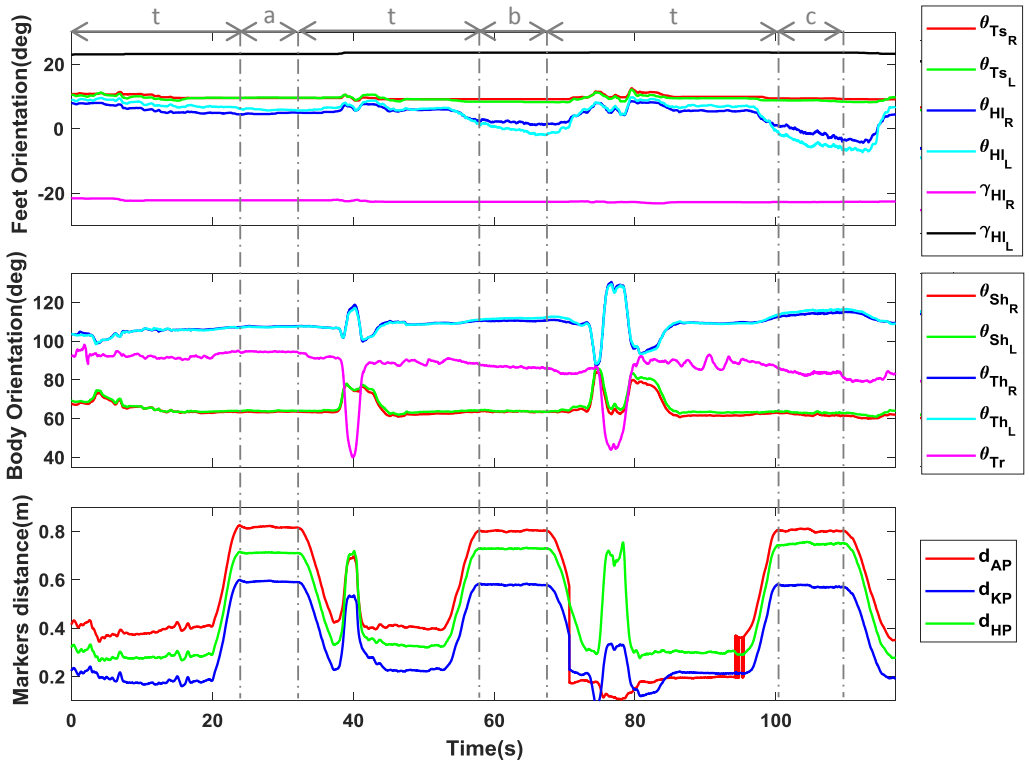

Fig. 44– The upper plot shows the orientation in the AKHFE plane, while the lifting task on a flat on a 10° upward slope was performed, of the right and left toe (θ_{Ts_R}, θ_{Ts_L}) and of the right and left heel (θ_{Hl_R}, θ_{Hl_L}) as well as the placement of the right and left foot with respect to the sagittal plane (γ_R, γ_L); the middle plot presents the pose in the AKHFE plane of the left and right user's shank (θ_{Sh_L}, θ_{Sh_R}), of the left and right user's thigh (θ_{Th_L}, θ_{Th_R}) and of the user's trunk (θ_{Tr}) in the sagittal plane; the bottom plot reports the distance in the sagittal plane between each lower joint and payloads. The ankle-payload distance, the knee-payload distance and the hip-payload distance are respectively indicated as d_{AP}, d_{KP} and d_{HP}.

Results:

Although care was taken by the subject, Fig. 44 and Table 3 highlight the subject's difficulty to keep the same posture during the task. The upper and middle plot of Fig. 44 depict the orientation of the user's lower limbs during the experiment, while the bottom plot show the distance of the leg joints with respect to the payload position. Although the subject kept a symmetrical posture with respect to the sagittal plane, the body posture did not remain constant among the different phases of the task. In particular, in the upper plot is evident that in phases (b) and (c) heels lift up ($\theta_{Hl_R}, \theta_{Hl_L}$); in the middle plot the orientation of the subject's thighs ($\theta_{\mathrm{Th}_L}, \theta_{Th_R}$) and trunk ($\theta_{Tr}$) change, while in the bottom plot the distance between the hip and payloads (d_{HP}) sensibly vary.

Table 3 on its left part, for each phase (j), reports the mean (m) between the orientation of the left and the right side (${}^{j}\theta_{k}^{m}$) of each type of body segment (k), while, on its right part, the distance (${}^{j}d_{iP}$), in the sagittal plane, between each leg joint (i) and the payload (P) held by the subject are depicted. As Fig. 44 shows, Table 3 highlights the subject's posture variation during the experiment. The variation of the orientation of the heels (${}^{j}\theta_{Hl}^{m}$) can be noticed, as well as the different posture of the thighs (${}^{j}\theta_{Th}^{m}$) and the increment of the distance between the hip and the payloads (${}^{j}d_{HP}$). On the other hand, the orientation of the toes (${}^{j}\theta_{Ts}^{m}$) of the shanks (${}^{j}\theta_{Sh}^{m}$) and of the feet (γ_R, γ_L), following the external-internal rotation of the legs with respect to the sagittal plane, can be considered constant along the task. In particular, the orientation of the toes highlights the accuracy of the front subassembly of the iT-Shoes to detect the inclined surface.

TABLE 3 BODY POSTURE VARIATION ON A INCLINED TERRAIN

Body Segment *(k)*	**Mean orientation in the AKHFE plane in phases (a), (b) and (c) (deg)**			**Leg joint *(i)***	**Distance with respect to the payload in the transverse plane (cm)**		
	$^{a}\boldsymbol{\theta}_{\boldsymbol{k}}^{\boldsymbol{m}}$	$^{b}\boldsymbol{\theta}_{\boldsymbol{k}}^{\boldsymbol{m}}$	$^{c}\boldsymbol{\theta}_{\boldsymbol{k}}^{\boldsymbol{m}}$		$^{a}\boldsymbol{d}_{\boldsymbol{iP}}$	$^{b}\boldsymbol{d}_{\boldsymbol{iP}}$	$^{c}\boldsymbol{d}_{\boldsymbol{iP}}$
Toes *(Ts)*	+ 9,6	+8,8	+9,0	Ankle *(A)*	81,7	80,2	80,4
Heel *(Hl)*	+5,4	+0,8	-2,8	Knee *(K)*	59,3	58,0	57,4
Shank *(Sh)*	+63,8	+63,7	+62,6	Hip *(H)*	71,1	72,9	74,9
Thigh *(Th)*	+107,5	+111,2	+114,8				
Trunk *(Tr)*	+94,5	+86,7	+83,6				

As Fig. 44 and Table 3 highlight, the assumption of a constant posture of the subject during the experiment was not verified. As it will be further discussed, from the difference between the torques estimated in the unloaded and loaded conditions by the SLLE the torque contribution generated by the variations of body posture have to be compensated in order to obtain the torque generated solely by the weights.

Fig. 45 shows the interaction of the subject's feet with the ground measured by the four force/torque sensors of the iT-Shoes. In the upper plot the sum of the vertical GRF is also depicted as well as its mean values during each phase of the task. The trend of the vertical GRF sum highlights clearly the payload increment during the experiment, while its mean values the accuracy of the iT-Shoes. The error in the estimation of the lifted weight in phase (b) is around the 5,5%, while in the phase (c) is about the 9,5%. The middle plot of Fig. 45 depicts the horizontal GRF in the AKHFE planes. As mentioned previously in the methodology paragraph, the values of the horizontal GRF, computed with respect to the ankle frames, should not be affected by the payload increment. Moreover since there are no external horizontal forces or fast dynamic motions creating horizontal forces (i.e. static friction), the measured horizontal GRF should ideally remain constant and close to zero. However in the middle plot of Fig. 45 can be seen that the horizontal GRF measured by the left and the right iT-Shoe show an increment as the payloads are lifted up. This discrepancy from the expected zero value might be the result of a non-optimal calibration of the force/torque sensors of the iT-Shoes, which seems to not resolve with high precision

the applied wrench at the foot sensor. In our experience, this could be rectified by an adaptation of the calibration mechanical setup and will be considered as part of future work.

On the other hand, in the bottom plot of Fig. 45, the GRT measured by the iT-Shoes are reported. Their trends are similar and consistent with respect to the different phases of the experiment. Indeed, their increment in phase (b) and (c) are determined by the shifting of the subject's body weight on the extremity of the front subassembly of the iT-Shoes and by the payloads lifting. Finally, in Fig. 45 an asymmetry between the interactions measured at the left and right foot can be explained by a slight asymmetry in the subject's stance and feet placement, refer to Fig. 44.

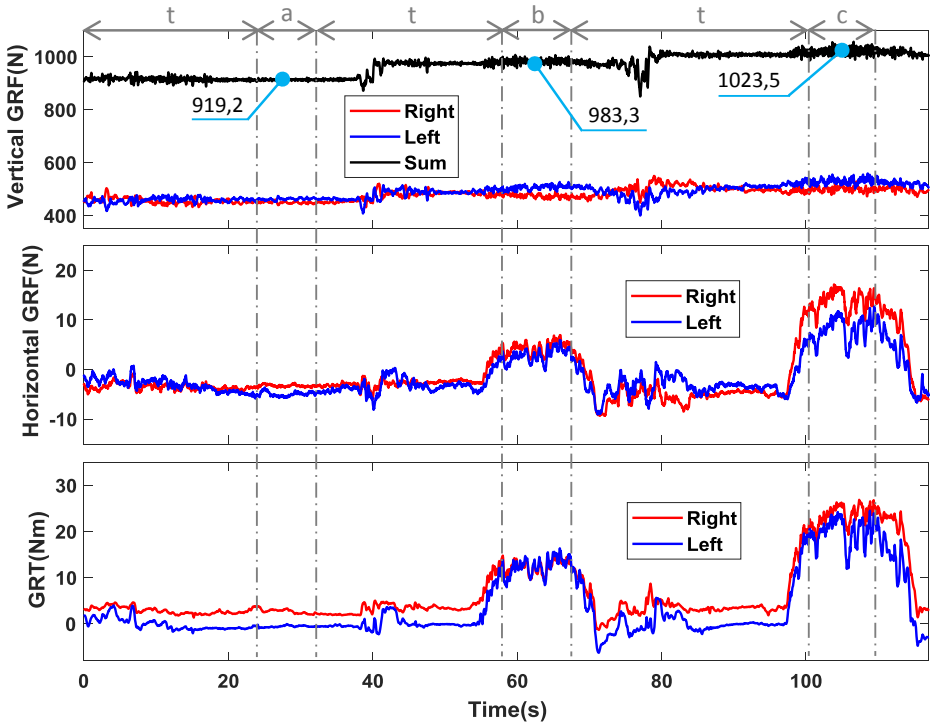

Fig. 45– Measurements of the GRF and of the GRT monitored by left and right iT-Shoe during the lifting task on a 10° upward slope are shown. The values are expressed with respect to the ankle frame, refer to Fig. 21, in the AKHFE planes. In the upper plot the trend of the sum of the GRF is also reported.

The torques estimated by the SLLE method are shown in Fig. 46. The torques show the expected trends according to the lifted weights. For an increment of the payloads, the effort of the extensor muscles of the ankle and of the hip joints increase, while for

the knees the activity of the extensor muscles decrease. Indeed, in phases (b) and (c) the CoM position of all the elements above each leg joint moved progressively toward the payload CoM position, generating the aforementioned effort variation in the leg muscles to balance the action of the gravity.

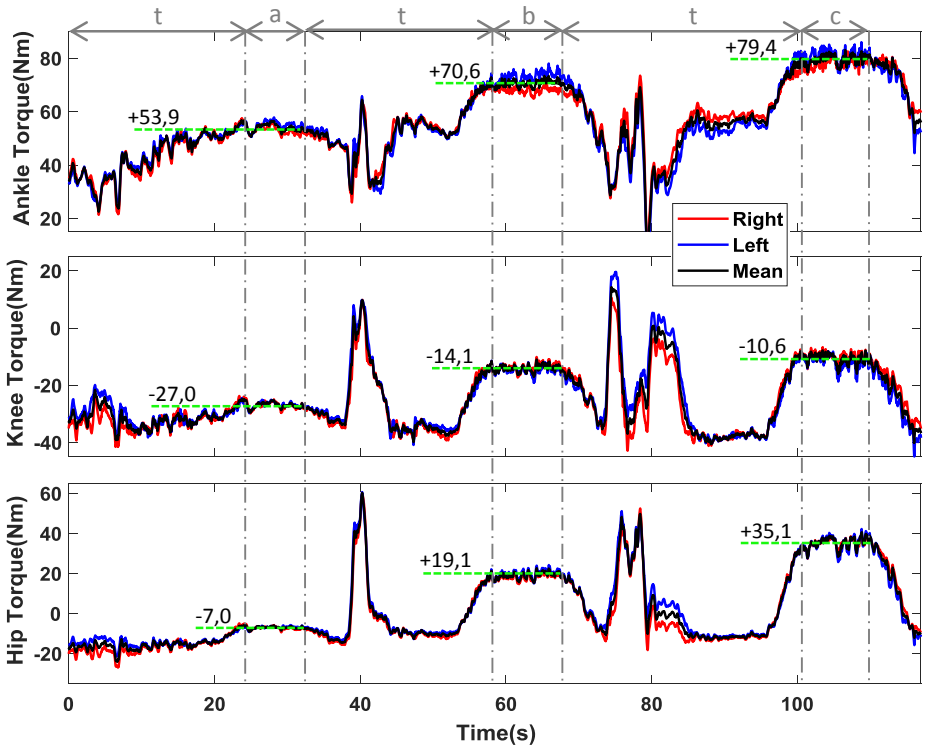

Fig. 46– Torques estimated by the SLLE method for both legs in the AKHFE planes during a lifting task on a 10° upward slope. The values are expressed in the joint coordinate frame, refer to Fig. 21 and Fig. 22. Black lines represent the mean between the right and the left legs, red and blue lines respectively. In each phase the mean value of the black trend is depicted.

To compare the differences between the torque estimated by the SLLE method in the unloaded and loaded conditions with respect to the expected torques estimated by the Optitrack, the torque contributions generated by the variations of body posture had to be compensated. To this end, the influence of the variation of posture was estimated using the implemented lower limbs model and an approximate model for the upper body taking the IMUs outputs. These bias values for the torques at the ankle, knee, and hip were subtracted to the values estimated by the SLLE method, defining the effective torque variation computed by the proposed approach. In Table 4 the effective

torque variations estimated by SLLE are reported. ${}^{ba}\Delta\tau_i^{m^e}$ represents the variation between phases (a) and (b), while ${}^{ca}\Delta\tau_i^{m^e}$ the variation between phases (a) and (c) for each joint (i).

TABLE 4 SLLE METHOD: OUTPUT COMPARISON ON A INCLINED TERRAIN

	SLLE Effective Torque Variation between phases (b-a) and (c-a) (Nm)		**Expected Torque Variation in phases (b-a) and (c-a) (Nm)**		**Percentage Error (between torques)**	
Joint *i*	$^{ba}\boldsymbol{\Delta\tau_i^{m^e}}$	$^{ca}\boldsymbol{\Delta\tau_i^{m^e}}$	$^{ba}\boldsymbol{\Delta\tau_i^{*}}$	$^{ca}\boldsymbol{\Delta\tau_i^{*}}$	$^{ba}\boldsymbol{e_i}$%	$^{ca}\boldsymbol{e_i}$%
Ankle	+19,6	+30,3	+21,7	+35,2	9,6	13,9
Knee	+16,0	+24,5	+15,7	+25,1	1,7	2,6
Hip	+22,1	+36,8	+19,8	+32,8	12,1	12,1

The expected torque variations ($^{ja}\Delta\tau_i^{*}$), calculated using the known weight of the payload (m_jg) and its distance from the joints ($^{j}d_{iP}$) tracked by Optitrack on the transverse plane, are reported in Table 4 and computed in (8). $cos(\gamma^m)$ accounts for the non-parallel disposition of the subject's feet with respect to the sagittal plane projecting in the AKHFE planes the desired torque. The mean of the values in module (γ^m) along the task was almost constant a 23°.

Discussion:

The obtained results validate the iT-Shoes and the SLLE method. Even if the horizontal GRF were not resolved with high precision, the iT-Shoes showed sufficiently accurate measurement of the contact wrenches at the feet. The SLLE method between phases (b-a) and (c-a) get respectively a mean percentage error of $^{ja}e_i$% of 7,8% and 9,5 %. Assuming negligible optical tracking errors in the measurement of $^{j}d_{iP}$, then in phase (b) the 3,1 kg payload held by the subject in each hand is estimated with a mean error of 0,24 kg, while in phase (c) the 4,85 kg payload with 0,25 kg of error. Possible sources of errors in the presented data are: inaccuracies on the upper body model adopted; inaccuracy on the measurement of the feet-ground interactions monitored by the iT-Shoes; errors in the lower limb orientation

measurement (i.e. imperfect alignment of the limbs and the IMUs); inaccuracy in the tracking of the joint positions by imprecise placement of the markers, affecting the calculation of the expected joint torques; errors induced by the approach of tracking only one side of the user's body and assuming a symmetrical body posture with respect to sagittal plane.

5.3.6 Lifting task on an irregular surface

The goal of this experiment was to evaluate the effectiveness of the SLLE method and of the second prototype of the iT-Shoes in estimating the effort generated by the user's lower limbs at the ankles, knees and hips to lift payloads, standing on an irregular terrain, without any information about the user's upper body and about the lifted loads.

Task:

The user was instructed to hold, on an irregular terrain, a specific posture for a few seconds, refer to Fig. 47 with no payload, phase (a), with 3,1 kg weights in each hand, phase (b) and with 4,85 kg in each hand, phase (c). During the task the subject was instructed to keep a symmetrical posture with respect to the sagittal plane. To focus on the results of interest, the transition (t) between each phase of the experiment will be not discussed.

Setup:

As in the previous experiments, the experimental setup was enriched with an IMUs attached to the torso and an Optitrack tracking system. The IMUs was placed on the user's trunk to track its orientation (θ_{Tr}), while the Optitrack tracking system was used to monitor the user's ankle, knee, and hip location as well as the payload's CoM position. To track the payload's CoM location a marker was located at the center of the user's hand and the addition of an appropriate offset was considered. The Optitrack system monitored only the user's left side since a symmetrical posture with

respect to the sagittal plane was assumed to be adopted by the subject during the experiment.

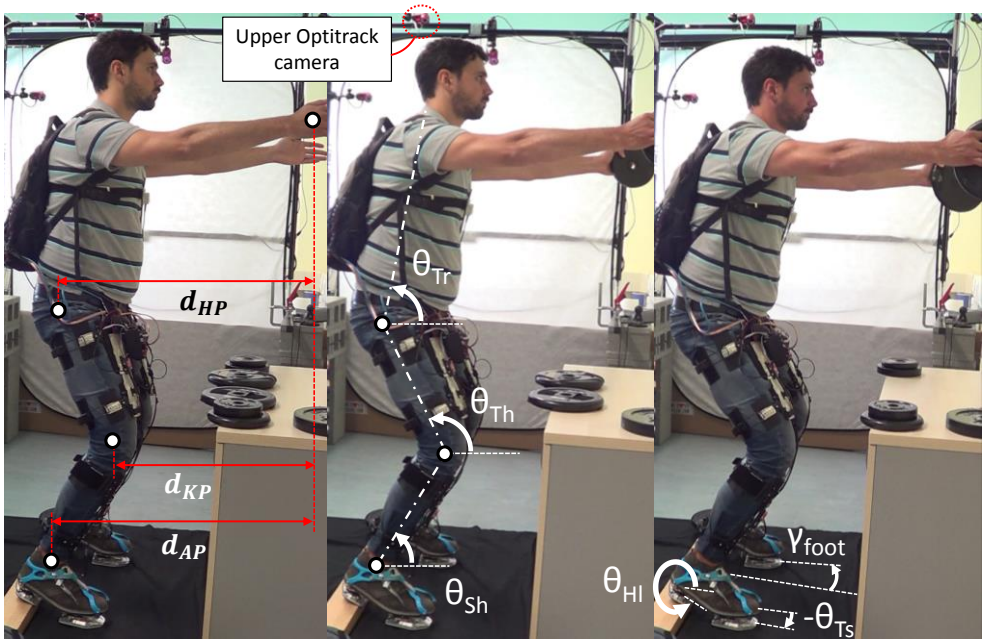

(a) (b) (c)

Fig. 47– The lifting task is shown while the subject was holding a position with no payload (a), with 3,1 kg weights in each hand (b) and with 4,9 kg in each hand (c) on an irregular terrain. In (a) the distances monitored by the Optitrack are depicted.

Methodology:

The procedure adopted in this experiment is the same used in sections 5.3.4 and 5.3.5. To validate the iT-Shoes the values of the GRF measured by the proposed sensing system were analyzed. According with the task described, during the experiment, the horizontal GRF, projected in the ankle frame, as Fig. 21 depicts, should not be affected by the payload increment. Moreover since there are no external horizontal forces or fast dynamic motions creating horizontal forces (i.e. static friction), the measured horizontal GRF should ideally remain constant and close to zero. The vertical GRF, instead, projected in the ankle frame, should vary according with the payload increments. To evaluate the SLLE method the torques computed for the ankle, hip and knee joints between the experimental phases (b-a) and (c-a) were investigated. These torques were compared with the torques generated by the lifted

weights multiplied by the distances, computed by the Optitrack, between each leg joint and the payloads, refer to Fig. 47.c. In the rest of the this section these torques computed by the Optitrack will be referred to as the expected torque variations. Crucial, in this experiment, is the user's ability to maintain a constant body posture between the unloaded and loaded conditions to avoid that the torques variation between the experimental phases (b-a) and (c-a) were generated not only by the payload presence, but also affected by the torque generated by variations of the body posture. Finally, looking at the toque differences between the unloaded and loaded conditions allowed to investigate the ability of the SLLE method to estimate the joint torques without being affected by possible inaccuracies in the parameters adopted for the lower limbs model.

Results:

Although care was taken by the subject, Fig. 48 and Table 5 highlight the subject's difficulty to keep the same posture during the task. The upper and middle plot of Fig. 48 depict the orientation of the user's lower limbs during the experiment, while the bottom plot show the distance of the leg joints with respect to the payload position. Trends of the orientation of the toes (θ_{Ts_R}, θ_{Ts_L}), as well as of the shanks (θ_{Sh_L}, θ_{Sh_R}) highlight the subject's difficulty to maintain a symmetric posture over an irregular terrain. The subject's body posture did not remain constant during the different phases of the task. In particular, in the upper plot is evident the different orientation of the heels (θ_{Hl_R}, θ_{Hl_L}); in the middle plot the orientation of the subject's thighs (θ_{Th_L}, θ_{Th_R}) and trunk (θ_{Tr}) change, while in the bottom plot the distance between the hip and payloads and between the ankle and the payload (d_{AP}, d_{HP}) sensibly vary. This is also visible in Fig. 47 where the distance between the user's head and the upper camera of the Optical track changes, highlighting the bending of the legs and his leaning forward when loaded.

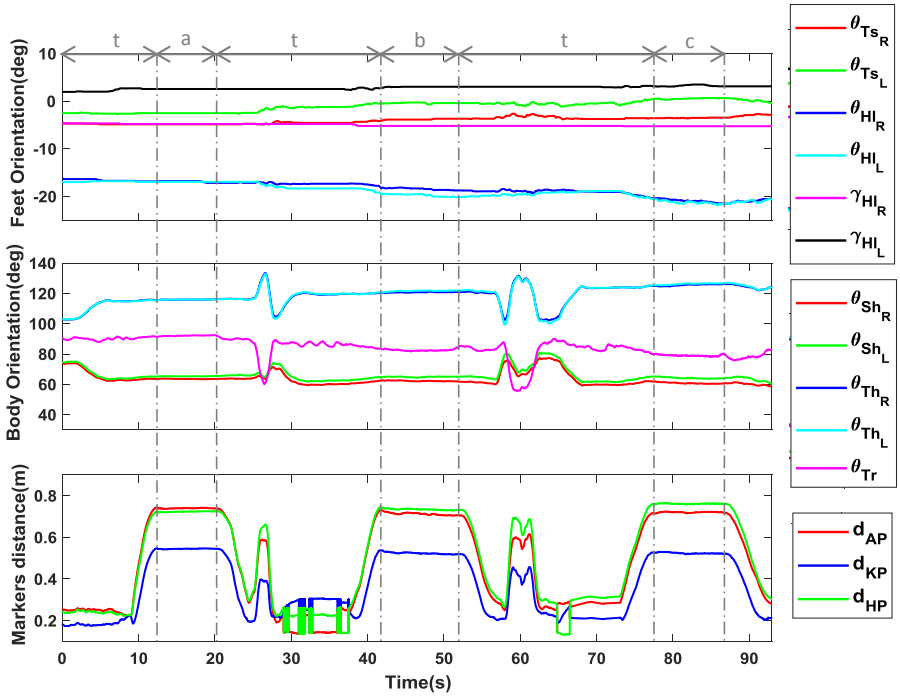

Fig. 48– The upper plot shows the orientation in the AKHFE plane, while the lifting task on an irregular terrain was performed, of the right and left toe ($\theta_{Ts_R}, \theta_{Ts_L}$) and of the right and left heel ($\theta_{Hl_R}, \theta_{Hl_L}$) as well as the placement of the right and left foot with respect to the sagittal plane (γ_R, γ_L); the middle plot presents the pose in the AKHFE plane of the left and right user's shank ($\theta_{\mathrm{Sh}_L}, \theta_{\mathrm{Sh}_R}$), of the left and right user's thigh ($\theta_{\mathrm{Th}_L}, \theta_{Th_R}$) and of the user's trunk (θ_{Tr}) in the sagittal plane; the bottom plot reports the distance in the sagittal plane between each lower joint and payloads. The ankle-payload distance, the knee-payload distance and the hip-payload distance are respectively indicated as d_{AP}, d_{KP} and d_{HP}.

Table 5, on its left part, for each phase (j), reports the mean (m) between the orientation of the left and the right side (${}^{j}\theta_{k}^{m}$) of each type of body segment (k), while, on its right part, the distance (${}^{j}d_{iP}$), in the sagittal plane, between each leg joint (i) and the payload (P) held by the subject are depicted. As Fig. 48 shows, Table 5 highlights the subject's posture variation during the experiment. The mean orientation of the toes (${}^{a}\theta_{Ts}^{m}$) and heels (${}^{a}\theta_{Hl}^{m}$) reflect the irregularity of the terrain, while their trends during loading show evidence of an elongation of the foot plantar fascia due to the payload acceptance. In phases (b) and (c) despite the subject's effort to maintain his posture while loaded, the mean orientation of the thighs, ${}^{b}\theta_{Th}^{m}$ and ${}^{c}\theta_{Th}^{m}$, and of the trunk, ${}^{b}\theta_{Tr}^{m}$ and ${}^{c}\theta_{Tr}^{m}$, differ considerably from those in phase (a).

This can be also noticed in the increasing trend of ${}^{j}d_{HP}$. On the other hand, the orientation of the feet (γ_R, γ_L), following the external-internal rotation of the legs with respect to the sagittal plane, can be considered constant along the task.

TABLE 5 BODY POSTURE VARIATION ON AN IRREGULAR TERRAIN

Body Segment *(k)*	**Mean orientation in the AKHFE plane in phases (a), (b) and (c) (deg)**			**Leg joint *(i)***	**Distance with respect to the payload in the transverse plane (cm)**		
	${}^{a}\boldsymbol{\theta}_{\boldsymbol{k}}^{\boldsymbol{m}}$	${}^{b}\boldsymbol{\theta}_{\boldsymbol{k}}^{\boldsymbol{m}}$	${}^{c}\boldsymbol{\theta}_{\boldsymbol{k}}^{\boldsymbol{m}}$		${}^{a}\boldsymbol{d}_{\boldsymbol{iP}}$	${}^{b}\boldsymbol{d}_{\boldsymbol{iP}}$	${}^{c}\boldsymbol{d}_{\boldsymbol{iP}}$
Toes *(Ts)*	-3,7	-2,1	-1,5	Ankle *(A)*	73,9	72,1	72,0
Heel *(Hl)*	-16,9	-19,0	-21,1	Knee *(K)*	54,5	52,3	52,4
Shank *(Sh)*	+64,5	+63,3	+62,3	Hip *(H)*	72,3	73,4	76,2
Thigh *(Th)*	+116,0	+121,1	+125,9				
Trunk *(Tr)*	+92,1	+82,5	+79,0				

As Fig. 48 and Table 5 highlight, the assumption of a constant posture of the subject during the experiment was not verified. As it will be further discussed, from the difference between the torques estimated in the unloaded and loaded conditions by the SLLE the torque contribution generated by the variations of body posture have to be compensated in order to obtain the torque generated solely by the weights.

Fig. 49 shows the interaction of the subject's feet with the ground measured by the four force/torque sensors of the iT-Shoes. In the upper plot the sum of the vertical GRF is also depicted as well as its mean values during each phase of the task. The trend of the vertical GRF sum highlights clearly the payload increment during the experiment, while its mean values the accuracy of the iT-Shoes. The error in the estimation of the lifted weight in phase (b) is around the 5%, while in the phase (c) is about the 8%. The middle plot of Fig. 49, instead, depicts the horizontal GRF in the AKHFE planes. As mention in the methodology paragraph, the values of the horizontal GRF, computed with respect to the ankle frames, should not be affected by the payload increment. Moreover since there are no external horizontal forces or fast dynamic motions creating horizontal forces (i.e. static friction), the measured horizontal GRF should ideally remain constant and close to zero. However in the

middle plot of Fig. 49 can be seen that the horizontal GRF measured by the right iT-Shoe show an increment as the payloads are lifted up. This discrepancy from the expected zero value might be the result of a non-optimal calibration of the force/torque sensors of the right iT-Shoe, which seems to not resolve with high precision the applied wrench at the foot sensor. In our experience, this could be rectified by an adaptation of the calibration mechanical setup and will be considered as part of future work.

On the other hand, in the bottom plot of Fig. 49, the GRT measured by the iT-Shoes are reported. Their trends are similar and consistent with respect to the different phases of the experiment. Indeed, their increment in phase (b) and (c) are determined by the shifting of the subject's body weight on the extremity of the front subassembly of the iT-Shoes and by the payloads lifting. Finally an asymmetry between the interactions measured at the left and right foot can be explained by the asymmetry in the subject's stance and feet placement, refer to Fig. 48.

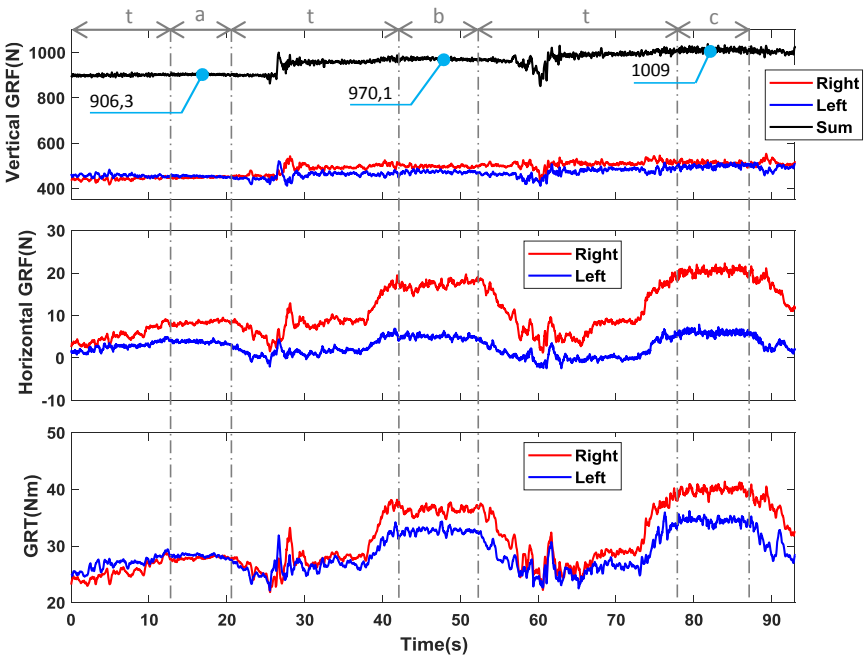

Fig. 49– Measurements of the GRF and of the GRT from the left (Left) and right (Right) iT-shoes in the AKHFE planes with respect to the ankle frame, during the lifting task on irregular terrain, are shown. In the upper plot the trend of the sum of the GRF is also reported.

The torques estimated by the SLLE method are shown in Fig. 50. The torques show the expected trends according to the lifted weights. For an increment of the payloads, the effort of the extensor muscles of the ankle and of the hip joints increase, while for the knees the activity of the extensor muscles decrease. Indeed, in phases (b) and (c) the CoM position of all the elements above each leg joint moved progressively toward the payload CoM position, generating the aforementioned effort variation in the leg muscles to balance the action of the gravity.

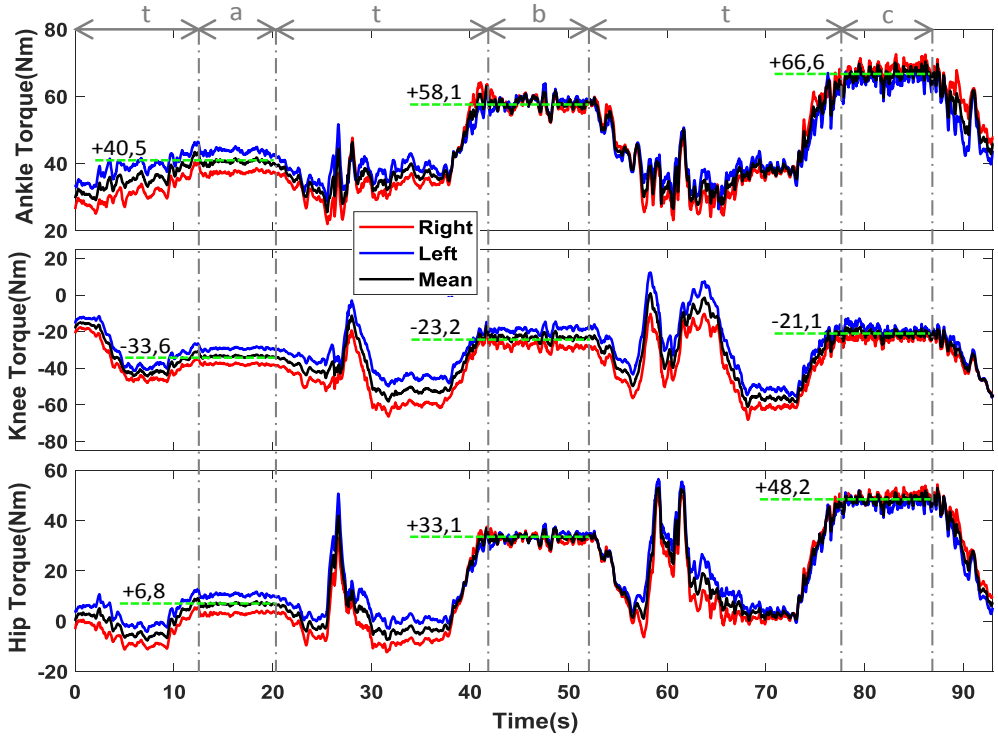

Fig. 50– Torques estimated by the SLLE method for both legs in the AKHFE planes during a lifting task on irregular terrain. The values are expressed in the joint coordinate frame, refer to Fig. 21 and Fig. 22. Black lines represent the mean between the right and the left legs, red and blue lines respectively. In each phase the mean value of the black trend is depicted.

To compare the differences between the torque estimated by the SLLE method in the unloaded and loaded conditions with respect to the expected torques estimated by the Optitrack, the torque contributions generated by the variations of body posture had to be compensated. To this end, the influence of the variation of posture was estimated using the implemented lower limbs model and an approximate model for the upper

body taking the IMUs outputs. These bias values for the torques at the ankle, knee, and hip were subtracted to the values estimated by the SLLE method, defining the effective torque variation computed by the proposed approach. In Table 6 the effective torque variations estimated by SLLE are reported. ${}^{ba}\Delta\tau_i^{m^e}$ represents the variation between phases (a) and (b), while ${}^{ca}\Delta\tau_i^{m^e}$ the variation between phases (a) and (c) for each joint (i).

TABLE 6 SLLE METHOD: OUTPUT COMPARISON ON AN IRREGULAR TERRAIN

	SLLE Effective Torque Variation between phases (b-a) and (c-a) (Nm)		**Expected Torque Variation in phases (b-a) and (c-a) (Nm)**		**Percentage Error (between torques)**	
Joint *i*	${}^{ba}\boldsymbol{\Delta\tau_i^{m^e}}$	${}^{ca}\boldsymbol{\Delta\tau_i^{m^e}}$	${}^{ba}\boldsymbol{\Delta\tau_i^{*}}$	${}^{ca}\boldsymbol{\Delta\tau_i^{*}}$	${}^{ba}\boldsymbol{e_i}\%$	${}^{ca}\boldsymbol{e_i}\%$
Ankle	+21,6	+31,3	+20,9	+34,3	3,4	8,5
Knee	+16,7	+22,9	+15,4	24,9	8,9	8,2
Hip	+23,3	+34,2	+21,6	+36,2	8,0	5,2

The expected torque variations (${}^{ja}\Delta\tau_i^{*}$), calculated using the known weight of the payload (m_jg) and its distance from the joints (${}^{j}d_{iP}$) tracked by Optitrack on the transverse plane, are reported in Table 6 and computed in (8). $cos(\gamma^m)$ accounts for the non-parallel disposition of the subject's feet with respect to the sagittal plane projecting in the AKHFE planes the desired torque. The mean of the values in module (γ^m) along the task was almost constant a 4°.

Discussion:

The obtained results validate the iT-Shoes and the SLLE method. Even if the horizontal GRF were not resolved with high precision, the iT-Shoes showed sufficiently accurate measurement of the contact wrenches at the feet. The SLLE method between phases (b-a) and (c-a) get respectively a mean percentage error of ${}^{ja}e_i\%$ of 6,8% and 7,3 %. Assuming negligible optical tracking errors in the measurement of ${}^{j}d_{iP}$, then in phase (b) the 3,1 kg payload held by the subject in each hand is estimated with a mean error of 0,21 kg, while in phase (c) the 4,85 kg payload

with 0,37 kg of error. Possible sources of errors in the presented data are: inaccuracies on the upper body model adopted; inaccuracy on the measurement of the feet-ground interactions monitored by the iT-Shoes; errors in the lower limb orientation measurement (i.e. imperfect alignment of the limbs and the IMUs); inaccuracy in the tracking of the joint positions by imprecise placement of the markers, affecting the calculation of the expected joint torques; errors induced by the approach of tracking only one side of the user's body and assuming a symmetrical body posture with respect to sagittal plane.

5.3.7 Pushing task

Due to the ability of the iT-Shoes to measure the full contact wrench between the subject and the ground, the goal of this experiment was to validate the iT-Shoes and the SLLE method on a pushing task, where the horizontal GRF, exchanged between the user's feet and the ground, have a relevant importance, refer to Fig. 51.

Task:

A subject was instructed to push on a force torque sensor (model ATI mini45) placed against the wall for a few seconds, phase (a); to stop pushing and only rest the hand on the sensor for few seconds, phase (b). This sequence was repeated several times. Fig. 53 shows a representative pushing cycle. During the experiment the subject was instructed to maintain a body posture constant and symmetric with respect to the sagittal plane.

Setup:

The experimental setup was enriched with an IMUs attached to the torso and an Optitrack tracking system. The IMUs was placed on the user's trunk to track its orientation (θ_{Tr}), while the Optitrack tracking system was used to monitor the user's ankle, knee, and hip location as well as the position of the F/T sensor placed on the wall. To track the F/T sensor location a marker was located at the center of the user's

hand and the addition of an appropriate offset was considered. The Optitrack system monitored only the user's left side since a symmetrical posture with respect to the sagittal plane was assumed to be adopted by the subject during the experiment.

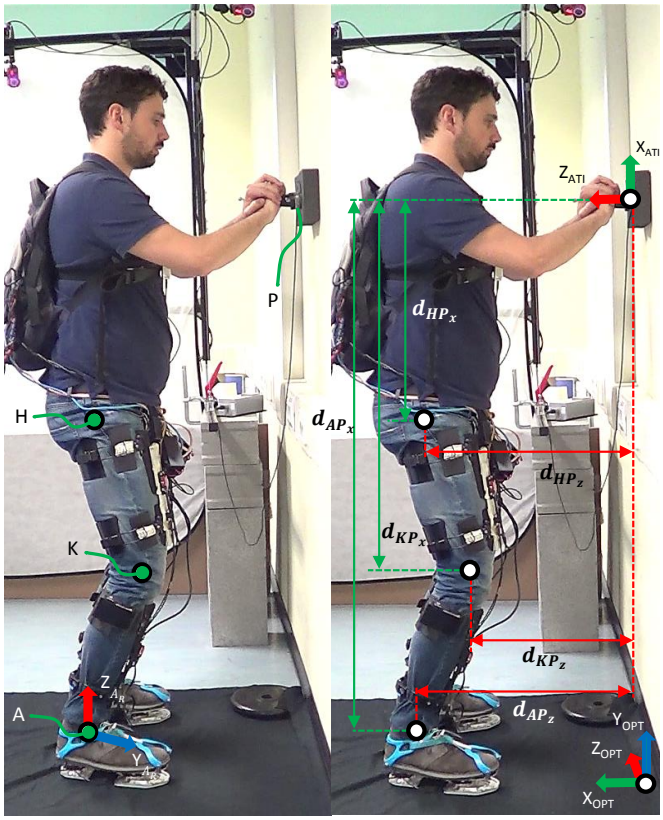

(a) (b)

Fig. 51– The pushing task against the wall is shown in phases: (a) while the subject was keeping the hands in contact with the ATI F/T sensor; in (b) while he was pushing against it. Between the ATI F/T sensor and the wall a deformable object was placed to visually highlight the subject's action. In (b) the distance used for the computation of the joint torques.

Methodology:

To validate the iT-Shoes the values of the GRF measured by the proposed sensing system were compared with the forces measured by the F/T sensor during the user's upper body interactions with the wall. In particular, the horizontal GRF, projected in the ankle frame as Fig. 21 depicts, should result equivalent to the forces measured by the F/T sensor in its *y-z* plane, refer to Fig. 51.b. The vertical GRF, instead, without

considering the user's body weight, should be equivalent to the forces generated by the user's upper body during the interaction with the wall along the X_{ATI} direction. To evaluate the SLLE method the torques computed for the ankle, hip and knee joints between the two experimental phases were investigated. These torques were compared with the torques computed using the posture measured by Optitrack and the upper body interaction loads measured by the ATI F/T sensor placed on the wall, refer to Fig. 51.b. In the rest of the this section these torques computed by the Optitrack will be referred to as the expected torque variations. Crucial, in this experiment, is the user's ability to maintain a constant body posture between the pushing and resting conditions to avoid that the torques variation between the experimental phases were generated not only by the interactions generated by the subject's action against the wall, but also affected by the torque generated by variations of the body posture. Finally, looking at the torque differences between the unloaded and loaded conditions allowed to investigate the ability of the SLLE method to estimate the joint torques without being affected by possible inaccuracies in the parameters adopted for the lower limbs model.

Results:

Posture data for this test are shown in Fig. 52 and summarized in Table 7. In particular, Fig. 52 depicts, along the all experiment, the orientation of the feet (upper plot), of the shanks, thighs and trunk (middle plot) as well as the distance between each leg joint and the F/T sensor placed on the wall. Table 7, for phases (a) and (b), reports the mean (m) orientation between the user's lower limbs, the trunk's inclination and the distance between each leg joint and the F/T sensor placed on the wall. Data show a small variation of the posture between phases, which is expected since the subject was putting effort into the pushing task. Nevertheless, their values allow to considered constant the user's posture during the experiment.

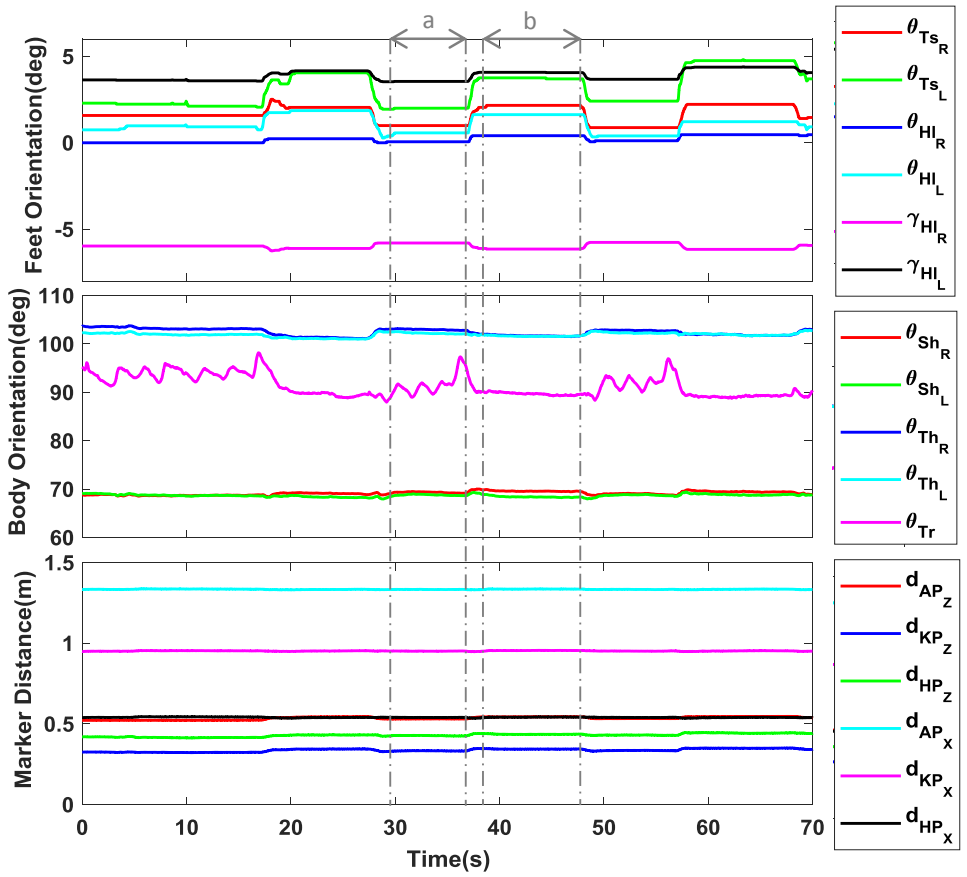

Fig. 52– The upper plot shows the orientation in the AKHFE plane, while the pushing task was performed, of the right and left toe ($\theta_{Ts_R}, \theta_{Ts_L}$) and of the right and left heel ($\theta_{Hl_R}, \theta_{Hl_L}$) as well as the placement of the right and left foot with respect to the sagittal plane (γ_R, γ_L); the middle plot presents the pose in the AKHFE plane of the left and right user's shank ($\theta_{\mathrm{Sh}_L}, \theta_{\mathrm{Sh}_R}$), of the left and right user's thigh ($\theta_{\mathrm{Th}_L}, \theta_{Th_R}$) and of the user's trunk (θ_{Tr}) in the sagittal plane; the bottom plot reports the distance in the sagittal plane between each lower joint and payloads. The ankle-payload distance, the knee-payload distance and the hip-payload distance are respectively indicated as d_{AP}, d_{KP} and d_{HP}.

TABLE 7 PUSHING TASK: BODY POSTURE VARIATION

Body Segment *(k)*	**Mean orientation in phases (a) and (b) (deg)**		**Leg joint** *(i)*	**Distance with respect to the payload (m)**			
	$^{a}\boldsymbol{\theta}_{\boldsymbol{k}}^{\boldsymbol{m}}$	$^{b}\boldsymbol{\theta}_{\boldsymbol{k}}^{\boldsymbol{m}}$		$^{a}\boldsymbol{d}_{\boldsymbol{iP}_x}$	$^{b}\boldsymbol{d}_{\boldsymbol{iP}_x}$	$^{a}\boldsymbol{d}_{\boldsymbol{iP}_z}$	$^{b}\boldsymbol{d}_{\boldsymbol{iP}_z}$
Toes *(Ts)*	+1,5	+3,0	Ankle *(A)*	1,333	1,336	0,532	0,544
Heel *(Hl)*	+0,3	+1,0	Knee *(K)*	0,951	0,955	0,333	0,344
Shank *(Sh)*	+69,0	69,0	Hip *(H)*	0,540	0,542	0,427	0,435
Thigh *(Th)*	+102,6	+101,7					
Trunk *(Tr)*	+92,1	89,7					

Fig. 53 shows the GRF measured by the iT-Shoes and the wrench measured by the ATI sensor at the hands. Care was taken to keep the *x* axis of the ATI frame aligned with the *z* axis of the of the iT-Shoes. Then, the GRF in the transverse plane (transvGRF) and the difference between the vertical GRF and the body weight (vGRF –BW) can be respectively associate with the ATI_{Fyz} and ATI_{Fx} to compare the forces exchange at the wall and at the ground level. Both phases are clearly perceived by the iT-Shoes and a good overlap among the transvGRF and the ATI_{Fyz} can be noticed.

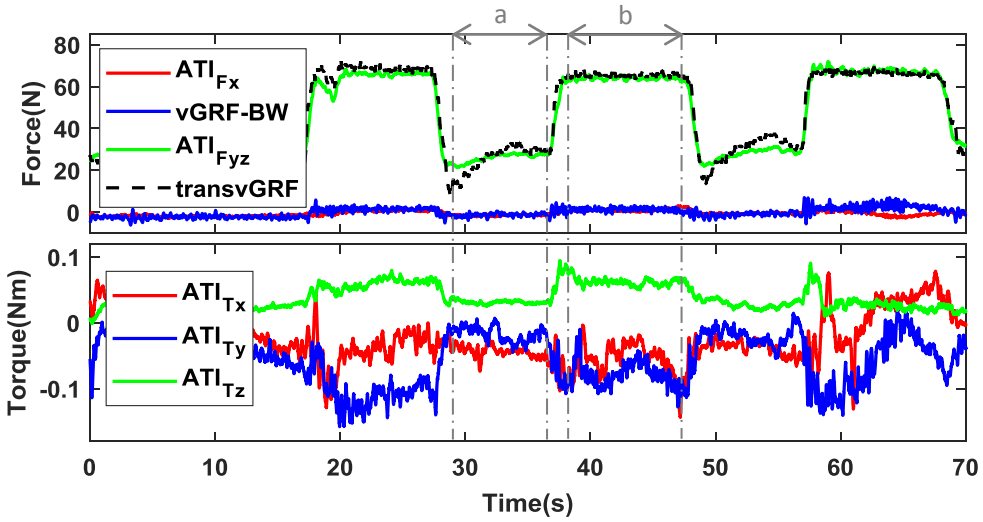

Fig. 53– The loads measured by the wall sensor, during the pushing task, are reported. ATI_{Fyz} represents the vector sum of the forces monitored by the wall F/T sensor on its *yz* plane. transvGRF and vGRF-BW represent respectively the vector sums of the forces measured by the iT-Shoes in the xy plane of the ankle frame and the vertical GRF minus the body weight value.

In Fig. 54 the GRF and the GRT are reported. Despite a similarity in the posture between the left and right side of the subject's body, the GRF and GRT reveal an asymmetry to the distribution of loads between the left and the right.

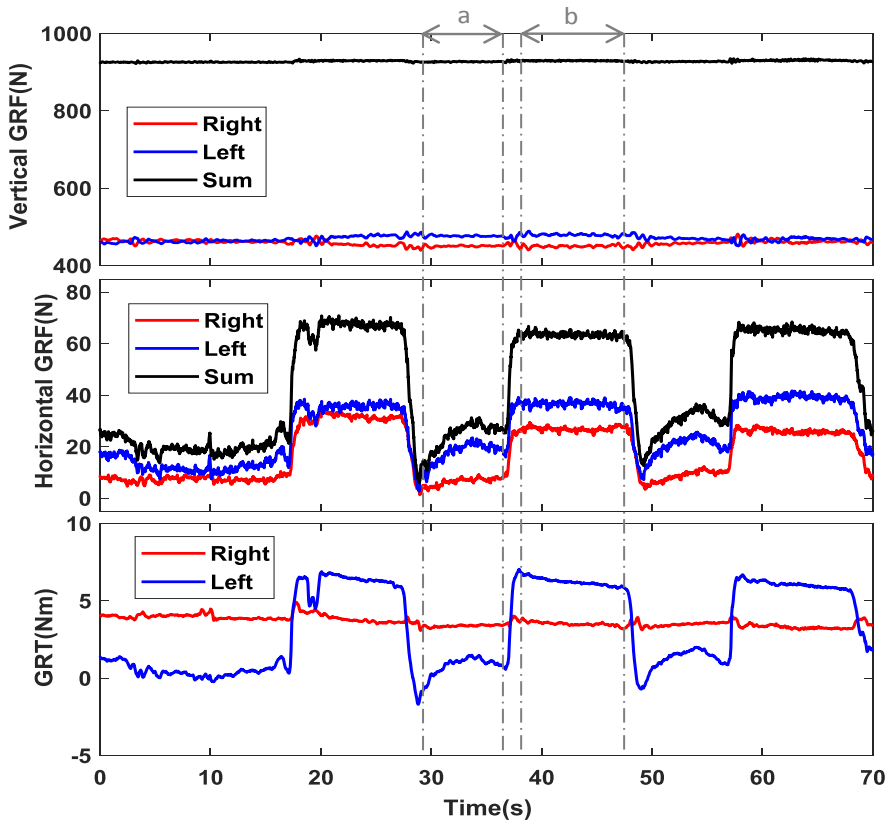

Fig. 54– The feet GRF and the GRT in the AKHFE planes during the pushing task are reported. The Left and Right trends represent for each foot the mean value between the forces or torques monitored by the iT-Shoes at the subject's heel and toe area.

The torques estimated by the SLLE method are depicted in Fig. 55 and summarized Table 8. In Fig. 55 the outputs of SLLE show a clear detection of the different phases of the experiment. The subject's pushing action against the wall causes a decrease to the effort at the ankles and an increase to the effort of the knees and hips while pushing and trying to maintain the same body posture. In (b) asymmetries in the estimated torques for the left and right side of the subject's leg joints are present. This can be explained by the subject's difficulty to push against the wall with the same intensity on each arm and the difficulty to maintain a strictly symmetrical posture.

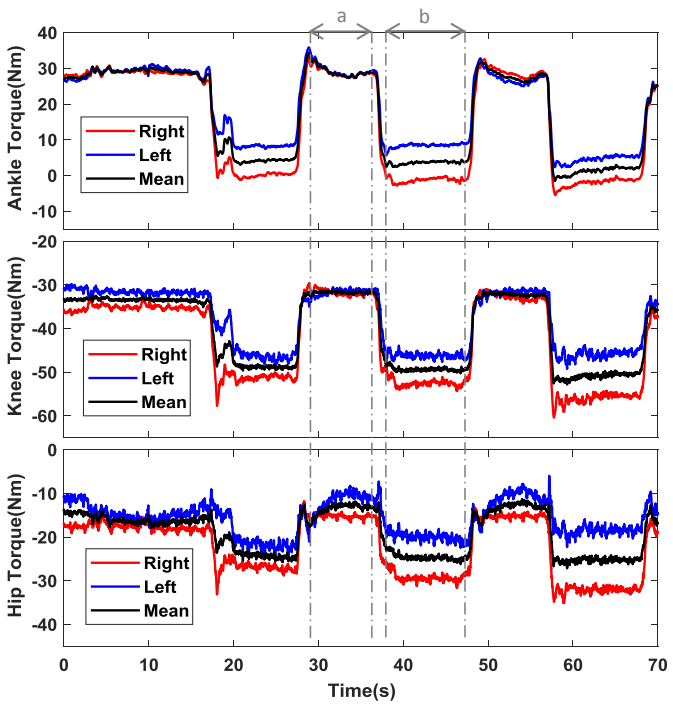

Fig. 55–Torques by the SLLE method for both legs in the AKHFE planes during the pushing task. Black lines represent the mean between the torque estimated on the right (red trend) and on the left (blue trend) side.

TABLE 8 PUSHING TASK: THE SLLE ESTIMATED TORQUES

	SLLE Torque Variation torque in phases (a) and (b) (Nm)		**Standard deviation of the mean torque in phases (a) and (b) (±Nm)**	
Joint *i*	$^{a}\boldsymbol{\tau}_{i}^{m}$	$^{b}\boldsymbol{\tau}_{i}^{m}$	$^{a}\boldsymbol{\sigma}_{\tau_i^m}$	$^{b}\boldsymbol{\sigma}_{\tau_i^m}$
Ankle	+29,2	+3,6	0,3	4,9
Knee	-31,8	-49,6	0,5	3,3
Hip	-12,1	-23,6	3,2	6,3

TABLE 9 PUSHING TASK: COMPARISON OF SLLE ESTIMATED AND EXPECTED TORQUE DIFFERENCES

	SLLE Estimated Torque Difference between phases (b-a) (Nm)	**Expected Torque Difference between phases (b-a) (Nm)**	**Percentage Error (between torques)**
Joint *i*	$\boldsymbol{\Delta\tau_i^{m^e}}$	$\boldsymbol{\Delta\tau_i^{*}}$	$\boldsymbol{e_i}^{\%}$
Ankle	-26,2	-24,8	5,8
Knee	-17,7	-17,8	0,4
Hip	-9,4	-9,8	4,6

The torque difference estimated by SLLE for each leg joint ($\Delta\tau_i^{m^e}$), between phase (a) and (b), and the expected torque differences ($\Delta\tau_i^*$), where *i* represent a lower joint, are reported in Table 9. $\Delta\tau_i^*$ are computed by (9) and they represent the torques generated by the increment of the torque ($\Delta\tau_y$) and of the forces (ΔF_{xz}) monitored by the ATI sensor in its *x*-*z* plane.

$$\Delta\tau_i^* = \left(\Delta\tau_y + \Delta F_{xz} \text{ x } {}^b d_{iP}\right) cos(\gamma^m)\, 0{,}5 \quad (9)$$

where ${}^b d_{iP}$ represents the distance between the ATI sensor and each leg joint in the sagittal plane, computed as the difference between the markers monitored by the optical tracking system with the assumption of a parallel disposition between the sagittal plane, the *x*-*z* plane of the ATI sensor and the *x*-*y* plane of Optitrack, refer to Fig. 51.b. A coefficient of 0,5 is add to the formula to considered only the expected torque differences that the joints of a single leg should generate. Finally $cos(\gamma^m)$ accounts for the non-parallel disposition of the subject's feet with respect to the sagittal plane, projecting the desired torque on the AKHFE planes. A value of 5° was registered for γ^m as mean between γ_R and γ_L.

Discussion:

The obtained results validate the iT-Shoes and the SLLE method. In particular iT-Shoes showed sufficiently accurate measurement of the GRF, while the SLLE method was capable of resolving the pushing task. As Table 9 reports, the $e_i{}^{\%}$ between the estimated torque variations and the expected torque differences does not exceed the 5,8% for each joint.

5.4 iT-Knee Bipedal System

This section presents two different assistive tasks conducted with the iT-Knee Bipedal System. In particular an assisted lifting task and an assisted walking task are described. These experiments aim to test the capability of iT-Knee exoskeleton to deliver the requested assistance to the user's knees and to test the capability of iT-Shoes and of the SLLE method to estimate online the torque generated by the user's knees while a dynamic task is performed.

5.4.1 Assisted lifting task

This experiment assess the capability of the iT-Knee Bipedal System to apply an assistive torque to the user's knees while a lifting task is performed.

Task:

A subject, wearing the iT-Knee Bipedal System and carrying 5 kg in each hand, with the arms initially resting along the body, was instructed to squat from a standing position, phase (a), to lift his arms bringing the payload in front of him, phase (b), to hold this posture for a few seconds, phase (c), before bringing back his arms down along the body, phase (d). The user kept the torso vertical during the entire task. The motion is depicted on Fig. 56.

Methodology:

To assist the user according with his motion, the torque inputs (τ_d) for the torque controllers of the exoskeleton motors were settled as the 20% of the knees torques estimated by the SLLE method, see Fig. 57. The experiment was performed with the first prototype version of the iT-Shoes and the ankles' torques were computed by the SLLE method based on (4).

(a) (b) (c) (d)

Fig. 56– Different body postures corresponding, from right to left, to the user's motion during the phases "a", "b", "c" and "d" defined in Fig. 58.

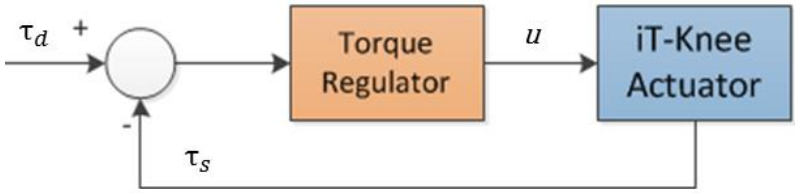

Fig. 57– Torque control scheme of the iT-Knee devices.

Results:

The upper plot of Fig. 58 depicts the torques, estimated by the SLLE method, that the user's knees were generating to performed the described task. Trends show the capability of the SLLE method to account for changes of the payload's CoM location in the calculation of the knees' torques. In the middle plot of Fig. 58, both the reference torque and the actual torques applied by the knee exoskeletons are presented. Their trends are mostly overlapped. This exhibits the capability of the iT-Knee exoskeleton to provide the required assistance in static condition to the user's knees. Finally the bottom plot of Fig. 58 depicts the vertical GRF monitored by the first version of the iT-Shoes.

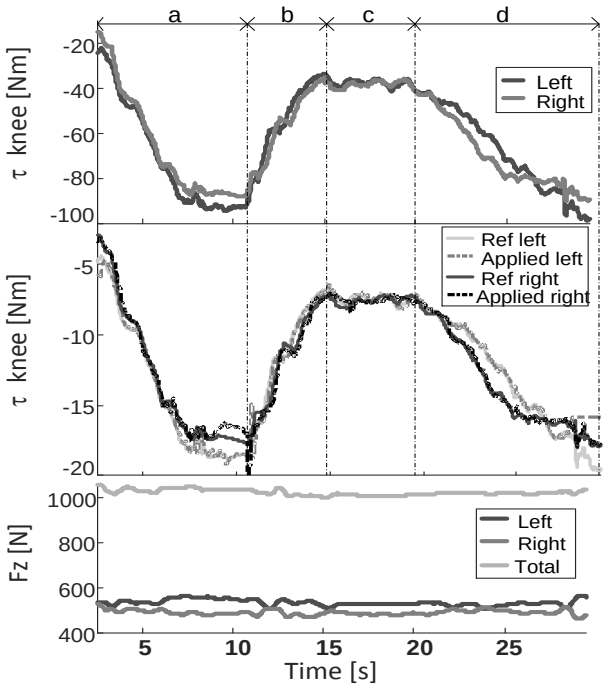

Fig. 58– The upper plot shows the torque generated at the knees joints (Left and Right), estimated by the proposed method (SLLE), while the subject was performing the motions represented in Fig. 56; the middle plot presents the assistive torque references (computed as 20% of the estimated torques) and the applied torques; the bottom plot reports the vertical force of the user carrying the payload (Total) as measured by the foot force sensors (Left and Right).

Discussion:

The experimental results presented in this section indicate: the capability of the SLLE method to effectively estimate the knee torques required to maintain the whole body balance while an object of considerable mass is lifted without a priori information of its mass and its CoM location during the task; the capability of the iT-Knee exoskeleton to provide, in static condition, the required assistive torque to the user's knees. Finally, the subject reported a positive experience with respect to the system's wearability (i.e. attachments of the exoskeleton) and with respect to its ergonomics during the torque delivering.

5.4.2 Assisted walking task

The objectives of this experiment were twofold. Firstly, to test the hardware of the iT-Knee Bipedal System in a locomotion task. Secondly, to test the control architecture of the iT-Knee Bipedal System in providing assistance in a sequence of different and not periodic activities, such as walking on flat terrain and climbing stairs.

Task:

A subject was assisted by the iT-Knee Bipedal System while he was walking on a flat surface and climbing stairs, shown in Fig. 59. In particular, the flexion/extension of the knees were assisted by the iT-Knee exoskeletons. Torque references for the iT-Knee actuators were generated based on the values estimated online by the SLLE method and modulated by the implemented state machine, refer to Section 4.3.1. In particular, in State 1 the torque references for the iT-Knee actuators (τ_{des}) was set to 40% of the torque estimated by the SLLE (τ_{c}). A maximum torque of 25 Nm was imposed to ensure safety.

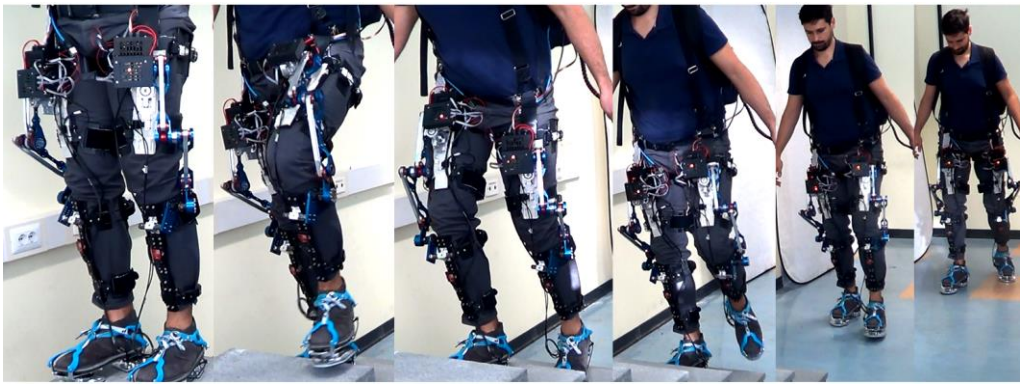

Fig. 59–The assistive task conducted with the iT-Knee Bipedal System.

Methodology:

To test the effectiveness of the iT-Knee Bipedal System, the interactions with the ground, monitored by the iT-Shoes, and the assistive torques, delivered by the iT-Knee exoskeletons, were recorded. Then, the compatibility of their trends across the different phases of the experiment were analyzed. On the other hand, to test the

robustness of the implemented assistive control strategy, the torque references generated for the iT-Knee exoskeletons and the evolution of the state machines during the task were recorded. Hence, the compatibility of their trends with the different phases of the task were investigated.

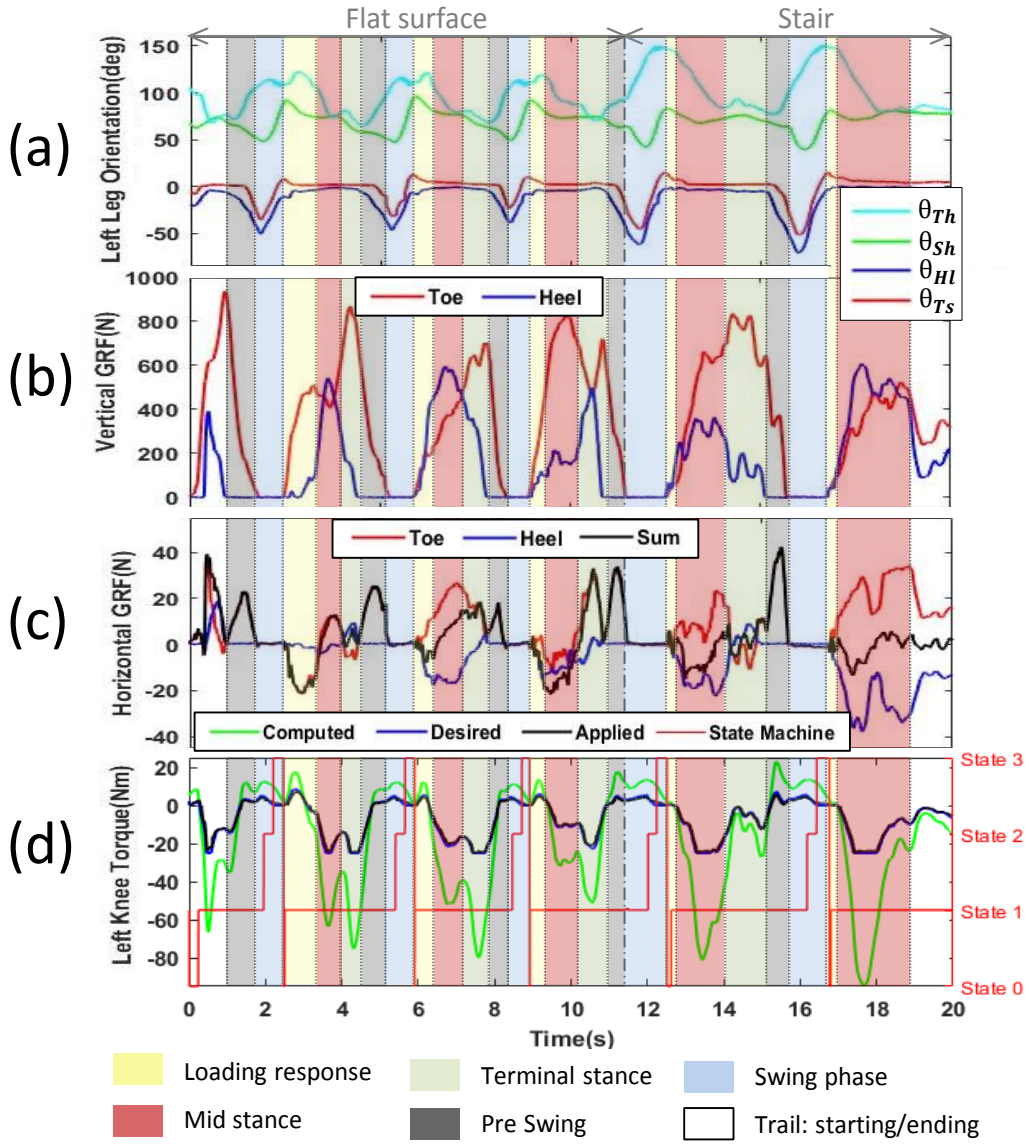

Fig. 60– In (a): θ_{Hl}. θ_{Ts}, θ_{Sh}, and θ_{Th} represent the orientation of the user's left heel, toe, shank and thigh in the AKHFE plane. In (b) and (c) the vertical and the horizontal ground reaction forces at the toe and heel measured by the left foot iT-Shoe in the AKHFE plane are shown. In (d) the knee torque estimated by SLLE, the desired torque generated by the state machine, the applied torque measured by the torque sensor of the iT-Knee actuator, described in [65], and the state of the state machine are depicted.

Results:

Fig. 60 shows representative plots of relevant signals of the assistive exoskeleton system and the SLLE method during walking and stair climbing for the different phases of the gait. These phases have been defined based on [56] and are represented by different background colors of the plot canvas. With the assumption of symmetrical behavior of the body with respect to the sagittal plane, data only of the left iT-Knee, iT-Shoe and state machine are presented. In particular, the upper plot of Fig. 60 shows the orientation of the body segments of the left lower limb of the subject; in Fig. 60.b and Fig. 60.c the vertical and horizontal GRF are depicted; while, in Fig. 60.d the knee torque estimated by SLLE, the desired torque generated by the state machine, the applied torque measured by the torque sensor of the iT-Knee actuator as well as the evolution of the state machine along the task are reported.

Discussion:

The transition between the two activities of the experiment (i.e. the walking task on a flat surface and the stair climbing task) is clearly highlighted by an increase in the amplitude and period of the measured link angles. The non-periodicity of the gait cycle is especially evident while the subject was walking on a flat surface. In particular, the vertical GRF highlight how the areas of the foot that go as first in contact with the ground can be different at each step.

Based on [56], the subject's gait is decomposed in its phases in order to analyze the trend of the GRF and of the torque computed by SLLE (τ_C). The loading response phase, characterized by the impact of the foot with the ground, is more evident during the walking phase rather than the climbing one. It is defined by: the acceptance of the weight as the GRF depict; by a knee flexion as the peak of θ_{Th} describes; and by the contraction of the muscles responsible for the flexion of the knee as the positive value of τ_c represents. The mid stance is characterized by peaks of the negative τ_c representing the activation of the knee extension muscles (quadriceps) to counteract the action of gravity. The transition from mid to terminal stance during walking is characterized by a gradual decrease of the vertical GRF at the heel, an increase of the

vertical GRF at the toe and a momentary decrease of the τ_c. This is followed by a negative peak of τ_c in the terminal stance representing the knee's extension effort for propulsion in the direction of motion of the body. The pre-swing phase is characterized by the toe push off, seen as a peak in the horizontal GRF signal at the toe, to finalize the leg propulsion. The toe push off in the pre-swing phase is assisted by the exoskeleton as seen in the positive peaks of τ_c while in the swing phase continues to provide a positive τ_c representing an assistance to lift the shank.

During the experiment, the state machine went through its states in a cyclic manner as shown in Fig. 60.d. In particular, the state machine was able to detect the different phases of the gait cycle even if the subject walked on different terrains with a non constant velocity. Torque control performances are depicted in the bottom plot, where a good overlap between the desired (τ_{des}) and the applied torque is shown. The applied torque was monitored by the torque sensor in the iT-Knee actuator.

Finally, the subject reported that, especially in the loading response phase, the assistive action of the exoskeletons was clearly perceived. In these phases, the exoskeleton was felt acting as a parallel spring with respect to the knee helping the leg to absorb the initial impact with the ground.

6 CONCLUSIONS AND FUTURE WORK

6.1 Conclusion

Exoskeletons have a huge potential impact in our future society. People with disabilities, elderly people as well as post-surgical patients and healthy subjects could benefit from such technology in their everyday life. The work presented in this thesis was focused on the design, development and control of a lower limb exoskeleton for elderly and healthy people, the iT-Knee Bipedal System. Such a device aims to assist the flexion/extension of the human knees with improved ergonomics and intuitive use. Such aspects are fundamental for the acceptance of this wearable technology. The conclusion of these studies are addressed below.

6.1.1 Design Aspects

In order to become widespread in the society as wearable devises, exoskeletons should exhibit fast donning, removal and setup procedures, agile adaptability to different users' sizes, ergonomics, compactness and lightness. Their kinematics should be fully coupled with the assisted joints in order to not reduce the users' mobility and to not generate undesired forces that would lead in discomfort.

To this end, part of the work presented in this thesis was focused on the design of a novel knee exoskeleton capable of addressing some of the aforementioned mechanical requirements. In particular, the iT-Knee exoskeleton does not impose motion constraints to the user's knees, while it minimizes the parasitic forces and torques generated on the skin by its attachment points. This is achieved thanks to the design of a novel under-actuated 6-DoF mechanism that makes the iT-Knee exoskeleton fully

kinematic coupled with the assisted joint. Moreover, its 5 passive DoF make the structure fast to wear, setup and remove, while they also make it self-adjustable to different users' size.

The study of the human knee biomechanics was the starting point of the design process of the iT-Knee exoskeleton. In particular, the kinematics and the range of motion of the knee joint were analyzed. This information defined the requirements that the iT-Knee exoskeleton had to satisfied in order to result fully kinematic coupled with the human knee. Structural requirements were then derived from data of a standing-up motion obtained from the literature. The actuation unit was selected as the trade of between the requirements defined by a standing-up motion and the walking activity. Even if being a prototype, iT-Knee targets an overall compact design with low mass/inertia and a small form factor. Finally, as distinguish characteristic, the iT-Knee exoskeleton, on the thigh area, as distinguishable characteristic, on the thigh area, the iT-Knee exoskeleton favors a frontal over the more classical lateral implementation/mounting of the actuation and transmission mechanisms. Experiments confirmed the ergonomic performance of the iT-Knee exoskeleton in terms of unconstrained user's RoM, pure torque transmission along with the mechanism and the reduction of the parasitic forces and torques generated at the user's skin.

Another important aspect to improve the effectiveness of exoskeletons in daily life scenarios is their sensing system. In unknown environments, where, for safety reasons, preplanned behaviors are not recommended, an accurate monitoring of the user's state is necessary. Moreover, in outdoor scenarios, this information should be acquired by portable sensing systems in order to not reduce the user's workspace. To this end, in this work, the design of a novel sensing system to monitor the interactions of the user's feet with the ground was presented. In particular, the iT-Shoe is a sensorized add-on system for shoes that integrates two 6axis Force/Torque sensors with dedicated embedded MEMS IMUs in their electronic to monitor respectively the full contact wrench and the feet orientation. Thanks to their design, iT-Shoes accommodate the plantar flexion and they are adjustable to different users' foot size. Experiments confirmed the effectiveness and reliability of the system on different ground

conditions (i.e. flat ground, upward slope, irregular terrains and stairs) and task typologies (i.e. payloads holding, payloads lifting, pushing task, walking).

6.1.2 Control Aspects

The control system of an assistive/power augmentation exoskeleton is responsible to detect the user's intentions and properly modulates the assistance of exoskeletons synchronously with such information. These aspects are even more crucial in daily life scenarios where irregular and noncyclic locomotion activities, unexpected ground conditions as well as unpredicted interactions with the environment can occur. As a consequence, a call for control strategies that exhibit robust behaviors in such operative conditions is issued. Moreover, if exoskeletons want to be used outdoor, their control strategies should rely on sensory information that are portable, ergonomic and as less invasive as possible. To achieve this, thanks to the development of the iT-Shoes, a novel method to estimate online the torques experienced by the user's ankles, knees and hips, the SLLE method, was presented. As major advantage, the proposed method does not require any information of the user's upper body (i.e. pose, weight and center of mass location) or on any interaction of the interaction of the user's upper body with the environment (i.e. payload handling or pushing and pulling task). Thanks to the knowledge of the user's feet-ground interactions, the method applies an inverse dynamic approach on the user's lower limbs to estimate online the torque at each user's leg joint. A fully wearable, ergonomic and portable setup is achieved since a minimalistic sensory system is required. Indeed, only sensorized shoes, to monitor the orientation of the feet and their interaction with the ground, and IMU sensors, to track the orientation of the shanks and thighs, are necessary. Finally, based on the torques estimated by the SLLE method, a state machine has been developed to generate reference torques for the actuators of the iT-Knee Bipedal System in order to modulate their assistance synchronously with the phases of walking tasks. The state machine combines posture and interaction force measurements that allow the design of more robust control strategies in daily life scenarios. Experimental results showed the

effectiveness and the validity of the SLLE method system on different ground conditions (i.e. flat ground, upward slope, irregular terrains and stairs) and task typologies (i.e. payloads holding, payloads lifting, pushing task, walking). Finally, an assistive walking-climbing task was performed with the iT-Knee Bipedal System to highlight the efficacy of the implemented state machine and the potentiality of the entire system.

6.2 Future work

A number of possible future research activities are suggested by the work reported in this dissertation:

- Enhancement of the iT-Knee exoskeleton design (i.e. mechanism and actuation unit disposition), presented in Chapter 3.2, to reduce its form factor .

- Extension of the iT-Knee exoskeleton to the hips and ankles in order to design a modular and configurable full lower limb exoskeleton.

- Enhancement of the attachment area of the iT-Knee to improve the system ergonomics.

- Enhancement of the iT-Shoes, presented in Chapter 3.3, to obtain a more accurate sensing system, compact and light, to be used in dynamic tasks.

- Extension of the SLLE method, presented in Section 4.3.1, to dynamic effects.

- Enhancement of the skeletal model of the human's lower limbs adopted by the SLLE method to account for the complexity of the human biomechanics.

- Perform a statistical analysis on the results of the SLLE method, to better show the significance level of the results compared to the golden standard.

- Development of a method to estimate subject-specific body parameters such as the length of his segments, their masses and inertia. This allows obtaining more accurate results from the SLLE method.

- Enhancement of the state machine, presented in Section 4.3.1, toward the detection of an increased number of user's state. This will improve the robustness of the control system of the iT-Knee Bipedal System.

- Implementation of different control strategies with respect to the user's intentions detected by the proposed state machine. This will increase the adaptability of the system to the different user's needs.

- Testing the effectiveness of the exoskeleton system from a metabolic cost point of view, involving a higher number of users.

- Testing the exoskeleton system while it assists the user's walking on different types of terrains.

- Testing the iT-Knee Bipedal System in more demanding conditions, when the exoskeleton has to provide more assistance to the user, exceeding the limit of 25 Nm as maximum output torque.

7 REFERENCES

[1] N. Yagn, "Apparatus for facilitating walking," ed: Google Patents, 1890.

[2] V. Patoglu, "Exoskeleton," ed: Google Patents, 2012.

[3] H. A. M. Engineering. (2016). *Lokomat Rehabilitation Device*. Available: www.hocoma.com

[4] J. F. Veneman, R. Ekkelenkamp, R. Kruidhof, F. C. T. v. d. Helm, and H. v. d. Kooij, "Design of a series elastic- and Bowden cable-based actuation system for use as torque-actuator in exoskeleton-type training," in *Rehabilitation Robotics, 2005. ICORR 2005. 9th International Conference on*, 2005, pp. 496-499.

[5] N. Vitiello, T. Lenzi, S. Roccella, S. M. M. De Rossi, E. Cattin, F. Giovacchini, *et al.*, "NEUROExos: A Powered Elbow Exoskeleton for Physical Rehabilitation," *Robotics, IEEE Transactions on*, vol. 29, pp. 220-235, 2013.

[6] B. Celebi, M. Yalcin, and V. Patoglu, "AssistOn-Knee: A self-aligning knee exoskeleton," in *Intelligent Robots and Systems (IROS), 2013 IEEE/RSJ International Conference on*, 2013, pp. 996-1002.

[7] Y. Sankai, "Wearing Type Behavior Help Device, Wearing Type Behavior Help Device Calibration Device, and Calibration Program," ed: Google Patents, 2008.

[8] H. Kawamoto, L. Suwoong, S. Kanbe, and Y. Sankai, "Power assist method for HAL-3 using EMG-based feedback controller," in *Systems, Man and Cybernetics, 2003. IEEE International Conference on*, 2003, pp. 1648-1653 vol.2.

[9] R. Horst and R. Marcus, "FlexCVA: A Continuously Variable Actuator for Active Orthotics," in *Engineering in Medicine and Biology Society, 2006. EMBS '06. 28th Annual International Conference of the IEEE*, 2006, pp. 2425-2428.

[10] R. W. Horst, "A bio-robotic leg orthosis for rehabilitation and mobility enhancement," in *Engineering in Medicine and Biology Society, 2009. EMBC 2009. Annual International Conference of the IEEE*, 2009, pp. 5030-5033.

[11] A. M. Technologies. (2014). *ReWalk*. Available: http://www.rewalk.com.

[12] H. Kazerooni, N. H. Harding, and R. Angold, "Lower extremity exoskeleton," ed: Google Patents, 2011.

[13] K. A. Strausser and H. Kazerooni, "The development and testing of a human machine interface for a mobile medical exoskeleton," in *Intelligent Robots and Systems (IROS), 2011 IEEE/RSJ International Conference on*, 2011, pp. 4911-4916.

[14] V. A. D. Cai, P. Bidaud, V. Hayward, F. Gosselin, and E. Desailly, "Self-adjusting, isostatic exoskeleton for the human knee joint," in *Engineering in Medicine and Biology Society, EMBC, 2011 Annual International Conference of the IEEE*, 2011, pp. 612-618.

[15] M. S. Jung-Hoon Kim, Dong Hyun Ahn, Byoung Jong Son, Suk-Young Kim, Deog Young Kim, Yoon Su Baek and Baek-Kyu Cho, "Design of a Knee Exoskeleton Using Foot Pressure and Knee Torque Sensors.," *International Journal of Advanced Robotic System*, vol. 12, 2015.

[16] K. J. Kim, M. S. Kang, Y. S. Choi, J. Han, and C. Han, "Conceptualization of an exoskeleton Continuous Passive Motion(CPM) device using a link structure," in *2011 IEEE International Conference on Rehabilitation Robotics*, 2011, pp. 1-6.
[17] A. Zoss, H. Kazerooni, and A. Chu, "On the mechanical design of the Berkeley Lower Extremity Exoskeleton (BLEEX)," in *Intelligent Robots and Systems, 2005. (IROS 2005). 2005 IEEE/RSJ International Conference on*, 2005, pp. 3465-3472.
[18] A. B. Zoss, H. Kazerooni, and A. Chu, "Biomechanical design of the Berkeley lower extremity exoskeleton (BLEEX)," *IEEE/ASME Transactions on Mechatronics,* vol. 11, pp. 128-138, 2006.
[19] R. Sarcos. *XOS-"Exoskeleton suit"*. Available: http://www.sarcos.com/
[20] L. Martin. (2016). *HULC-"Exoskeleton suit"* Available: http://www.lockheedmartin.com/us/products/exoskeleton/hulc.html
[21] M. R. Tucker, J. Olivier, A. Pagel, H. Bleuler, M. Bouri, O. Lambercy, *et al.*, "Control strategies for active lower extremity prosthetics and orthotics: a review," *Journal of NeuroEngineering and Rehabilitation,* vol. 12, p. 1, 2015// 2015.
[22] N. C. Karavas, N. G. Tsagarakis, and D. G. Caldwell, "Design, modeling and control of a series elastic actuator for an assistive knee exoskeleton," in *2012 4th IEEE RAS & EMBS International Conference on Biomedical Robotics and Biomechatronics (BioRob)*, 2012, pp. 1813-1819.
[23] I. Sarakoglou, N. G. Tsagarakis, and D. G. Caldwell, "Occupational and physical therapy using a hand exoskeleton based exerciser," in *Intelligent Robots and Systems, 2004. (IROS 2004). Proceedings. 2004 IEEE/RSJ International Conference on*, 2004, pp. 2973-2978 vol.3.
[24] T. Yan, M. Cempini, C. M. Oddo, and N. Vitiello, "Review of assistive strategies in powered lower-limb orthoses and exoskeletons," *Robotics and Autonomous Systems,* vol. 64, pp. 120-136, 2// 2015.
[25] M. Cempini, S. M. M. D. Rossi, T. Lenzi, M. Cortese, F. Giovacchini, N. Vitiello, *et al.*, "Kinematics and design of a portable and wearable exoskeleton for hand rehabilitation," in *2013 IEEE 13th International Conference on Rehabilitation Robotics (ICORR)*, 2013, pp. 1-6.
[26] A. Chiri, M. Cempini, S. M. M. D. Rossi, T. Lenzi, F. Giovacchini, N. Vitiello, *et al.*, "On the design of ergonomic wearable robotic devices for motion assistance and rehabilitation," in *Engineering in Medicine and Biology Society (EMBC), 2012 Annual International Conference of the IEEE*, 2012, pp. 6124-6127.
[27] T. Lenzi, S. D. Rossi, N. Vitiello, A. Chiri, S. Roccella, F. Giovacchini, *et al.*, "The neuro-robotics paradigm: NEURARM, NEUROExos, HANDEXOS," in *2009 Annual International Conference of the IEEE Engineering in Medicine and Biology Society*, 2009, pp. 2430-2433.
[28] M. Cempini, S. M. M. D. Rossi, T. Lenzi, N. Vitiello, and M. C. Carrozza, "Self-Alignment Mechanisms for Assistive Wearable Robots: A Kinetostatic Compatibility Method," *IEEE Transactions on Robotics,* vol. 29, pp. 236-250, 2013.
[29] E. S. G. a. J. W. Suntay, "A Joint Coordinate System for the Clinical Description of Three-Dimensional Motions: Application to the Knee," *Journal of Biomechanics,* vol. 105, 1983.
[30] G. Wu, F. C. T. van der Helm, H. E. J. Veeger, M. Makhsous, P. Van Roy, C. Anglin, *et al.*, "ISB recommendation on definitions of joint coordinate systems of

various joints for the reporting of human joint motion—Part II: shoulder, elbow, wrist and hand," *Journal of Biomechanics*, vol. 38, pp. 981-992, 5// 2005.

[31] D. G. Caldwell, N. G. Tsagarakis, S. Kousidou, N. Costa, and I. Sarakoglou, ""SOFT" EXOSKELETONS FOR UPPER AND LOWER BODY REHABILITATION — DESIGN, CONTROL AND TESTING," *International Journal of Humanoid Robotics*, vol. 04, pp. 549-573, 2007/09/01 2007.

[32] N. G. Tsagarakis and D. G. Caldwell, "Development and Control of a 'Soft-Actuated' Exoskeleton for Use in Physiotherapy and Training," *Autonomous Robots*, vol. 15, pp. 21-33, 2003// 2003.

[33] N. Karavas, A. Ajoudani, N. Tsagarakis, J. Saglia, A. Bicchi, and D. Caldwell, "Tele-Impedance based stiffness and motion augmentation for a knee exoskeleton device," in *Robotics and Automation (ICRA), 2013 IEEE International Conference on*, 2013, pp. 2194-2200.

[34] N. Karavas, A. Ajoudani, N. Tsagarakis, J. Saglia, A. Bicchi, and D. Caldwell, "Tele-impedance based assistive control for a compliant knee exoskeleton," *Robotics and Autonomous Systems*, vol. 73, pp. 78-90, 11// 2015.

[35] A. H. A. Stienen, E. E. G. Hekman, F. C. T. v. d. Helm, and H. v. d. Kooij, "Self-Aligning Exoskeleton Axes Through Decoupling of Joint Rotations and Translations," *IEEE Transactions on Robotics*, vol. 25, pp. 628-633, 2009.

[36] A. Otten, C. Voort, A. Stienen, R. Aarts, E. v. Asseldonk, and H. v. d. Kooij, "LIMPACT:A Hydraulically Powered Self-Aligning Upper Limb Exoskeleton," *IEEE/ASME Transactions on Mechatronics*, vol. 20, pp. 2285-2298, 2015.

[37] Y. L. Park, B. r. Chen, D. Young, L. Stirling, R. J. Wood, E. Goldfield, *et al.*, "Bio-inspired active soft orthotic device for ankle foot pathologies," in *2011 IEEE/RSJ International Conference on Intelligent Robots and Systems*, 2011, pp. 4488-4495.

[38] M. Wehner, B. Quinlivan, P. M. Aubin, E. Martinez-Villalpando, M. Baumann, L. Stirling, *et al.*, "A lightweight soft exosuit for gait assistance," in *2013 IEEE International Conference on Robotics and Automation*, 2013, pp. 3362-3369.

[39] A. T. Asbeck, R. J. Dyer, A. F. Larusson, and C. J. Walsh, "Biologically-inspired soft exosuit," in *2013 IEEE 13th International Conference on Rehabilitation Robotics (ICORR)*, 2013, pp. 1-8.

[40] K. Anam and A. A. Al-Jumaily, "Active Exoskeleton Control Systems: State of the Art," *Procedia Engineering*, vol. 41, pp. 988-994, // 2012.

[41] T. Hayashi, H. Kawamoto, and Y. Sankai, "Control method of robot suit HAL working as operator's muscle using biological and dynamical information," in *2005 IEEE/RSJ International Conference on Intelligent Robots and Systems*, 2005, pp. 3063-3068.

[42] C. Fleischer and G. Hommel, "A Human--Exoskeleton Interface Utilizing Electromyography," *IEEE Transactions on Robotics*, vol. 24, pp. 872-882, 2008.

[43] N. Karavas, A. Ajoudani, N. Tsagarakis, J. Saglia, A. Bicchi, and D. Caldwell, "Tele-Impedance based stiffness and motion augmentation for a knee exoskeleton device," in *2013 IEEE International Conference on Robotics and Automation*, 2013, pp. 2194-2200.

[44] C. Castellini, P. Artemiadis, M. Wininger, A. Ajoudani, M. Alimusaj, A. Bicchi, *et al.*, "Proceedings of the first workshop on Peripheral Machine Interfaces: going

beyond traditional surface electromyography," *Frontiers in Neurorobotics*, vol. 8, 2014-August-15 2014.

[45] H. Kazerooni, "Exoskeletons for human power augmentation," in *2005 IEEE/RSJ International Conference on Intelligent Robots and Systems*, 2005, pp. 3459-3464.

[46] H. Kazerooni, J. L. Racine, H. Lihua, and R. Steger, "On the Control of the Berkeley Lower Extremity Exoskeleton (BLEEX)," in *Proceedings of the 2005 IEEE International Conference on Robotics and Automation*, 2005, pp. 4353-4360.

[47] Y. Ikeuchi, J. Ashihara, Y. Hiki, H. Kudoh, and T. Noda, "Walking assist device with bodyweight support system," in *2009 IEEE/RSJ International Conference on Intelligent Robots and Systems*, 2009, pp. 4073-4079.

[48] J. E. Pratt, B. T. Krupp, C. J. Morse, and S. H. Collins, "The RoboKnee: an exoskeleton for enhancing strength and endurance during walking," in *Robotics and Automation, 2004. Proceedings. ICRA '04. 2004 IEEE International Conference on*, 2004, pp. 2430-2435 Vol.3.

[49] T. Nakamura, K. Saito, W. ZhiDong, and K. Kosuge, "Realizing model-based wearable antigravity muscles support with dynamics terms," in *2005 IEEE/RSJ International Conference on Intelligent Robots and Systems*, 2005, pp. 2694-2699.

[50] B. Ugurlu, M. Nishimura, K. Hyodo, M. Kawanishi, and T. Narikiyo, "A framework for sensorless torque estimation and control in wearable exoskeletons," in *2012 12th IEEE International Workshop on Advanced Motion Control (AMC)*, 2012, pp. 1-7.

[51] W. Huo, S. Mohammed, and Y. Amirat, "Observer-based active impedance control of a knee-joint assistive orthosis," in *2015 IEEE International Conference on Rehabilitation Robotics (ICORR)*, 2015, pp. 313-318.

[52] D. Sasaki, T. Noritsugu, and M. Takaiwa, "Development of pneumatic lower limb power assist wear driven with wearable air supply system," in *2013 IEEE/RSJ International Conference on Intelligent Robots and Systems*, 2013, pp. 4440-4445.

[53] C. J. Walsh, D. Paluska, K. Pasch, W. Grand, A. Valiente, and H. Herr, "Development of a lightweight, underactuated exoskeleton for load-carrying augmentation," in *Proceedings 2006 IEEE International Conference on Robotics and Automation, 2006. ICRA 2006.*, 2006, pp. 3485-3491.

[54] F. Negrello, M. Garabini, M. G. Catalano, J. Malzahn, D. G. Caldwell, A. Bicchi, *et al.*, "A modular compliant actuator for emerging high performance and fall-resilient humanoids," in *Humanoid Robots (Humanoids), 2015 IEEE-RAS 15th International Conference on*, 2015, pp. 414-420.

[55] N. G. Tsagarakis, D. G. Caldwell, F. Negrello, W. Choi, L. Baccelliere, V. G. Loc, *et al.*, "WALK-MAN: A High-Performance Humanoid Platform for Realistic Environments," *Journal of Field Robotics*, vol. 34, pp. 1225-1259, 2017.

[56] D. A. Neumann, *Kinesiology of the musculoskeletal system: Foundations for rehabilitation*. St. Louis, Mo: Mosby/Elseviser, 2010.

[57] L. Zhao, W. Zhao, S. Huang, and R. Jiang, "The study of kinematics parameters for human treadmill walking," in *2015 8th International Conference on Biomedical Engineering and Informatics (BMEI)*, 2015, pp. 386-390.

[58] L. Saccares, A. Brygo, I. Sarakoglou, and N. G. Tsagarakis, "A Novel Human Effort Estimation Method for Knee Assistive Exoskeletons," in *ICORR 2017- 15th IEEE International Conference on Rehabilitation Robotics*, 2017.

[59] H. M. Schepers, H. F. J. M. Koopman, and P. H. Veltink, "Ambulatory Assessment of Ankle and Foot Dynamics," *IEEE Transactions on Biomedical Engineering*, vol. 54, pp. 895-902, 2007.

[60] G. G. Chernyĭ and S. A. Regirer, *Contemporary problems of biomechanics*: Mir Publishers, 1990.

[61] P. de Leva, "Adjustments to Zatsiorsky-Seluyanov's segment inertia parameters," *Journal of Biomechanics*, vol. 29, pp. 1223-1230.

[62] C. P. Witana, S. Xiong, J. Zhao, and R. S. Goonetilleke, "Foot measurements from three-dimensional scans: A comparison and evaluation of different methods," *International Journal of Industrial Ergonomics*, vol. 36, pp. 789-807, 9// 2006.

[63] A. Young and D. Ferris, "State-of-the-art and Future Directions for Robotic Lower Limb Exoskeletons," *IEEE Transactions on Neural Systems and Rehabilitation Engineering*, vol. 25, pp. 1-1, 2016.

[64] H. Khan, R. Featherstone, D. G. Caldwell, and C. Semini, "Bio-inspired knee joint mechanism for a hydraulic quadruped robot," in *Automation, Robotics and Applications (ICARA), 2015 6th International Conference on*, 2015, pp. 325-331.

[65] L. Saccares, I. Sarakoglou, and N. G. Tsagarakis, "iT-Knee: An exoskeleton with ideal torque transmission interface for ergonomic power augmentation," in *2016 IEEE/RSJ International Conference on Intelligent Robots and Systems (IROS)*, 2016, pp. 780-786.